SHP2 DELETION IN POST-MIGRATORY NEURAL CREST CELLS

RESULTS IN IMPAIRED CARDIAC SYMPATHETIC INNERVATION

Jacquelyn D. Lajiness

May 2014

Accepted by the Graduate Faculty, of Indiana University, in partial
fulfillment of the requirements for the degree of Doctor of Philosophy.

_____

David A. Ingram, Jr., M.D.,
Administrative Chair

_____

Maureen A. Harrington, Ph.D.

Doctoral Committee

_____

Raghu G. Mirmira, M.D., Ph.D.

March 21, 2014

_____

R. Mark Payne, M.D.

_____

Michael Rubart, M.D.

DEDICATION

This thesis is dedicated to my wonderful family and friends. I could not have

accomplished this without your love and support. You guys are the best!

ACKNOWLEDGEMENTS

I would first like to acknowledge Simon Conway, PhD. Thank you for putting in the time and effort to train me as your student. During my time in your lab I have not only learned laboratory techniques but how to think more like a scientist and what kind of mentor I want to be for my future students. I would also like to thank the past and current members of the Conway lab. Thank you for sharing your time and expertise. It has been an honor to work with you.

I would also like to acknowledge the members of my research committee: Drs. Maureen Harrington, David Ingram, Mark Payne, and Michael Rubart. Thank you for guiding me and helping to shape my project with your insight. I have learned much about how to be a scientist from your tutelage. I cannot envision a better collection of mentors. Thank you for all of your support! I owe much of my success throughout this process to you and your collective encouragement, patience, and input.

To the educators who helped foster my love for science and put up with me throughout the years. Especially Mrs. Williams, my 9th grade science teacher and

Dr. Krueger, my undergraduate research mentor. I would not have considered pursuing a PhD without your encouragement and guidance.

Thank you to all of the students and staff that make up the MSTP. I count myself incredibly lucky to be surrounded by such amazing people.

A special thanks to Jan Receveur, you truly are a phenomenal person, and the extra effort you put into everything you do has helped make the IU MSTP more than just a program to us students. You not only make sure we show up to meetings and jump through the right hoops, but you exemplify the warmth and camaraderie that makes our MSTP a wonderful place to be.

To the directors of the MSTP that I have had the pleasure of working with during my time at IUSM: Drs. Wade Clapp, Maureen Harrington, and Raghu Mirmira, thank you for your mentorship and support. The time and effort you have put into my training as well as your council and guidance have been instrumental to my success.

To Brandon and Jeff, thanks for being my partners in crime. We endured classes together as a team and shared countless laughs and lunches as well as a few protocols. I could always count on you guys! Thank you for your friendship.

Jacquelyn D. Lajiness

SHP2 DELETION IN POST-MIGRATORY NEURAL CREST CELLS RESULTS

IN IMPAIRED CARDIAC SYMPATHETIC INNERVATION

Autonomic innervation of the heart begins *in utero* and continues during the neonatal phase of life. A balance between the sympathetic and parasympathetic arms of the autonomic nervous system is required to regulate heart rate as well as the force of each contraction. Our lab studies the development of sympathetic innervation of the early postnatal heart in a conditional knockout (cKO) of *Src homology protein tyrosine phosphatase 2* (Shp2). Shp2 is a ubiquitously expressed non-receptor phosphatase involved in a variety of cellular functions including survival, proliferation, and differentiation. We targeted Shp2 in post-migratory neural crest (NC) lineages using our novel *Periostin-Cre*. This resulted in a fully penetrant mouse model of diminished cardiac sympathetic innervation and concomitant bradycardia that progressively worsen.

Shp2 is thought to mediate its basic cellular functions through a plethora of signaling cascades including extracellular signal-regulated kinases (ERK) 1 and 2. We hypothesize that abrogation of downstream ERK1/2 signaling in NC lineages is primarily responsible for the failed sympathetic innervation phenotype observed in our mouse model. *Shp2* cKOs are indistinguishable from control littermates at birth and exhibit no gross structural cardiac anomalies; however, *in vivo* electrocardiogram (ECG) characterization revealed sinus bradycardia that

develops as the *Shp2* cKO ages. Significantly, 100% of *Shp2* cKOs die within 3 weeks after birth. Characterization of the expression pattern of the sympathetic nerve marker tyrosine hydroxylase (TH) revealed a loss of functional sympathetic ganglionic neurons and reduction of cardiac sympathetic axon density in *Shp2* cKOs. *Shp2* cKOs exhibit lineage-specific suppression of activated pERK1/2 signaling, but not of other downstream targets of Shp2 such as pAKT (phosphorylated-Protein kinase B). Interestingly, restoration of pERK signaling via lineage-specific expression of constitutively active MEK1 (Mitogen-activated protein kinase kinase1) rescued TH-positive cardiac innervation as well as heart rate. These data suggest that the diminished sympathetic cardiac innervation and the resulting ECG abnormalities are a result of decreased pERK signaling in post-migratory NC lineages.

David A. Ingram, Jr., M.D., Administrative Chair

TABLE OF CONTENTS

LIST OF TABLES

LIST OF FIGURES

LIST OF ABBREVIATIONS

AAA	Aortic arch arteries
A/C6	Adenylate cyclase 6
AHA	American Heart Association
ANS	Autonomic nervous system
APSA	American Physician Scientist Association
AraC	Cytosine arabinoside
AV	Atrioventricular
β1AR	Beta-1 adrenergic receptor
bp	Base pairs
BPM	Beats per minute
caMEK1	constitutively active Mitogen-activated protein kinase kinase
cAMP	Cyclic adenosine monophosphate
cDNA	complementary DNA
cKO	conditional knock out
DNA	Deoxyribonucleic acid
DRG	Dorsal root ganglia
DMSO	Dimethyl sulfoxide
E	Embryonic day
ECG	Electrocardiograph
EMT	Epithelial-mesenchymal transition
GAP	GTPase-activating protein
H&E	Hemotoxylin and eosin
IHC	Immunohistochemistry
JAK	Janus Kinase
LS	LEOPARD syndrome
MAG	Myelin-associated glycoprotein
MAPK	Mitogen-activated protein kinase
MBP	Myelin Basic Protein
MEK	Mitogen-activated protein kinase kinase
mRNA	messenger ribonucleic acid

NC	Neural crest
NFAT	Nuclear factor of activated T-cells
NGF	Nerve Growth Factor
NIH	National Institutes of Health
Nrg-1	Neuregulin-1
Nrp1	Neuropilin1
NS	Noonan syndrome
NSβT	Neuron specific beta tubulin
OFT	Outflow tract
P	Postnatal day
pAKT	phosphorylated-Protein kinase B
PBS	Phosphate-buffered saline
PBST	Phosphate-buffered saline Tween-20
PI3K	Phosphoinositide 3-kinase
PCR	Polymerase Chain Reaction
pERK	phospo-Extracellular Signal-Regulated Kinase
PTP	Protein Tyrosine Phosphatase
qPCR	quantitative Polymerase Chain Reaction
R26r	ROSA26 reporter
RTK	Receptor Tyrosine Kinase
SA	Sinoatrial
SC	Schwann cell
SCP	Schwann cell precursor
SEM	Standard error of the mean
SH2	Src homology2
Shp2	Src homology protein tyrosine phosphatase 2
Stat	Signal transduces and activators of transcription
tAKT	total-Protein kinase B
TEM	Transmission electron microscopy
tERK	total-Extracellular Signal-Regulated Kinase
TH	Tyrosine hydroxylase
TrkA	Tropomyosin-related receptor A
TUNEL	Terminal Deoxynucleotidyl Transferase Mediated dUTP Nick End Labeling

Some of the text in this dissertation was originally published in the Proceedings of the National Academy of Sciences USA. Lajiness et al. SHP-2 deletion in post-migratory neural crest cells results in impaired cardiac sympathetic innervation. *Proceedings of the National Academy of Sciences*. 2014; published ahead of print March 24, 2014, doi:10.1073/pnas.1319208111. © Proceedings of the National Academy of Sciences USA.

INTRODUCTION

The neural crest

The neural crest (NC) is a multipotent and transient migratory embryonic lineage that gives rise to a wide variety of cell types, tissues, and organs[1-4]. The NC is derived from the ectoderm, but is often referred to as the "fourth germ layer" because of the key role it plays in development. NC cells are required at different developmental stages for normal development of diverse tissues such as the facial skeleton, melanocytes, as well as the dermis, smooth muscle and adipose tissue associated with the skin in the head and neck region, the outflow tract septum of the heart, the smooth muscle associated with arteries derived from the aortic arches, and the peripheral nervous system (including the sensory, enteric, and autonomic nervous systems)[3, 5-10]. NC cells originate within early embryo neural folds. Although these cells are epithelial in nature while in the neural folds, they undergo epithelial-mesenchymal transition (EMT), delaminate from the neural folds, and migrate to target sites throughout the body where they differentiate into a variety of different cell types. The processes of NC induction, delamination, EMT, migration, and differentiation are extremely complex and subject to many influencing factors such as bone morphogenic proteins and various growth factors[2, 10].

The NC is often categorized by the rostral-caudal region from which the NC cells migrate. There are five regional classifications that correlate roughly with

functional designations: cranial, cardiac, vagal, trunk, and sacral NC (Figure 1). Cranial NC cells originate from the forebrain, midbrain and hindbrain regions of the neuroepithelium. The cranial NC will give rise to the pharyngeal arches which will eventually form the connective tissue and skeletal framework of the face and middle ear as well as the cranial nerves and associated glia, and the thymus, parathyroid, and thyroid glands[9, 11]. The cardiac NC develops from the region associated with somite 1-3 in embryos. These cells colonize the aortic arches, the endocardial cushions, and the outflow tract of the heart eventually contributing to aortic arch remodeling, valve development and outflow tract septation events[4, 12]. Abnormalities in the cardiac NC can lead to developmental cardiac defects such as persistent truncus arteriosus, double outlet right ventricle, and transposition of the great arteries (reviewed in [13]). The cardiac NC region overlaps with the vagal NC which extends from somite 1-7. The vagal NC cells, in conjunction with the sacral NC (posterior to somite 28), migrate to the gut and give rise to the enteric ganglia (parasympathetic in nature). Failure of the vagal and sacral NC cells to migrate results in loss of enteric ganglia. In the absence of ganglia, peristaltic movement in the intestine is not established which can result in obstruction[14-16]. The remaining NC population (somites 8-28) is collectively referred to as trunk NC which migrate along one of two migratory pathways. The trunk NC cells that migrate dorsolaterally give rise to many of the pigmented cells found throughout the body such as melanocytes. The remaining trunk NC cells migrate along the ventral pathway and give rise to the adrenal medulla (specifically derived from cells arising from somite 18-24), along with the

majority of the peripheral nervous system including the dorsal root ganglia (DRG) and associated sensory nervous system, sympathetic, and parasympathetic nervous systems as well as associated Schwann cells (SCs).
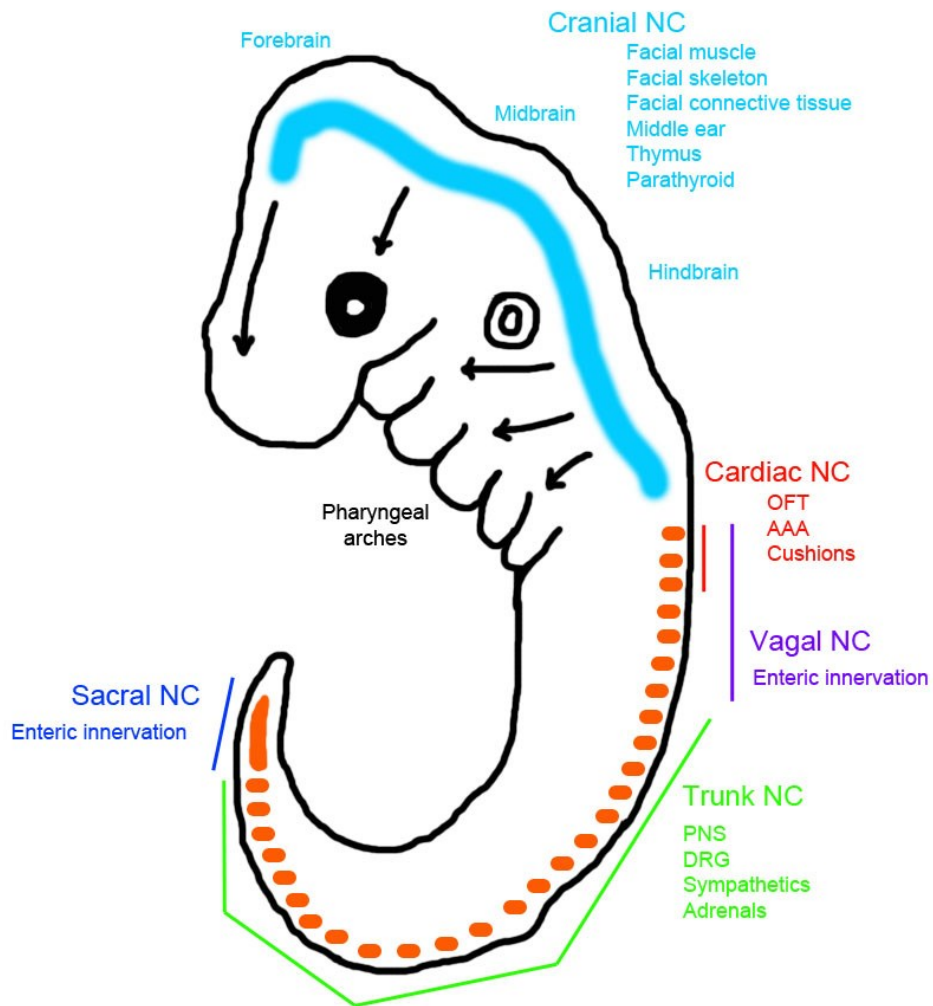
Figure 1. Subsets of NC and the structures derived from them. Figure

depicts a schematic of a developing embryo (~E10/11). The cranial NC cells are

derived from the forebrain, midbrain, and hindbrain (represented in light blue).

These cells give rise to the pharyngeal arches which form the components listed.

The somites of the developing embryo are depicted in orange. Cardiac NC cells

(somites 1-3; red) give rise to the cardiac outflow tract (OFT), aortic arch arteries

(AAA) and the cushions which will form the valves of the heart. Vagal NC

(somites 1-7; purple) and sacral NC (after somite 28; blue) cells collectively

contribute to the innervation of the gut. Trunk NC cells (somites 8-28; green) give

rise to the various components listed.

Due to the multistep process of NC morphogenesis (*i.e.* delamination, EMT, migration, and differentiation), NC cells are especially vulnerable to both environmental and genetic influences. Many congenital birth defects are thought to be due to aberrant NC morphogenesis[17], and NC ablation can result in various structural abnormalities including craniofacial defects such as mandibular hypoplasia and cleft palate, myelination and innervation defects, several different cardiac defects (reviewed in [17]) as well as abnormal electrical function of the embryonic heart[18, 19]. The extremely versatile yet susceptible nature of the NC lineage makes it an incredibly interesting area of study; however, investigations are often limited by the availability of genetic tools and the severity of the phenotypes observed as many mouse models with altered NC development are embryonically lethal and thus more subtle phenotypes or those occurring later in development go unexamined.

Various Cre lines instituted in NC studies

Cre recombinase is an enzyme used for genetic recombination of genomic DNA in animal models. Sophisticated mouse models have been developed where the spatiotemporal expression of Cre recombinase (referred to as "Cre" for short) is controlled by the promoter that drives its expression. By selecting a promoter that has a restricted temporal and anatomic expression pattern, it is possible for researchers to generate an animal model with precise genetic manipulation. A "Cre line" is a mouse line carrying a particular promoter used to drive Cre expression. This mouse line can be crossed to any number of transgenic mouse

lines with a floxed region of DNA (*i.e.* DNA flanked by LoxP sites) to drive genetic recombination. There is more than one way that Cre can be used as a genetic tool; however, in this study it is used to excise genomic DNA that is surrounded by introduced LoxP sites. A LoxP site is a palindromic sequence of DNA that is recognized and spliced by Cre. Once Cre is expressed in a cell, it permanently alters genomic DNA in that cell specifically[20]. Because genomic DNA is altered, any progeny of a cell that expressed Cre is also genetically modified even if Cre itself is never expressed in the progeny.

As spatiotemporal precision is an essential aspect to Cre-mediate genetic recombination technology, a reporter system capable of indicating when and where Cre is expressed was developed. The reporter system utilized in this study is the ROSA/LacZ reporter system (illustrated in Figure 5). Briefly, a transgene containing the constitutively active ROSA26 promoter, a neo cassette flanked by LoxP sites, and the *lacZ* gene followed by a polyadenylation sequence is introduced in a mouse line[21]. When crossed onto the background of a Cre-expressing mouse line, Cre will delete the neo cassette and allow for transcription of the *lacZ* gene which encodes β-galactosidase. β-galactosidase expression, thus, occurs only in cells expressing Cre and can then be detected via X-Gal staining. Thus, all genetically modified cells can be identified. This technique is referred to as lineage mapping.

There are several mouse lines in which Cre recombinase is expressed in different subsets of developing NC cells at varying time points throughout development. One of the earliest Cre lines to be expressed in a significant NC population is *AP2-α-Cre*. Cre is expressed as early as E7 in the cranial NC which contributes to all pharyngeal arches and in the caudal ectoderm overlying what will become the pharyngeal arches[22, 23]. *AP2-α-Cre* is a useful tool for extremely early investigations into development; however, its utility in NC investigations is often limited by the confounding factor that it is also expressed in the ectoderm. As the ectoderm releases factors critical to NC survival, migration, and differentiation, it becomes difficult to determine whether a genetic alteration driven by *AP2-α-Cre* causes a primary defect in the NC itself to give rise to a particular phenotype or if the observed effect is secondary in nature due to an alteration of the neural ectoderm overlying the neural crest which indirectly affects the NC cells.

The "classical" NC Cre line is *Wnt1-Cre* in which Cre is expressed in the dorsal neural folds and neural tube prior to delamination and emigration of the NC (E8)[23-25]. At E8.5 Cre is expressed in the majority of migratory NC cells and the complete pattern of expression is observed by E11.5[23, 24, 26]. In the *Wnt1-Cre* model, many NC derived tissues express Cre including the pharyngeal arches, outflow tract of the heart, aorto-pulmonary septum, dorsal root ganglia and peripheral nervous system as well as the Schwann cells supporting and myelinating those neurons[23]. This is the most complete and most widely used

Cre line for NC studies, however it does have its limitations. For example, there have been reports that *Wnt1-Cre* can induce phenotypes by ectopically activating endogenous Wnt signaling[25]. Furthermore, Cre expression in such a wide array of tissues from an early age (as early as E8) results in many phenotypes that are embryonically lethal and thus will not allow for investigation of more subtle phenotypes or phenotypes that arise postnatally[27].

A tamoxifen inducible form of *Wnt1-Cre* does exist which enables researchers to activate Cre expression at any time after the onset of Wnt-1 promoter activation. However, Cre is only expressed in cells that are actively utilizing the Wnt-1 promoter at the time of administration of tamoxifen. Further, the recombination efficiency is drastically reduced and the level of tamoxifen needed to induce recombination boarders on the level that will interfere with pregnancy[24]. While this Cre system may have specific applications, its utility in comprehensive NC development studies is tenuous.

Another Cre transgenic line that is expressed in NC lineages is the *P0-Cre*. Cre is expressed in NC derivatives such as the DRG, the sensory and enteric nervous systems, and pharyngeal arch derived craniofacial mesenchyme from E9 onward[23, 28]. In this model, the complete Cre expression pattern is observed by E12.5. Cre is expressed in a smaller subset of NC than observed in the *Wnt1-Cre* line. Furthermore, unlike the *Wnt1-Cre* line, the *P0-Cre* line expresses Cre in the notochord which is not derived from the NC[28].

There are two different Cre lines in which Cre expression is driven by the nestin gene promoter. *Nestin1-Cre* is expressed in several NC and non-NC lineages. The earliest Cre expression detected by reporter gene expression occurs at E7.5-8 and is observed in specified areas of the embryo as well as in extra-embryonic mesenchyme[29]. The branchial arches express Cre E8-10.5, and by E9 the heart contains Cre-positive cells. However, several non-NC lineages such as the entire central nervous system and pancreatic progenitors also express Cre by E14.5-15.5[29]. Unfortunately, although being expressed in NC lineages at important times, Cre expression in such a wide variety of non-NC lineages precludes *Nestin1-Cre* from being informative about isolated NC defects. Similarly, in the *Nestin2-Cre* Cre line, Cre is expressed in both NC lineages as well as the central nervous system (non-NC-derived). By E11.5 the DRG (NC-derived) as well as the ventricular zone of the telenecephalon and spinal cord (central nervous system) are Cre-positive[30].

In the *Advillin-Cre* model, Cre is expressed in NC-derived structures such as all peripheral sensory neurons including DRG, trigeminal ganglia, and nodose ganglia as well as the superior cervical ganglia (sympathetic nervous system) from E14.5-16.5[31]. Cre expression is also detected in the midbrain, brainstem, and tongue (non-NC-derived)[31]. As *Advillin-Cre* is expressed in a small subset of NC-lineages and is only activated relatively late in development, it, like all other Cre lines, has limitations in its applicability to the study of NC development.

Collectively, current transgenic lines expressing Cre in NC-derived tissues cover a relatively wide range of tissue subsets and developmental time points. Certain lineages such as the derivatives of the pharyngeal arches and the sensory nervous system and corresponding DRG are well represented at varying time points whereas other lineages such as the sympathetic nervous system have only partial expression or limited time points at which developmental requirement for particular genes can be investigated. As E8-E11 is a crucial developmental window in which NC cells migrate throughout the body and differentiate into various tissues, the more genetic tools available to manipulate NC cells in this timeframe, the more detailed our knowledge of NC cellular processes will become. The work herein describes using a Cre line developed in our lab (*Periostin-Cre*) to investigate the development of NC derivatives specifically focusing on the sympathetic arm of the autonomic nervous system.

Autonomic nervous system

The autonomic nervous system (ANS), as a subset of the peripheral nervous system, is derived from the NC. The ANS itself is divided into two diametrically opposed branches: the sympathetic and parasympathetic nervous systems. The sympathetic innervation ramps up the "fight or flight" responses while the parasympathetic innervation reverses these responses in favor of promoting "rest and digest" functions[32]. Together, these two arms maintain homeostasis; regulate the organism's responses to exercise, stress, and/or injury; and interact with the

endocrine system to control reproduction[33]. The word "autonomic" means "self-governing" and that is precisely what this aspect of the nervous system does; it controls all of the elements of daily life that you don't have to think about. It regulates blood pressure and heart rate, coordinates basal respiratory rate, controls body temperature, adjusts urinary output and salt retention, facilitates digestion and propulsion of food through the digestive tract, and maintains blood glucose levels[33, 34].

The classic structure of the ANS is a two-neuron chain. The cell body of the first neuron (the preganglionic fiber) resides in the interomediolateral horn of the spinal cord and projects out its axon to a peripheral ganglia where it synapses on the cell body and/or dendrites of the second neuron (the postganglionic fiber)[33-35]. The postganglionic fiber then synapses directly onto the target organ. Typically sympathetic neurons have short preganglionic axons and long postganglionic axons (*i.e.* the peripheral ganglia is located near the spinal cord) while the opposite is true for the parasympathetic neurons (the peripheral ganglia is located near/on the target organ)[34]. However, this does not hold true for some organs such as the heart and the gut which have more complex interactions between the sympathetic and parasympathetic innervation[33, 36-42].

There are two main neurotransmitters that transduce signals in the ANS: acetylcholine and norepinephrine. Acetylcholine is released at all ganglionic synapses (between the pre- and postganglionic fibers) and is recognized by

nicotinic cholinergic receptors on the postganglionic neuron[43]. Parasympathetic postganglionics also release acetylcholine which achieves its effects on the target organ through muscarinic receptors. In contrast, most sympathetic postganglionics release norepinephrine which signals through α–adrenergic or β–adrenergic receptors depending upon the tissue[44, 45]. The sympathetic innervation to the sweat glands and some blood vessels are important exceptions as they signal through the acetylcholine/muscarinic receptor pathway despite being part of the sympathetic nervous system[33]. All adrenergic receptors signal through G-proteins and primarily result in altered cAMP levels by either stimulating adenylate cyclase to increase cAMP levels or inhibiting it to decrease cAMP levels. Specificity for how an individual organ responds to sympathetic stimulation is achieved through which subsets of receptors (α1, α2, β1, and β2) are expressed and at what concentrations. Thus, the same sympathetic stimulus can effect different physiological changes in different tissues[43, 45].

α1–adrenergic receptors are located on peripheral smooth muscle cells and when stimulated with either epinephrine or norepinephrine result in the contraction of those muscles through increasing calcium levels[33, 46]. Physiologically, this results in dilation of the pupils and vasoconstriction of blood vessels. α2–adrenergic receptors serve and important negative feedback role in the autonomic nervous system[47, 48]. These receptors are located on vascular prejunctional synapses, and when stimulated with epinephrine or extremely high levels of norepinephrine, they signal through an inhibitory G-protein which inhibits

adenylate cyclase and decreases cAMP levels preventing further release of norepinephrine at that synapse[49]. β1–adrenergic receptors are expressed predominantly in the heart and are responsible for many of the "fight or flight" systemic response associated with sympathetic stimulation such as increased heart rate and cardiac output[35, 50]. These effects are achieved through an increase in cAMP levels in the pacemaker cells of the heart (the SA node) as well as in the cardiomyocytes. The elevated cAMP levels lead to an increase not only the heart rate but also the strength of each contraction. And finally, β2–adrenergic receptors are located on peripheral smooth muscle and when stimulated result in elevated cAMP levels leading to the relaxation of the associated smooth muscle cells[34, 51]. This allows for bronchodilation to increase oxygen intake as well as vasodilation to provide increased circulation to skeletal muscles in preparation for strenuous activity. These receptors are much more sensitive to epinephrine (released by the adrenal gland) as opposed to norepinephrine (released by sympathetic neurons)[33, 45].

While acetylcholine is commonly produced by many subsets of neurons, norepinephrine is unique to sympathetic neurons. Therefore, expression of enzymes critical in the synthetic pathway of catecholamines (norepinephrine and epinephrine) can be used to identify sympathetic innervation. One such enzyme is tyrosine hydroxylase (TH; the rate-limiting enzyme for catecholamine synthesis). TH catalyzes the conversion of tyrosine to L-DOPA (a key intermediate of catecholamine synthesis) and is commonly used as a definitive

marker of sympathetic innervation[52-55]. A less commonly used, but more specific

marker of sympathetic innervation is dopamine β-hydroxylase (DβH). DβH

converts dopamine to norepinephrine and is only expressed in noradrenergic

neurons and adrenal chromaffin cells. A small population of TH-positive, DβH-

negative neurons does exist. This population are dopaminergic neurons and are

primarily located in the central nervous system and the enteric nervous system[56].

Development of cardiac sympathetic innervation

Although autonomic innervation of the heart begins *in utero*, functional

neurocardiac coupling continues postnatally. Autonomic imbalance and irregular

cardiac innervation density can result in deadly consequences such as cardiac

arrhythmias, heart failure, and sudden cardiac death[57-60]. While a balance

between the sympathetic and parasympathetic arms of the autonomic nervous

system is required to regulate heart rate, conduction velocity, and the force of

each contraction, sympathetic tone predominates in determining the basal heart

rate in rodents. This means that in a rodent if the heart were removed from all

sympathetic and parasympathetic input, it would beat slower. This is because the

stimulus to beat faster from the sympathetic innervation is, at rest, stronger than

the parasympathetic stimulus to slow the heart rate. Therefore, removing

sympathetic input has a greater physiologic effect on heart rate, and the heart

rate will decrease as a result.

The sympathetic nervous system arises from the neural crest lineage. In the case of sympathetic neurons innervating the heart, trunk NC cells delaminate and migrate ventrally through the somites to establish the sympathetic trunk ganglia near the dorsal aorta[8, 54, 61, 62]. Post-migration, cross-regulatory transcription factors such as Mash1, Phox2a and 2b as well as Gata3[63-69] are temporarily expressed. Expression of these transcription factors drives NC cells to acquire a neuronal fate and eventually to differentiate into sympathetic neurons expressing both neuron specific β-tubulin (NSβT) and TH [70-75]. Subsequently, a subset of sympathetic NC cells undergoes a second migration to the cervicothoracic and intrinsic cardiac ganglia to establish populations of sympathetic neurons which contribute to the cardiac plexus or "heart brain" [8, 40, 41]. Recent studies exploring the extensive complexity of autonomic cardiac innervation revealed multiple levels of regulation and interaction between parasympathetic and sympathetic arms of autonomic innervation that converges in the "heart brain" to control cardiac function[36-42]. This network seems to be particularly influential and dynamic in the first few weeks of life making our *Shp2* cKO model ideally situated to investigate this important developmental stage.

Sympathetic (*i.e.* TH-positive) innervation is first observed at the base (near the aorta and pulmonary artery) of the heart around embryonic (E) day 13.5. This innervation then extends onto the surface of the atria and eventually to the ventricles before following blood vessels into the atrial and ventricular walls to innervate the myocardium and project to the sinoatrial (SA) and atrioventricular

16

(AV) nodes[76]. Establishment of the sympathetic innervation of the heart is achieved gradually over a month, beginning in utero at E13.5 and culminating at approximately 3 weeks after birth.

Sympathetic innervation to the SA and AV nodes serves two purposes. The SA node is the pacemaker of the heart (the collection of cells that generates the action potential that results in the depolarization of the atria—corresponding to the P-wave of an ECG; Figure 2). Sympathetic stimulation of the SA node results in an overall increase in heart rate by decreasing the amount of time between each P-wave. The AV node, under normal physiological conditions, is responsible for delaying the action potential after the atria but before the ventricles so that the atria have enough time to finish emptying all of the blood that they contain into the ventricles before the ventricles begin contracting (it essentially controls the length of the PR interval; Figure 2). Sympathetic stimulation of the AV node also serves to increase heart rate by decreasing the duration of this "pause".
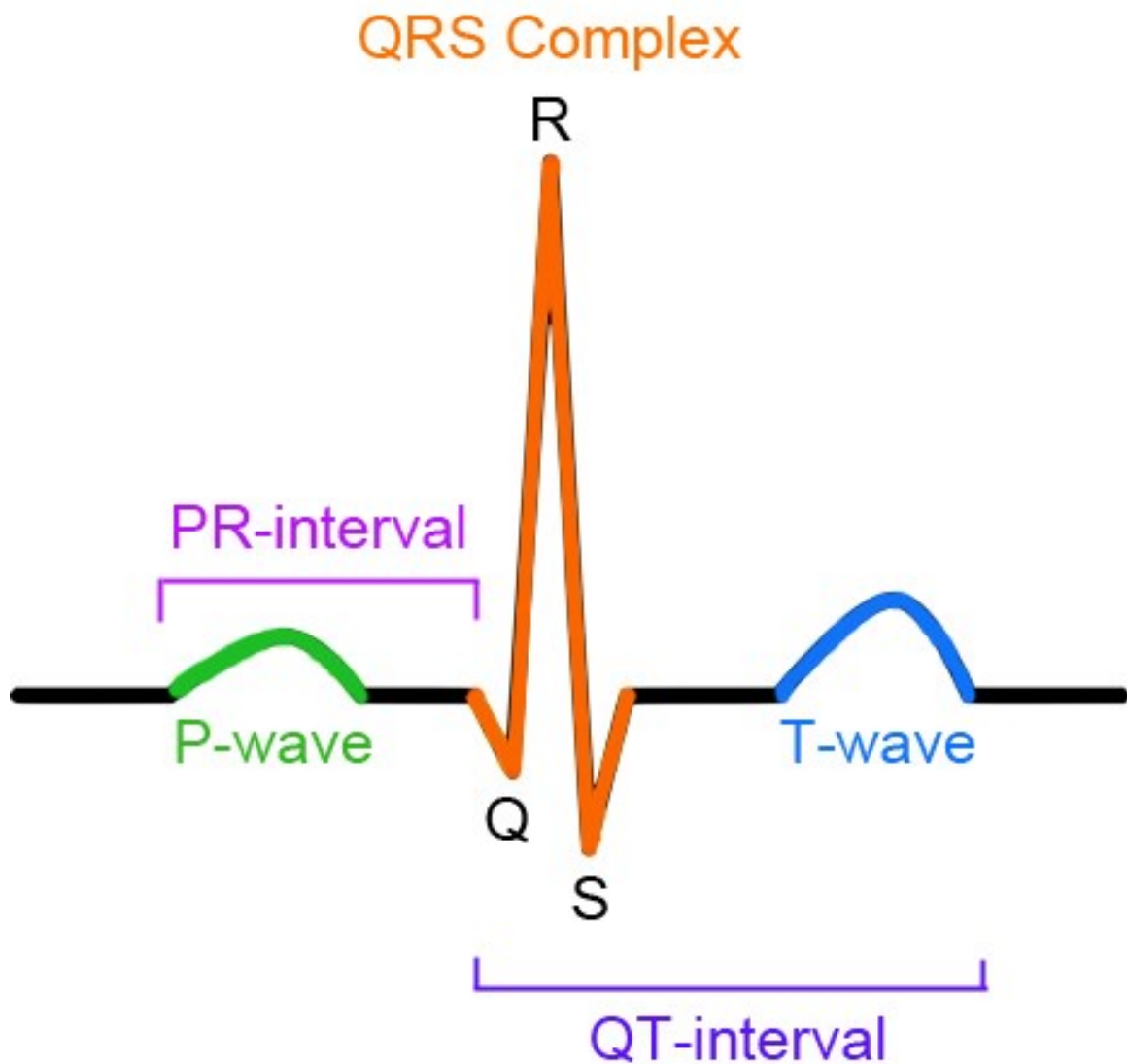
Figure 2. Standard ECG trace. The standard ECG is broken up into three main

waveforms and two clinically relevant intervals:

The P-wave (green) corresponds to the electrical depolarization of the atria. The

action potential responsible for generating the P-wave is initiated by SA node and

disseminates throughout the atria to signal a coordinated contraction. An absent

P-wave indicates abnormal SA node function.

The PR-interval corresponds to conduction delay at the AV node. A prolonged PR-interval indicates some degree of AV-block which if progresses, can result in arrhythmias and sudden death.

The QRS complex (orange) corresponds to the electrical depolarization of the ventricle.

The QT-interval corresponds to the length of the mechanical contraction of the ventricles. Prolongation or abbreviation of the QT-interval can predispose to ventricular tachycardia which can progress to ventricular fibrillation and sudden death.

The T-wave (blue) corresponds to ventricular repolarization.

Although present from *in utero* stages, the sympathetic innervation of the heart is not functionally relevant (*i.e.* does not control heart rate) until the second week of postnatal life in rodents[37, 53, 77]. While the number of primary dendrites emanating from sympathetic ganglia is set in the first postnatal week of life, the adult pattern of innervation achieved through extension and further branching of the primary dendrites is not fully formed until three weeks after birth[37, 78-80]. Nerve growth factor (NGF) is the signaling factor that primarily determines the density and complexity of sympathetic innervation and is absolutely essential in the first several weeks of postnatal life[79].

Role of NGF in establishment and maintenance of sympathetic innervation

The establishment of sympathetic innervation requires NGF production by the target organ—the myocardium in the case of the heart. NGF is the main neurotrophic factor in establishing and maintaining sympathetic innervation as well as a subpopulation of sensory neurons in the dorsal root ganglia[27, 81]. *In vitro* studies have shown that NGF stimulates the differentiation/neurite outgrowth of sympathetic neurons through the Shp2/ERK pathway while mediating the survival of those same neurons through the PI3K/AKT pathway[82-89]. Interestingly, NGF is not required early in embryonic development nor in adult animals once the sympathetic innervation has been established. However, NGF signaling is required for establishment of sympathetic innervation from E16.5 onward[90] and is essential for the survival of sympathetic neurons from P1-P40[91]. Understanding

this critical developmental window (from E16.5-1 month after birth) is key to investigations into sympathetic innervation.

NGF binds to its high-affinity receptor tropomyosin-related receptor A (TrkA). TrkA then results in the formation of a signaling complex including Src homology protein tyrosine phosphatase 2 (Shp2) which leads to activation of the Ras-RAF-MEK signaling cascade eventually resulting in sustained extracellular signal-regulated kinase (ERK) activation through phosphorylation. Once ERK is phosphorylated, it translocates to the nucleus where it modulates expression of genes controlling basic cellular functions such as proliferation and differentiation[86, 92]. Interestingly, mutating mitogen-activated protein kinase kinase (MEK) so that it is incapable of phosphorylating ERK blocks sympathetic neuronal differentiation in the model cell line (PC12 cells). Conversely, introducing an activating mutation in MEK induces differentiation and neurite outgrowth in sympathetic neurons even in the absence of differentiation factors such as NGF[86]. These experiments have shown that, at least *in vitro*, ERK phosphorylation is both necessary and sufficient for sympathetic neuron differentiation as defined by neurite outgrowth.

Interruption of the NGF signaling pathway at either the ligand (NGF) or receptor (TrkA) level results in pups that are viable at birth without any gross defects. However, the pups fail to gain weight, have decreased cross-sectional area of sympathetic neurons in ganglia and fewer dendrites, exhibit total loss of

sympathetic innervation by 10 days after birth, and all are dead by 4 weeks after birth (*Ngf* null) or ~8 weeks after birth (*TrkA* null)[27, 93-95]. NGF deprivation studies in which NGF antiserum was administered revealed that peripheral sympathetic innervation is affected by loss of NGF in the postnatal period but not in adulthood. This result indicates that there exists a critical window for NGF action and establishment of sympathetic innervation[94, 96]. Conversely, administering NGF to developing pups resulted in the expansion of arborization arising from sympathetic ganglia. Specifically, there was an increase in the number of primary dendrites as well as an increase in their length and number of branch points[79]. *In vitro* studies indicate that NGF administration promotes differentiation and thus neurite outgrowth and arborization but halts cellular division[86]. Other models of altered sympathetic innervation including a p75 (a low-affinity receptor of NGF) null mouse as well as a *Sema3a* (a neural chemorepellent for sensory and sympathetic axons) null mouse and mouse model involving NC-restricted deletion of the Sema3A receptor *Nrp1* all result in diminished sympathetic innervation of the heart and subsequent bradycardia[38, 97, 98]. Collectively, these studies illustrate that interruptions in NGF signaling at the ligand or receptor disturb sympathetic innervation which, among other effects, can lead to sinus bradycardia. In the current study we are interested in understanding what effect downstream interruptions in NGF signaling (specifically at the level of signal transduction through Shp2) will have on the development of sympathetic innervation particularly in the heart.

Shp2 signaling and roles in development

Shp2 is a ubiquitously expressed non-receptor phosphatase containing two N-terminal Src homology2 (SH2) domains, a central protein tyrosine phosphatase (PTP) catalytic domain, and a C-terminus with tyrosyl phosphorylation sites and a proline-rich domain[99, 100]. It is involved in a variety of cellular functions including survival, proliferation, and differentiation[100-104]. *Shp2* gain-of-function mutations account for approximately 50% of Noonan syndrome (NS, OMIM 163950) characterized by postnatal reduced growth, dysmorphic facial features, skeletal abnormalities, and cardiac defects[105]. Conversely, loss of Shp2 catalytic activity results in LEOPARD syndrome (LS, OMIM 151100) which is characterized by lentigines (dark, freckle-like lesions covering the skin), electrocardiographic (ECG) abnormalities, ocular hypertelorism (wide-set eyes), pulmonary stenosis, abnormal genitalia, growth retardation resulting in short stature, sensory neural deafness as well as other neurologic and cardiac defects including hypertrophic cardiomyopathy[106]. It has often been commented in the literature how LS and NS have striking clinical similarities despite manifesting opposite effects on Shp2 activity and downstream signaling cascades. This is predominantly thought to reflect a narrow physiologic range of downstream MAPK signaling that is conducive for proper development[102, 107].

There are seven Shp2 mutations associated with LS, all of which are concentrated in the catalytic core of the protein. These mutations have been shown *in vitro* to cause a decrease in catalytic activity of Shp2 and diminished

MAPK signaling[102, 108, 109]; however there is still debate as to the mechanism for how Shp2 facilitates Ras/MAPK activation. It has been hypothesized that Shp2 can act by any of the following mechanisms or a combination thereof: dephosphorylating binding sites on RasGAP receptors, inactivating Grb2/Sos inhibitors, and/or activating Src family kinases resulting in sustained Ras and subsequent ERK activation[102, 110, 111]. While the specific mechanism has yet to be elucidated, it is known that activation of Shp2 via a ligand binding a receptor tyrosine kinase (RTK) results in increased RAS activity and subsequent phosphorylation of ERK1/2 which then translocate to the nucleus to alter transcription and regulate cellular processes (Figure 3).
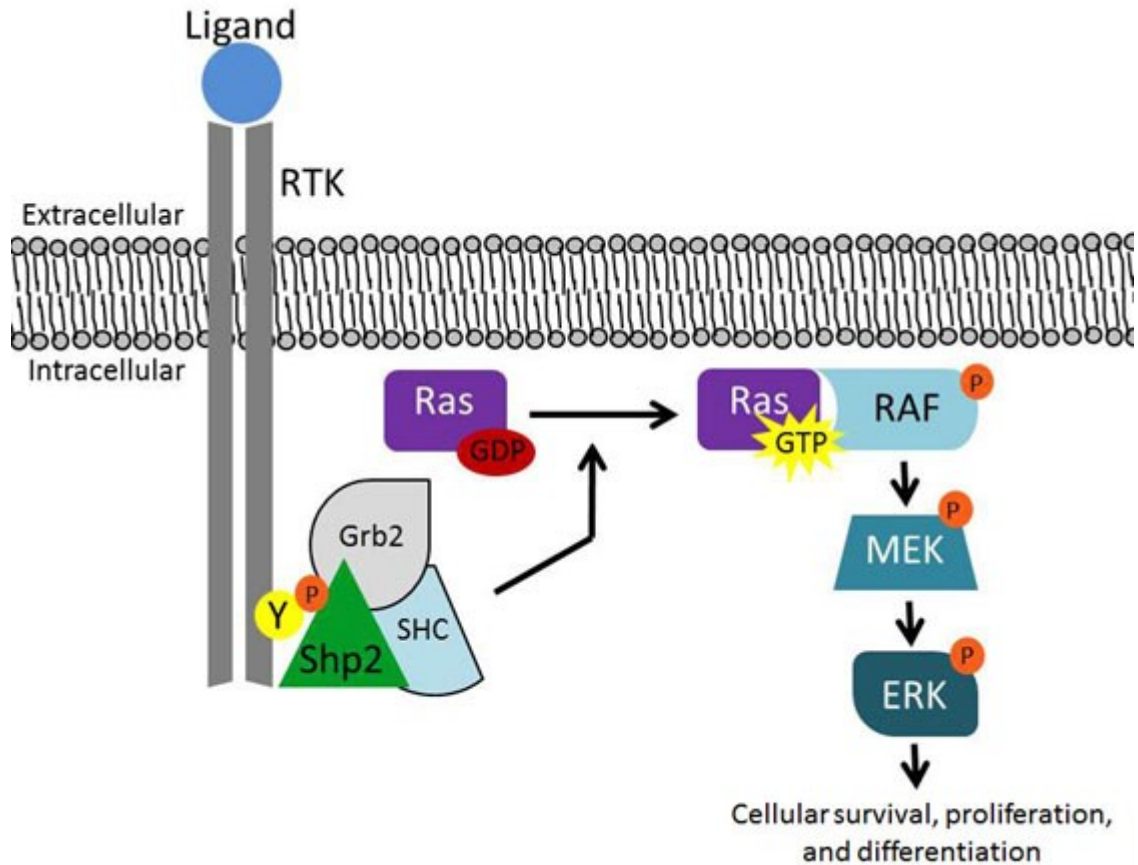
Figure 3. Schematic of Shp2/MAPK signaling cascade. A ligand (*i.e.* growth

factor) binds to a receptor tyrosine kinase (RTK) which is associated with a

complex including Shp2. Propagation of signaling results in localization of Ras to

the membrane where GDP is exchanged for GTP. Ras bound to GTP activates

RAF via phosphorylation which continues the activating phosphorylation cascade

through MEK and ERK. Once phosphorylated, ERK translocates to the nucleus

where it regulates transcription to alter cellular survival, proliferation, and

differentiation. Schematic based off of work detailed in Rosario et al., 2007 [92].

It is generally accepted that many of the phenotypes observed in models of altered Shp2 signaling are a direct result of aberrant pERK levels. By extension, this would suggest that many of the clinical manifestations of diseases such as LS and NS are likewise associated with altered MAPK signaling[107]. LS itself is characterized by a constellation of symptoms such as heart defects and ECG abnormalities including sinus bradycardia—although the ECG anomalies observed are often complicated by structural defects[112, 113]. LS patients can exhibit sudden cardiac arrest associated with ECG anomalies; however, they usually have a complex presentation including hypertrophic cardiomyopathy[114-116].

Indeed, other related disorders (*e.g.* Costello, Cardiofaciocutaneous, Neurofibromatiosis type-1, and Legius syndromes) all share clinical overlap and possibly a common pathogenetic mechanism with LS and NS, thus they have been grouped into the neurocardiofacialcutaneous syndrome family (or the RAS-opathies)[117, 118]. We are not proposing that *Shp2;Periostin-Cre* conditional knock outs (cKOs) are a mouse model for NS, LS or other RAS-opathies. Instead, we are hypothesizing that the arrhythmogenesis observed in some of these patients may be due to abnormal Shp2 function and misregulation of downstream MAPK signaling during sympathetic nervous system innervation of the heart.

Although Shp2 has been shown to signal through several different cascades such as PI3K, MAPK, NFAT, and JAK/Stat[104]; ERK1 and 2 are thought to be

particularly important for mediating aberrant Shp2 phenotypes[119, 120]. This was elegantly demonstrated via the rescue of various *Shp2* gain-of-function phenotypes by decreasing pERK signaling through genetic as well as pharmacologic manipulation[119, 120]. Specifically in sympathetic neurons, Shp2 and downstream activation of ERK have been shown to be required for differentiation (as indicated by neurite outgrowth) *in vitro*[86, 121, 122]. Shp2 and downstream targets such as ERK are extremely important in the context of cardiac development and the mechanism of several human diseases, but our understanding of the direct roles of these signaling molecules *in vivo* is incomplete.

Knocking out Shp2

Due to its pivotal developmental role, systemic *Shp2* deletion results in early embryonic lethality[123, 124]; however, several cKO mouse models have been used to investigate the *in utero* requirement of Shp2 using various Cre drivers. These mouse models, although primarily embryonically lethal, have demonstrated Shp2 can play a role in NC-mediated events such as cardiac outflow track development, septation of the ventricles of the heart, semilunar valvulogenesis[125], craniofacial development, and Schwann cell-mediated myelination of the peripheral nervous system[101, 126] as well as NC-independent events such as limb development[127] and Ca^{2+} oscillations in cardiac fibroblasts[128]. Of particular relevance to the studies herein are the *Shp2* cKO phenotype resulting from *Nestin2-Cre*[30] and the *Erk1/2* cKO phenotype driven by

Advillin-Cre[101]. Both *Nestin2-Cre* and *Advillin-Cre* are expressed in subsets of

NC cells as well as the central nervous system and exhibit postnatal growth

retardation, motility abnormalities, and death by approximately 3 weeks of age.

Additional *in vitro* studies have shown that Shp2 is a key downstream factor in

NGF signaling during sympathetic neuronal differentiation and subsequent

neurite outgrowth[86, 121, 122]. However, the *in vivo* postnatal requirement of Shp2

within NC lineages has remained unclear due to the predominance of

embryonically lethal phenotypes observed in models of Shp2 loss in the NC. Our

work focuses on addressing this gap in knowledge specifically regarding the role

of Shp2 in development of sympathetic innervation of the heart.

Role of Shp2 in myelination

Shp2 signaling is critical for the migration and establishment of Schwann cells

(SCs) and their precursors (SCPs) as well as the ability of those cells to

effectively myelinate the peripheral nervous system. SCPs are derived from NC

cells at approximately E12-13. SCPs then develop into immature SCs (E15-birth

(E20)). Immature SCs adopt one of two fates postnatally: they either associate

with a single large caliber axon and become myelinating SCs or they associate

with many small caliber axons and become non-myelinating SCs as part of a

Remak bundle[129, 130] (Figure 4). Interestingly, SCs can dedifferentiate back to

immature SCs and reenter the cell cycle before undergoing differentiation

again[131]. The level of Neuregulin-1 (Nrg-1; a ligand for the EGFR family of

receptors) type III expressed by the axon appears to be, at least in *in vitro* models, an essential determinant of commitment to a myelinating phenotype[130, 132]. This is achieved through promoting expression of the Schwann cell transcription factors Oct-6 and Krox-20[101, 133].
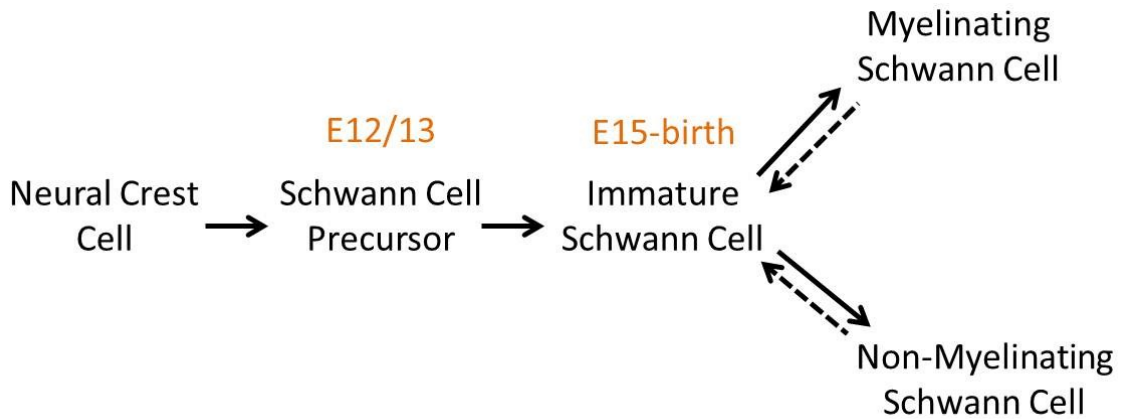
Figure 4. Schematic of Schwann cell development. This schematic illustrates the progression of a NC cell to a SCP, immature SC, and eventually to a myelinating or non-myelinating SC. Developmental time points for presence of each of these stages are indicated in orange. Interestingly, differentiated SCs can dedifferentiate to immature SCs and then redifferentiate as either myelinating or non-myelinating SCs. This is particularly common after nerve injury when the SCs are no longer associated with a particular axon. Adapted from Mirsky et al., 2002[129].

Shp2 is required for Nrg-1 signal transduction through ERK which serves different functions at various developmental time points[101, 126]. When ERK1/2 or Shp2 are deleted early in NC development (E8.5) via *Wnt1-Cre*, no SCPs are present on the axons of peripheral nerves[101, 126]. This thought to be due to the fact that at this stage in development ERK1 and 2 are required to suppress myelin basic protein (MBP) and myelin-associated glycoprotein (MAG) to prevent premature differentiation of glial cells[101]. In the absence of the suppressive effect of pERK1/2, it has been hypothesized that SCPs lose the ability to maintain their progenitor state which could explain their absence in ERK cKOs. There is also evidence that both MAPK and PI3K pathways must be simultaneously activated at E12 to prevent apoptosis in SCPs[134].

Interestingly, when ERK1/2 are deleted in SCPs using the *Dhh-Cre* (expressed at E13) or Shp2 is deleted using the *Krox20-Cre* (expressed E11-P4 depending on the lineage[135]), SCPs are present on peripheral axons, but they do not myelinate[101, 126]. These pups experience tremor and hindlimb paresis within 2 weeks of birth. In the absence of an inducible Cre model or comparison with Cres expressed at different times but with a very similar expression pattern, we cannot conclusively determine the temporal requirements of Shp2 and ERKs; however, these studies indicate that Shp2 is required early in development for SCP survival and presence on the developing peripheral nerves and later in development for myelination.

It has been shown *in vitro* and *in vivo* that Shp2 mutation in SCs impaired

sustained ERK1/2 signaling, but leaves PI3K/AKT activation unchanged[126]. This

result reinforces the idea that certain branches of downstream Shp2 signaling are

more important than others in various contexts. In *in vitro* culture, SCs lacking

Shp2 did not proliferate or migrate in response to Nrg1 indicating that Shp2

signaling through pERK is a key pathway essential for transducing Nrg1 signaling

in SCs[126].

Role of Shp2 in neonatal cardiac innervation

In the present study, we sought to explore the *in vivo* postnatal role of Shp2 and

its downstream effectors within the development and maintenance of cardiac

sympathetic innervation and neurocardiac coupling. We targeted Shp2 using a

Periostin-Cre transgenic line (Figure 5) that uses a partial Periostin gene

promoter to induce expression of Cre recombinase within post-migratory NC

lineages[136]. The resulting phenotype in mice is one of failed sympathetic cardiac

innervation and concomitant bradycardia. Molecular analysis indicated that

downstream phosphorylated-extracellular signal-regulated kinase1/2 (pERK) was

the primary signaling aberrancy within the sympathetic lineage. Further

investigation revealed that genetic restoration of the pERK deficiency via lineage-

specific expression of constitutively active mitogen-activated protein kinase

kinase-1 (caMEK1) was sufficient to rescue the sympathetic innervation deficit

and its physiological consequences. These results demonstrate that Shp2

signaling through pERK is required *in vivo* for the establishment of functional

sympathetic innervation within the postnatal heart. Moreover, these data provide

a mechanistic basis for understanding the lineage-specific aspects of clinical

presentations that can occur in diseases such as LS as well as other ECG

abnormalities resulting from disturbed pERK-dependent sympathetic innervation.
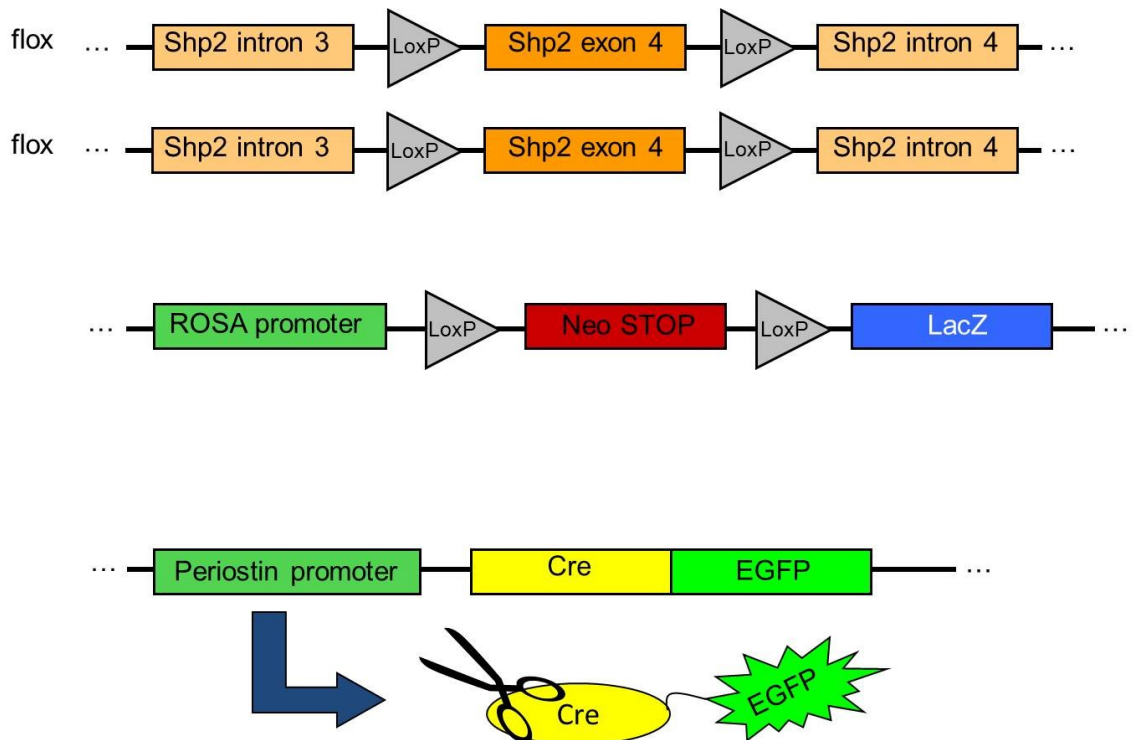
Figure 5. Genetic schematic of Shp2 cKO. Genetic recombination in this model is driven by the *Periostin-Cre* generated in our lab. Essentially, in cells that activate the periostin promoter (mainly post-migratory NC cells), Cre recombinase is expressed. Cre then excises pieces of genomic DNA that are flanked by "LoxP" sites. In our model, all cells which express Cre delete exon 4 of *Shp2* as well as the "stop" preceding the *lacZ* gene. Deletion of exon 4 of Shp2 leads to absence of Shp2 protein expression while deletion of the "stop" allows for β–galactosidase expression from the *lacZ* gene. Because the presence of β–galactosidase can be detected with staining, the ROSA promoter driving expression of the *lacZ* gene serves as our reporter system to identify all cells which express Cre or are derived from cells which expressed Cre.

MATERIALS AND METHODS

Generation of mice

Animal use was in accordance with institutional guidelines, and all experiments were reviewed and approved by the institutional Animal Care and Use Committee. Floxed *Shp2* mice[111] were obtained from G.S. Feng (Uni. of California San Diego) and intercrossed with *Periostin-Cre* [MGI:3775923] mice on a C57BL/6 background to generate lineage-restricted cKO offspring[136] containing a 3.9kb partial *Periostin* promoter that drives Cre expression within the NC-derived peripheral nervous system (including Schwann cells as well as sensory, enteric and sympathetic neurons)[137]. Initial cross was performed by Paige Snider, PhD.

To facilitate lineage mapping, floxed *Shp2;Periostin-Cre* mice were intercrossed with β–galactosidase indicator mice[21]. In order to reconstitute pERK expression within the *Shp2* cKO lineage, the floxed *Shp2;Periostin-Cre* mice were intercrossed with *CAG-caMEK1* mice[138] obtained from M. Krenz (Uni. Missouri-Columbia) which were on a pure FVB/N background. The resulting ♂*CAG-caMEK1Periostin-Cre;Shp2$^{f/+}$*mice were bred to existing ♀*Shp2$^{f/f}$;R26r/R26r* mice which yielded our desired compound mutant experimental genotype: *CAG-caMEK1;Periostin-Cre;Shp2$^{f/f;}$R26r* in the expected Mendelian ratio: 3:16.

To distinguish pups from littermates, their paws were tattooed in the first 5 days of life (Ketchum tattoo kit) to indicate a specific identity for each pup in the litter. This resulted in a permanent ID system with no morbidity noted.

For weight and survival data, pups were monitored and weighed daily. After the initial observation was made that no pups survived past P20 and that weight loss preceded death, weight and gross appearance were carefully monitored as indicators of overall health. As indicated, pups were humanely euthanized prior to lethality.

Genotyping mice lines

The following primer sequences and PCR protocols were used for genotyping from tail clippings and verification of Cre-mediated recombination of floxed *Shp2* locus in isolated sympathetic trunk ganglia and brain DNA via PCR: For tail clip samples, DNA was isolated by Proteinase K digestion followed by ethanol precipitation and extraction. Samples were resuspended in 10mM TRIS-HCl pH 8.5.

For recombination studies, whole bodies of P2 pups were processed for β-galactosidase staining. Following this procedure, sympathetic trunk ganglia (now easily visualized and separated from surrounding tissue) as well as brain tissue were collected. DNA isolation was carried out using the same method utilized for tail clip samples.

Periostin-Cre, sense 5'-ATGTTTAGCTGGCCCAAATG-3', antisense 5'-ACATGGTCCTGCTGGAGTTC-3'; PCR program: (1) 94 °C for 5 minutes, (2) 94 °C for 1 minute, (3) 60 °C for 1 minute, (4) 72 °C for 1 minute, (5) go to (2) and repeat for 33 cycles, (6) 72 °C for 10 minutes. Amplified PCR product: 550 bp. Primers and PCR protocol designed by Paige Snider, PhD[139].

Shp2 flox, sense 5'-ATGGGAGGGACAGTGCAGTG-3', antisense 5'-ACGTCATGATCCGCTGTCAG-3'; PCR program: (1) 94 °C for 3 minutes, (2) 94 °C for 30 seconds, (3) 57 °C for 30 seconds, (4) 72 °C for 1 minute, (5) go to (2) and repeat for 33 cycles, (6) 72 °C for 2 minutes. Amplified PCR product: wild-type 300 bp; flox 400 bp[111].

Shp2 null, sense 5'-TAGGGAATGTGACAAGAAAGCAGTC-3', antisense 5'-AAGAGGAAATAGGAAGCATTGAGGA-3'; PCR program: (1) 94 °C for 5 minutes, (2) 94 °C for 5 minutes, (3) 55 °C for 30 seconds, (4) 72 °C for 1 minute, (5) go to (2) and repeat for 40 cycles, (6) 72 °C for 5 minutes. Amplified PCR product: 350 bp[111].

CAG-caMEK1, sense 5'-TTGATCACAGCAATGCTAACTTTC-3', antisense 5'-GTACCAGCTCGGCGGAGACCAA-3'. PCR program: (1) 94 °C for 2 minutes, (2) 94 °C for 30 seconds, (3) 54 °C for 30 seconds, (4) 72 °C for 30 seconds, (5) go

to (2) and repeat for 30 cycles, (6) 72 °C for 5 minutes. Amplified PCR product: 460 bp. (Primers designed by Maike Krenz, PhD[138]).

Ube1x (gender determination primers), sense 5'-TGGTCTGGACCCAAACGCTGTCCACA-3', antisense 5'-GGCAGCAGCCATCACATAATCCAGATG-3'. PCR program: (1) 94 °C for 1 minute, (2) 98 °C for 15 seconds, (3) 66 °C for 20 seconds, (4) 72 °C for 1 minute, (5) go to (2) and repeat for 34 cycles. Amplified PCR product: male samples give two bands (217 and 198 bp), female samples produce only one band (217 bp)[140].

R26r genotyping was as described[21]. *ROSA*, (1) 5'-AAAGTCGCTCTGAGTTGTTAT-3', (2) 5'-GCGAAGAGTTTGTCCTCAACC-3', (3) 5'-GGAGCGGGAGAAATGGATATG-3'. PCR program: (1) 94 °C for 2 minutes, (2) 94 °C for 30 seconds, (3) 58 °C for 1 minute, (4) 72 °C for 45 seconds, (5) go to (2) and repeat for 33 cycles, (6) 72 °C for 5 minutes. Amplified PCR product: wild-type band 500 bp, mutant band 250 bp.

Histologic analysis, lineage mapping, and molecular marker analysis
Isolation of tissues, fixation, processing, and whole-mount staining for β-galactosidase was performed as described[141]. Prior to molecular analysis, all harvested hearts were morphologically and histologically analyzed as described[141].

Briefly, whole-mount β-galactosidase staining was achieved as follows: mouse pups ranging in age from E14.5-P20 were harvested (at least 3 age-matched littermate cKO and control at each age) and microdissected to enable efficient penetration of 4% paraformaldehyde fixative. Samples were fixed for 1.5 hours at 4 °C. Samples were then rinsed in cold PBS (two rinses for 5 minutes each) followed by 4 rinses of 15 minutes each with β-gal buffer. After final rinse, samples were placed in fresh β-gal buffer and left rocking at 4 °C over night. If any residual blood was present in the wells the next morning, a final wash with β-gal buffer was performed before addition of X-gal (substrate). After addition of X-gal, samples were wrapped in foil and kept at 37 °C for 2-5 days.

For whole-mount antibody analysis, following fixation overnight in 4% paraformaldehyde fixative at 4 °C, micro-dissected hearts were dehydrated at room temperature in increasing concentrations of methanol in 1% PBST, then bleached overnight at room temperature in a 3% H_2O_2 solution, rehydrated, blocked in 2% milk in PBST and DMSO, and then incubated in primary antibody (Tyrosine Hydroxylase; 1:1,000; Millipore) diluted in blocking solution for 3 days at 4 °C. The hearts were thoroughly rinsed in 1% PBST prior to secondary (goat anti-rabbit HRP; 1:200; Jackson Laboratories) application, then following a 3 day incubation at 4 °C were washed in 1% PBST overnight before being developed using DAB kit (Vector Laboratories).

For immunostaining slides were deparaffinized, rehydrated, and then processed using ABC kit (Vectorstain) as described[23]. The following primary antibodies were used: neuron-specific β3Tubulin (NSβT, 1:48,000; Abcam), tyrosine hydroxylase (TH, 1:10,000; Millipore), and TrkA (1:200; Millipore). Cell apoptosis was evaluated using TdT-FragEL[TM] DNA Fragmentation Kit (Calbochem) following manufactures protocol.

In situ hybridization of *Hcn4*, *Phox2a*, *Phox2b*, *Gata3*, *Mash1* and *Sox10* (plasmids[142] provided by P. Cserjesi, Columbia University) was performed by Jian Wang, MS on 10μm serial sections as described[143] using sense and anti-sense S[35]-labeled cRNA probes.

For transmission electron microscopy (TEM), samples were isolated and fixed in 2% paraformaldehyde, 2% gluteraldehyde fixative in 0.1M cacodylate buffer (pH 7.2) overnight, processed by the EM core facility, and imaged on a Phillips400 microscope (via IU EM Core) as described[144].

For all assays, serial sections were analyzed for at least 3 different mice of each genotype and at each developmental age.

Real-Time PCR and Western blot analysis

Total RNA isolated from individual isolated P2, P7 and P14 hearts using the Direct-zol[TM] RNA MiniPrep kit (Zymo Research Corp.). This RNA was reverse-transcribed and qPCR analysis of:

Ngf (Left: TATACTGGCCGCAGTGAGGT; Right: GGACATTGCTATCTGTGTACGG)*,*

β1Adrenergic receptor (Left: CATCATGGGTGTGTTCACG; Right: GGAAAGCCTTCACCACGTT)

A*denylate cyclase-6* (Left: GGGAGAAGGAGGAGATGGAG; Right: GGTCATAGGTGCTGGCATTT), and

Hprt (Left: TGGCCCTCTGTGTGCTCAA; Right: TGATCATTACAGTAGCTCTTCAGTCTGA)

mRNA expression levels were determined as described[145]. qPCR was carried out twice in duplicate (n=2). qPCR studies were done in collaboration with Emily Blue, PhD.

Efficiency of Cre recombination induction for *Shp2;Periostin-Cre* and quantification of Shp2, pERK, pAKT and TH levels were measured by Western in isolated heart/ganglia region, adrenal gland, and brain samples at E14.5, P7, and P14 as described in[145]. Blots were probed with pERK (1:1,000;Cell Signaling); tERK (1:1,000;Cell Signaling); pAKT (1:1,000;Cell Signaling); tAKT (1:1,000;Cell

Signaling); Shp2 (1:1,000;Santa Cruz); TH (1:1,000;Millipore); and normalized to the housekeeping α-tubulin loading control (1:10,000;Sigma). Signal was detected via ECL-plus (Amersham) with peroxidase-conjugated goat anti-rabbit secondary antibody (1:5000; Promega). Densitometric quantification of Western data (n=4-6 samples per genotype/age) was analyzed using the AlphaVIEW SA program.

Electrocardiograms

Using Model F-E2 electrodes (Grass Technologies), ISO-Dam biological amplifier (World Precision Instruments, Inc), and a DAQCardA1-16XE-50 analog-to-digital converter (National Instruments), longitudinal ECG data were collected starting at P4 every other day until death. The mice were anesthetized with isoflurane (~30 seconds for induction at 4 vol% at 2-liter oxygen flow and then maintained during ECG collection at 2% at 2-liter oxygen flow). Following induction, the mice were transferred onto a heat pad where 3 Model F-E2 electrodes (Grass Technologies) were inserted subcutaneously: where the right forelimb meets the trunk, where the left forelimb meets the trunk, and where the right hindlimb meets the trunk, respectively. Pilot studies done in collaboration with Michael Rubart, MD. Dr. Rubart graciously loaned me his ECG equipment to continue these studies.

Isoflurane was chosen as the anesthetic due to its minimal cardiac depression[146]; however, slight cardiac depression is observed over time. The reproducibility of

the electrode placement does affect the amplitude of the ECG trace, but it does not alter time intervals (the parameter of interest).

Data were acquired for ~5 mins, and then the mice were placed back with their mothers to recover. The pups recovered quickly (30 seconds to 1 minute) and resumed normal activity. Clampfit software was used for waveform analysis. ECG collection was done with and without isoproterenol (Sigma; i.p. 2µg/g of body weight[147]) and atropine (Sigma; 1.2µg/g[148]) challenge. For the atropine pharmacological studies, continuous ECG traces were collected for 25-30 minutes after injection in order to document any heart rate alterations as atropine's effects (if any are observed) peak at 20 minutes after injection[148].

Statistical analysis

Densitometric analysis was examined for statistical significance using Student's *t*-test. A P-value < 0.05 was regarded as significant. Error bars indicate standard error of the mean (SEM). Longitudinal heart rate data and isoproterenol challenge data were subjected to a two-way ANOVA followed by a Sidak's test for multiple comparisons. Heart rate data for the three genotypes were tested for significance with a one-way ANOVA followed by Tukey's multiple comparisons test. All statistical tests were performed using GraphPad Prism 6 statistical software.

RESULTS

Establishment of *Shp2* cKO mouse line

Conditional *Shp2* floxed mice containing a floxed exon 4[111] were intercrossed with *Periostin-Cre* transgenic mice to generate embryos that were deficient for Shp2 protein within many post-migratory NC lineages from embryonic day (E) 10 onward. *Periostin-Cre* mice express Cre under the control of a partial 3.9kb *Periostin* promoter (as demonstrated by *R26r* indicator mice[21]) within the peripheral nervous system (including autonomic, sensory, enteric nervous systems as well as glial components such as Schwann cells). Cre is also expressed in the pharyngeal arches, outflow tract of the heart, adrenal glands, endocardial cushion lineages and future valves, but is absent from the central nervous system (brain and spinal cord) as indicated by lineage mapping for all stages investigated[136, 137] (Figure 6). *Periostin-Cre* is also expressed in fetal and neonatal cardiac fibroblasts which are non-NC derived structures [149] but is absent from *in utero* and postnatal cardiomyocytes[149-151].

Homozygous *Shp2* cKO newborns were genotyped via PCR at expected Mendelian inheritance ratios (n=11 litters) and lineage mapping utilizing the *R26r* reporter[21] confirmed Cre-mediated recombination in a pattern suggestive of post-migratory NC lineages beginning at E10 with extensive recombination observable by E11.5 (Figure 6). This result demonstrated that our conditional gene-targeting strategy did disrupt normal Shp2 expression *in utero* but did not cause any gross

embryonic defects and circumvented the *in utero* lethality observed within other

NC-restricted models of Shp2 ablation[103, 123].
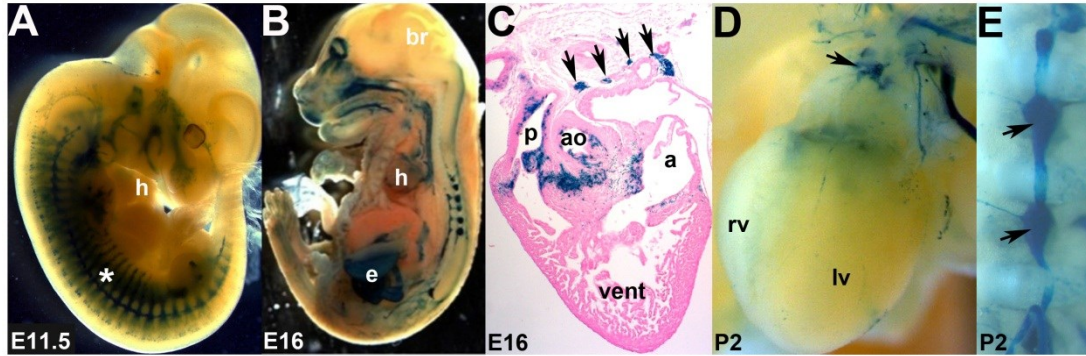
Figure 6. Lineage mapping of *Periostin-Cre* expression via β-galactosidase staining. Lineage mapping of *Periostin-Cre* expression via β-galactosidase staining of E11.5 embryo (A), E16 embryo (B,C) and P2 pup (D,E) demonstrated Cre expression pattern suggestive of post-migratory NC lineages including the craniofacial region, dorsal root ganglia, sympathetic trunk (* in A,B,E), enteric ganglia, and peripheral nerves including those innervating the heart (A-D; arrows in C). [Paige Snider, PhD is responsible for carrying out the initial cross to generate Shp2 cKOs and provided the images for panels A-C]. (Figure adapted from Lajiness et al., 2014).

Validation of molecular model

Lineage-specific recombination was verified in DNA isolated from mutant sympathetic trunk ganglia (Cre-expressing) but not brain (Cre-negative as indicated by *lacZ* expression for all ages of interest in this study) (Figure 7A). Deletion of exon 4 of *Shp2* resulted in decreased Shp2 protein levels in microdissected partial heart/cardiac ganglia samples (Figure 7B) and NC-containing adrenals (Figure 8). These tissues were chosen as they are enriched for *Periostin-Cre*-expressing cells (see Figure 6); however, it is important to remember that neither the partial heart/cardiac ganglia nor adrenal gland is entirely Cre positive so it is unlikely ubiquitous Shp2 would be completely eliminated in these samples.
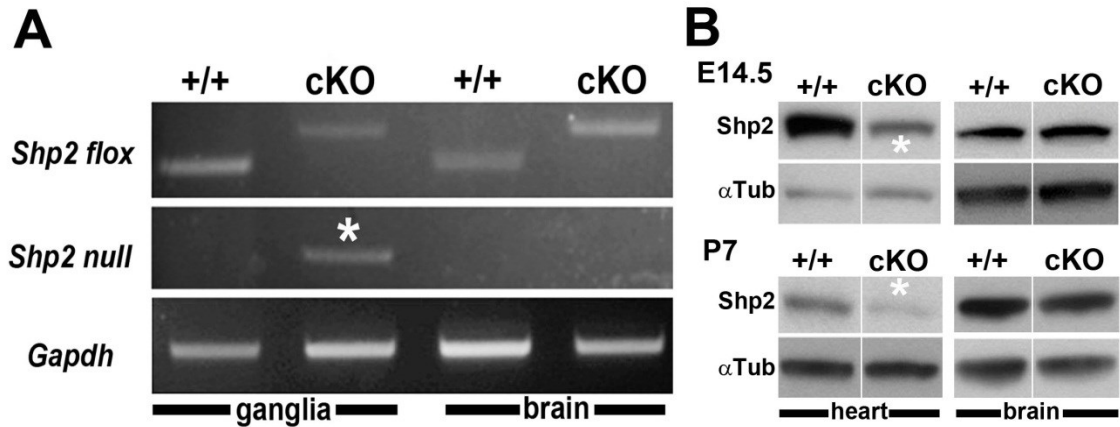
Figure 7. Molecular verification of model. (A) PCR analysis of recombination efficiency demonstrating the lineage-specific nature of *Shp2* knock out. Recombination efficiency was calculated via densitometry to be 78.8% within cKO ganglia (*). **(B)** Composite Western blot of heart and brain isolates confirming the lineage-specific nature of *Shp2* cKO at the protein level. Shp2 levels were decreased in heart (*) but not brain isolates both *in utero* and postnatally. (Figure adapted from Lajiness et al., 2014).
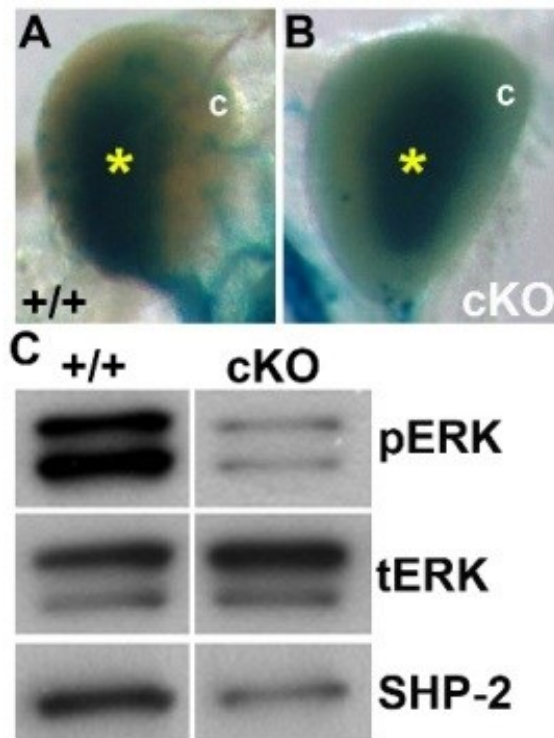
Figure 8. Shp2 and pERK levels are levels are decreased in NC-containing adrenal glands. (A, B) Whole-mount β-galactosidase staining of a *Periostin-Cre* expression in control (A) and mutant (B) P7 adrenal glands illustrating Cre-positive adrenal medulla (*) and Cre-negative cortex (c). **(C)** Composite Western blot illustrating decreased pERK and Shp2 protein levels in whole adrenal isolates, when normalized to total ERK levels (n=3). (Figure from Lajiness et al., 2014).

Shp2 cKOs are indistinguishable from control littermates at birth

Shp2 cKOs were indistinguishable from littermate controls at birth but by the 2nd week of life, the mutants exhibited diminished growth, and none survived past postnatal (P) day 21 (Figure 9). The initial lethality phenotype was found by Paige Snider, PhD and Rachel Young. Since a previously reported *Shp2* cKO model using *Nestin-Cre* exhibited an earlier and more severe phenotype in males[30], we used PCR analysis (using *Zfy* sex determination primers[140]) to determine gender of all neonatal mutants. However, we did not detect any sex-related bias in our model (n=24 cKOs; Figure 10).
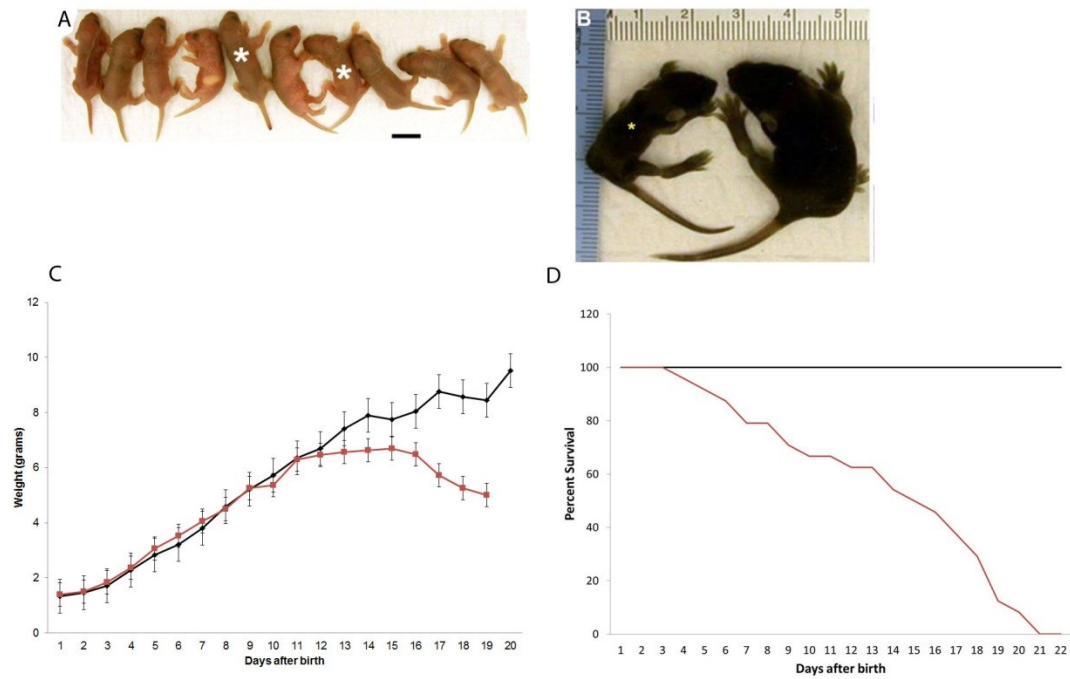
Figure 9. Growth and survival of *Shp2* cKOs. (A,B) Control and mutant (*)

pups at P2 (A) and P9 (B) (mutants indicated by asterisk). **(C)** Longitudinal

growth curve compiled from 7 litters. **(D)** Survival curve (n=24 cKOs). Error bars

indicate SEM. (Panel A adapted from Lajiness et al., 2014).
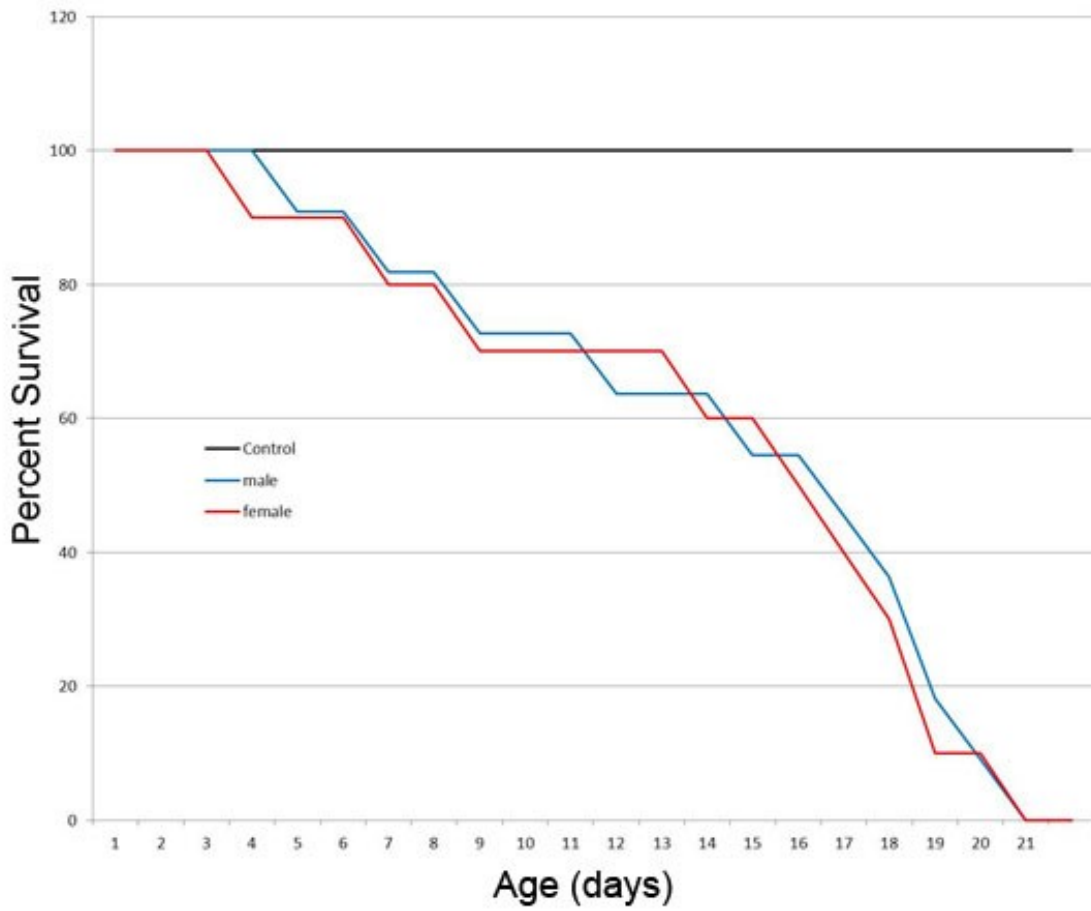
Figure 10. Survival curve of mutants separated by gender. Percent survival

of male and female *Shp2* cKOs over time (n=12).

Necropsy verified normal craniofacial (Figure 11) and cardiovascular development. Similarly, histology and *R26r* reporter analysis revealed that despite Cre expression within the embryonic outflow tract and valves, both outflow tract morphogenesis and valvular maturation were unaffected (Figure 12). However, diminished peripheral and enteric innervation were noted (Figure 13) and are thought to contribute to the failure to thrive and lethality observed in *Shp2* cKOs.
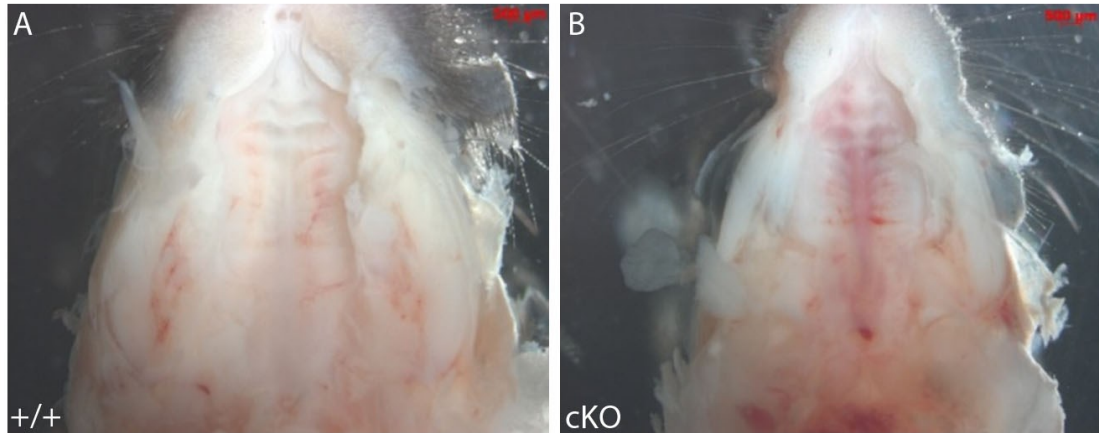
Figure 11. *Shp2* cKOs do not exhibit gross craniofacial malformations.

Gross image of P9 control (A) and mutant (B) hard and soft palates illustrating that no clefting or other gross defects are present (n=3).
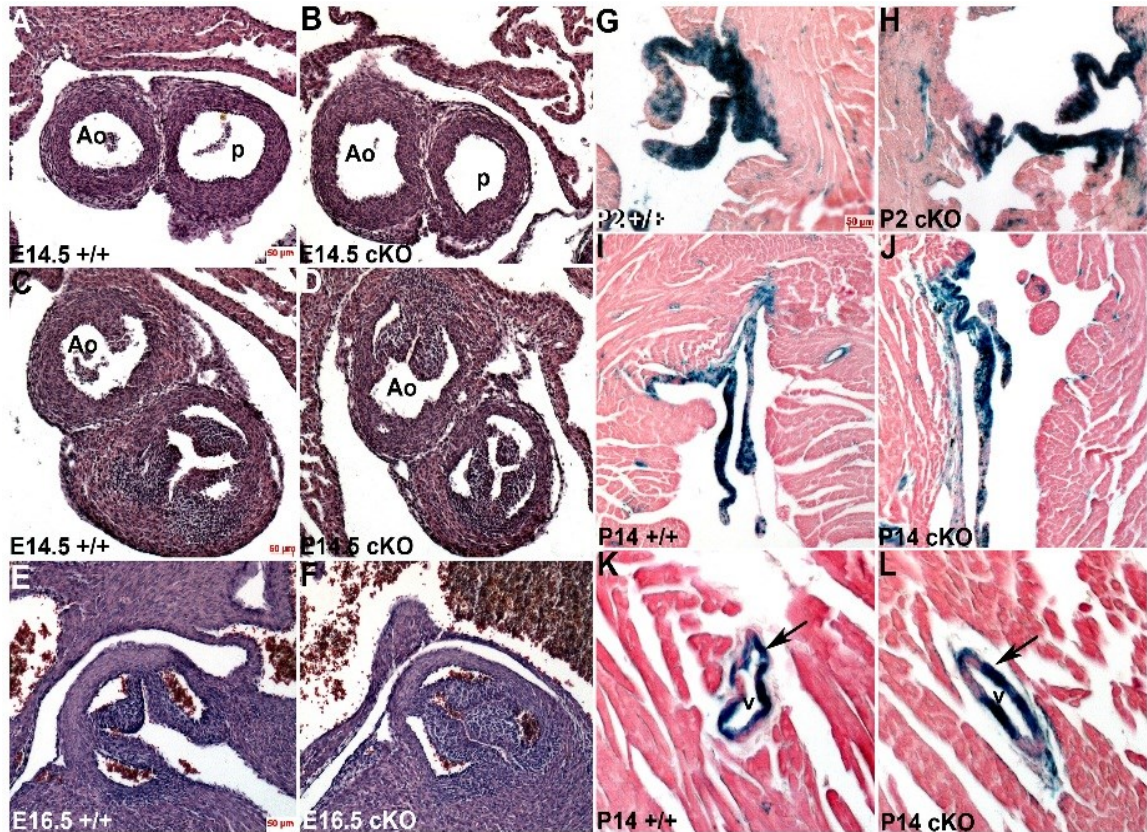
Figure 12. *Shp2* **cKO outflow tract and valves are normal**. **(A-D)** Hematoxylin

and eosin histological staining of transverse sections through the outflow vessels

(A,B) and valvular planes (C,D) of E14.5 wild-type (+/+) and cKO outflow tracts.

Note that both are normally septated and that the orientation of the separate

aorta (Ao) and pulmonary (p) trunks is similar. Additionally, the aortic and

pulmonary valve leaflets are positioned appropriately and of similar thickness.

(E,F) Histology of E16.5 wild-type and cKO fully formed aortic valves reveals

comparable maturation. **(G-J)** Lineage mapping of *Periostin-Cre* expression via

β-galactosidase staining and eosin counterstaining in histological sections

revealed morphologically normal aortic/pulmonic (G,H) and mitral/tricuspid (I,J)

valves in both the P14 mutant and littermate control despite Cre expression from

E10 onward. **(K,L)** Similarly, histology demonstrated normal architecture of

vascular smooth muscle cells within the myocardium of P14 *Shp2* cKOs. Scale bar in A-F and G-L is 50µm. (Figure adapted from Lajiness et al., 2014).
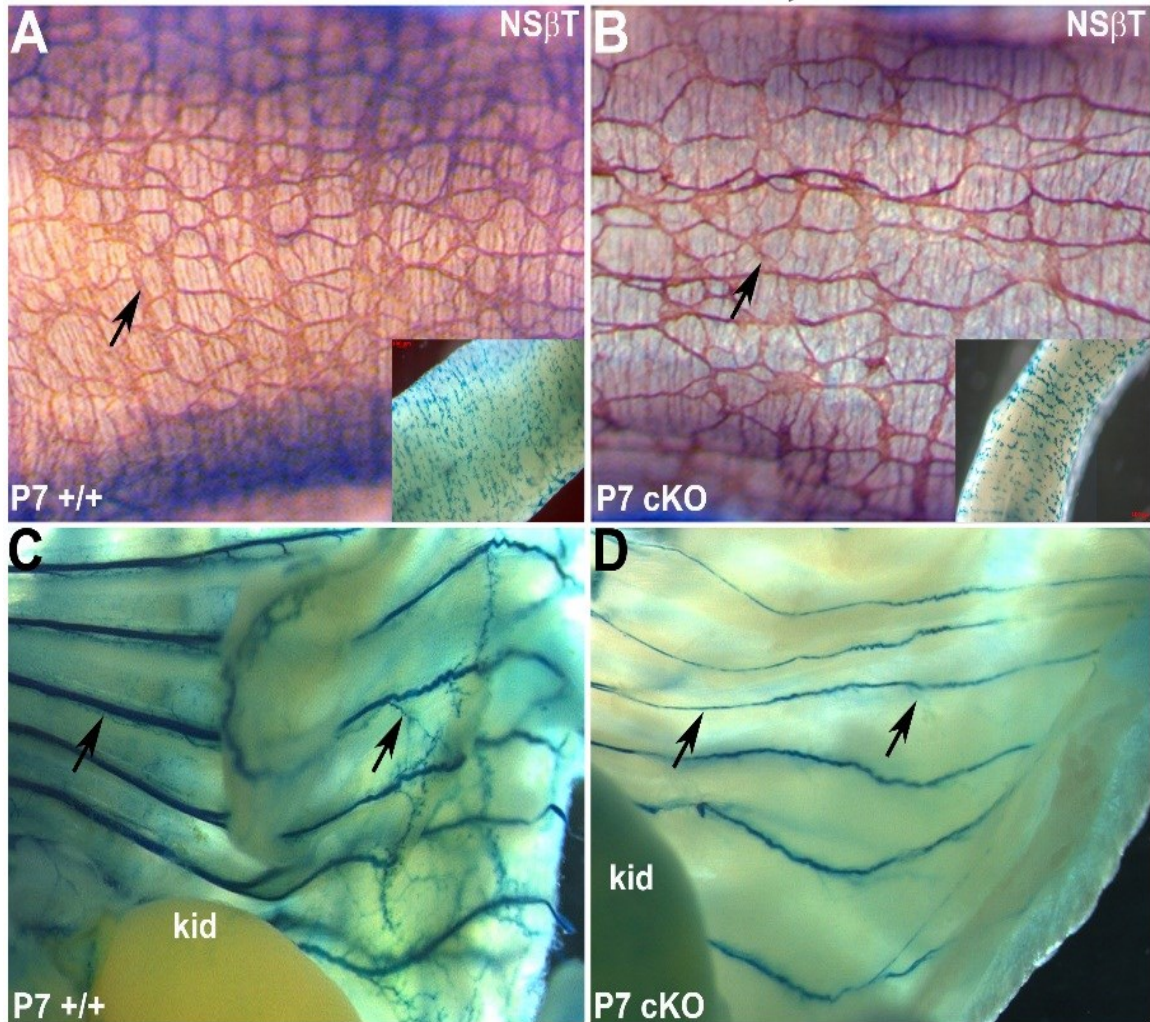
Figure 13. *Shp2* cKO enteric and peripheral nervous systems are diminished. (A,B) Postnatal day 7 guts were immunostained with neuron specific β3 tubulin (NSβT) antibody to detect the enteric nervous system embedded in the lining of the gastrointestinal tract. Note that the cKOs exhibit diminished enteric innervation (B) compared to wild-type control littermate (A). Insets are whole-mount *R26r* lineage mapping of *Periostin-Cre* in wild-type and cKO P7 GIs, verifying a paucity of enteric NC within the cKO GI. **(C,D)** Similarly, whole-mount β-galactosidase staining of control (C) and mutant (D) ribcages revealing diminished peripheral innervation in cKOs compared to littermate

controls. Thus, the observed failure to thrive and subsequent lethality observed in

this model is most likely multifactorial, and in conjunction with the diminished

sympathetic cardiac innervation and concomitant bradycardia, the diminished

peripheral and enteric innervation are most likely contributing factors to the

eventual lethality observed. (Figure adapted from Lajiness et al., 2014).

Shp2 cKOs exhibit abnormal peripheral innervation

To further investigate the diminished peripheral innervation observed and determine its relationship to the failure to thrive phenotype, the pups were observed for behavioral abnormalities and necropsies were performed immediately after death or at time of harvest. Necropsies often revealed present but decreased milk in the digestive tract of mutants as early as P6 in severe cases. This was frequently accompanied by air in the bowel. Culling littermates to reduce litter size did not affect mutant longevity nor necropsy results which indicate that mutant pups not only have trouble outcompeting littermates for food, but may also have difficulty ingesting food regardless of competition. Since peripheral innervation was suspected to be less robust due to the lineage mapping results (see Figure 13), innervation of the tongue was examined in mutants and controls via immunohistochemistry. This preliminary study revealed diminished overall innervation (both motor and sensory) to the tongue which may contribute to the failure of pups to access food (Figure 14).
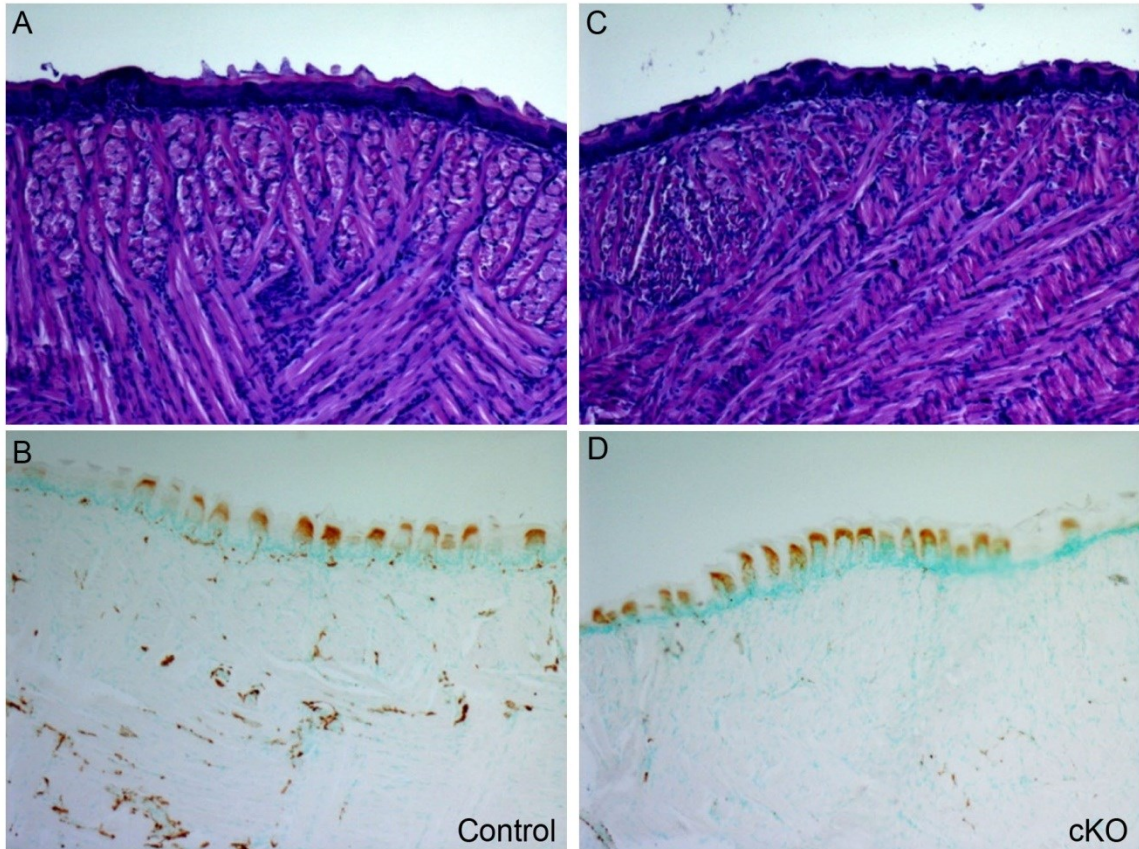
Figure 14. Abnormal innervation observed in *Shp2* cKOs. (A) H&E stained section of a P6 control tongue. **(B)** NSβT IHC of an adjacent slide. **(C)** H&E stained section of a P6 mutant tongue. **(D)** NSβT IHC of an adjacent slide. Notice the lack of innervation in the *Shp2* cKO tongue (n=2). As NSβT is a generic neuronal marker this study indicates an overall paucity of innervation. The innervation of the tongue includes sensory innervation which is a branch of the trigeminal nerve (cranial nerve V) for the anterior 2/3rds of the tongue and the glossopharyngeal nerve (cranial nerve IX) in the posterior 1/3rd; motor which is from the hypoglossal nerve (cranial nerve XII); and taste (gustatory neurons innervating the taste buds) which is from the facial nerve (cranial nerve VII) in the anterior 2/3[rds] of the tongue and the glossopharyngeal in the posterior 1/3rd of the tongue[152]. The complexity of the innervation present in the tongue makes

delineating specific contributions with NSβT IHC impossible, but the overall

diminished innervation indicates that there are, most likely, deficiencies in

multiple sources of innervation.

Postnatally, *Shp2* cKOs exhibit diminished neurite outgrowth from cardiac sympathetic ganglia

To investigate the NC-specific effects of *Shp2* KO in post-migratory NC lineages, we carried out lineage mapping using the *lacZ* reporter system[21]. The largest collection of the heart's sympathetic innervation is located on the dorsal surface of the heart, and there we observed significantly diminished neurite outgrowth from cKO TH-positive cardiac ganglia at both P2 and P14 (Figure 15). Whole-mount spatiotemporal analysis of β–galactosidase expression revealed that cardiac sympathetic ganglia in *Shp2* cKO mice have fewer projections and that the neurites that are present are less robust (Figure 15A,B,G,H) than those observed in age-matched littermate controls (Figure 15D,E,J,K). In the *Shp2* cKO mice the ganglia themselves, however, do not appear grossly atrophic or morphologically compromised. Detailed histology revealed typical neuronal architecture, namely, large dense nucleus with wavy axonal projections emanating from both the control (Figure 15 F,L) as well as the ganglia in the *Shp2* cKOs (Figure 15C,I).
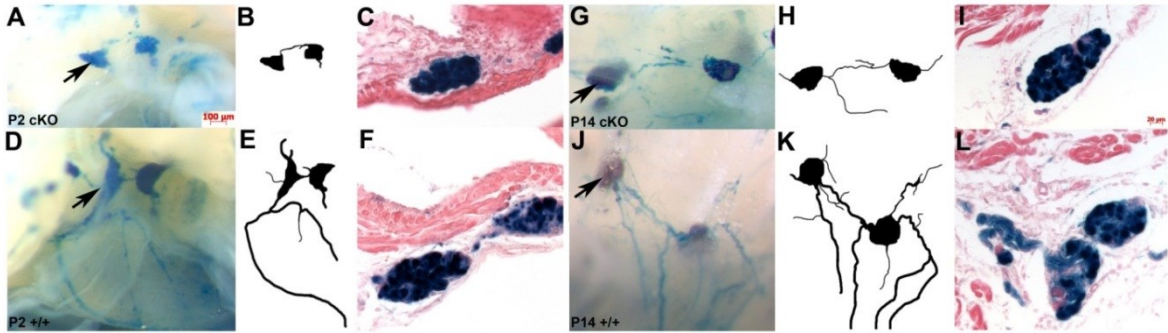
Figure 15. *Shp2* **cKOs exhibit diminished neurite outgrowth from cardiac ganglia. (A-C)** P2 *Shp2* cKO cardiac ganglia (arrows): whole-mount β-galactosidase staining (A), black and white reconstruction trace of surface neurite outgrowth (B), and histological section of β-galactosidase stained ganglia counterstained with eosin (C). **(D-F)** Same sequence of littermate P2 control. **(G-L)** Same sequence of P14 mutant (G-I) and littermate P14 control (J-L). Note both P2 and P14 cKOs exhibit reduced neurite outgrowth. Scale bar in A is 100μm and also applies to images in D,G, and J; scale bar in C is 20μm and also applies to the images in F,I, and L. (Figure adapted from Lajiness et al., 2014).

Decreased sympathetic innervation is observed in *Shp2* cKO hearts

In light of the decreased neurite outgrowth despite the normal gross anatomical appearance of the ganglia, molecular characterization of *Shp2* cKO cardiac ganglia utilizing immunohistochemistry techniques was conducted. Despite the *in utero* loss of Shp2, the ganglia of E14.5 *Shp2* cKOs consistently express neuron-specific NSβT, TrkA (the high-affinity receptor of NGF, required for sympathetic neuron survival) and the sympathetic neuronal marker TH (Figure 16A-C). A similar pattern was observed in the ganglia of the E16.5 *Shp2* cKOs (Figure 17). However, postnatally the expression of TH in ganglia from *Shp2* cKOs is diminished at all ages investigated (P7 (Figure 16F); P0, P6, P18 (Figure 17)) while NSβT and TrkA remain unaltered (Figure 16D,E). Moreover, the ganglia in postnatal Shp2 cKOs are similar in size and cellularity to ganglia in controls, and TUNEL staining did not detect any apoptotic cells (Figure 16G).
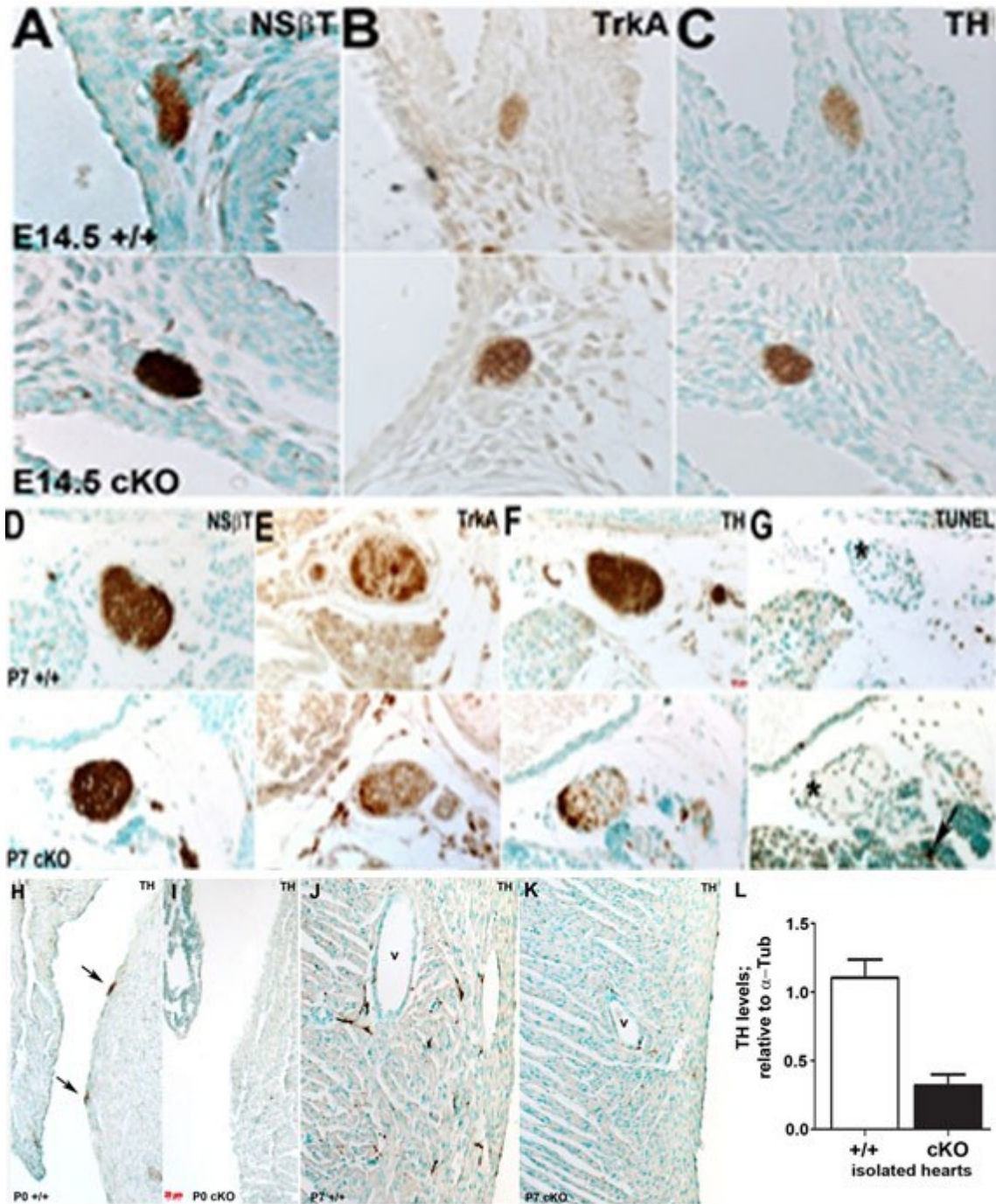
Figure 16. *Shp2* **cKOs demonstrate diminished cardiac sympathetic**

innervation. (A-C) Immunohistochemistry (IHC) demonstrating equivalent NSβT

(A), the NGF receptor TrkA (B), and TH (C) expression in E14.5 littermate pairs

of controls (top) and mutant (bottom)ganglia. **(D-G)** Adjacent sections of P7

ganglia (control, top panel; mutant: lower panel) examined using IHC NSβT (D),

TrkA (E), TH (F), and apoptosis (TUNEL; G). Note that P7 *Shp2* cKO ganglia

exhibited diminished TH expression but are not apoptotic. However, apoptotic

cells are seen in adjacent tissue (arrow in cKO G; n=3 littermate pairs with 2

slides containing 4-5 sections of tissue each analyzed). **(H,I)** IHC detection of

TH-positive nerves on the left ventricle of a P0 control (H) and mutant (I). **(J,K)**

TH IHC of P7 ventricle of a control (J) and mutant (K). Note the lack of

sympathetic innervation in the mutant heart at both ages, but normal surface

(arrows, H) and penetrating (J) TH-positive nerves around blood vessel (v) in

wild-types. **(L)** Densitometry quantification of TH protein levels as detected by

Western within isolated P14 hearts (n=5). *Shp2* cKO TH levels relative to loading

control (α-tubulin) were significantly decreased (*t*-test; p-value=0.0010). Error

bars represent SEM. (Figure adapted from Lajiness et al., 2014).
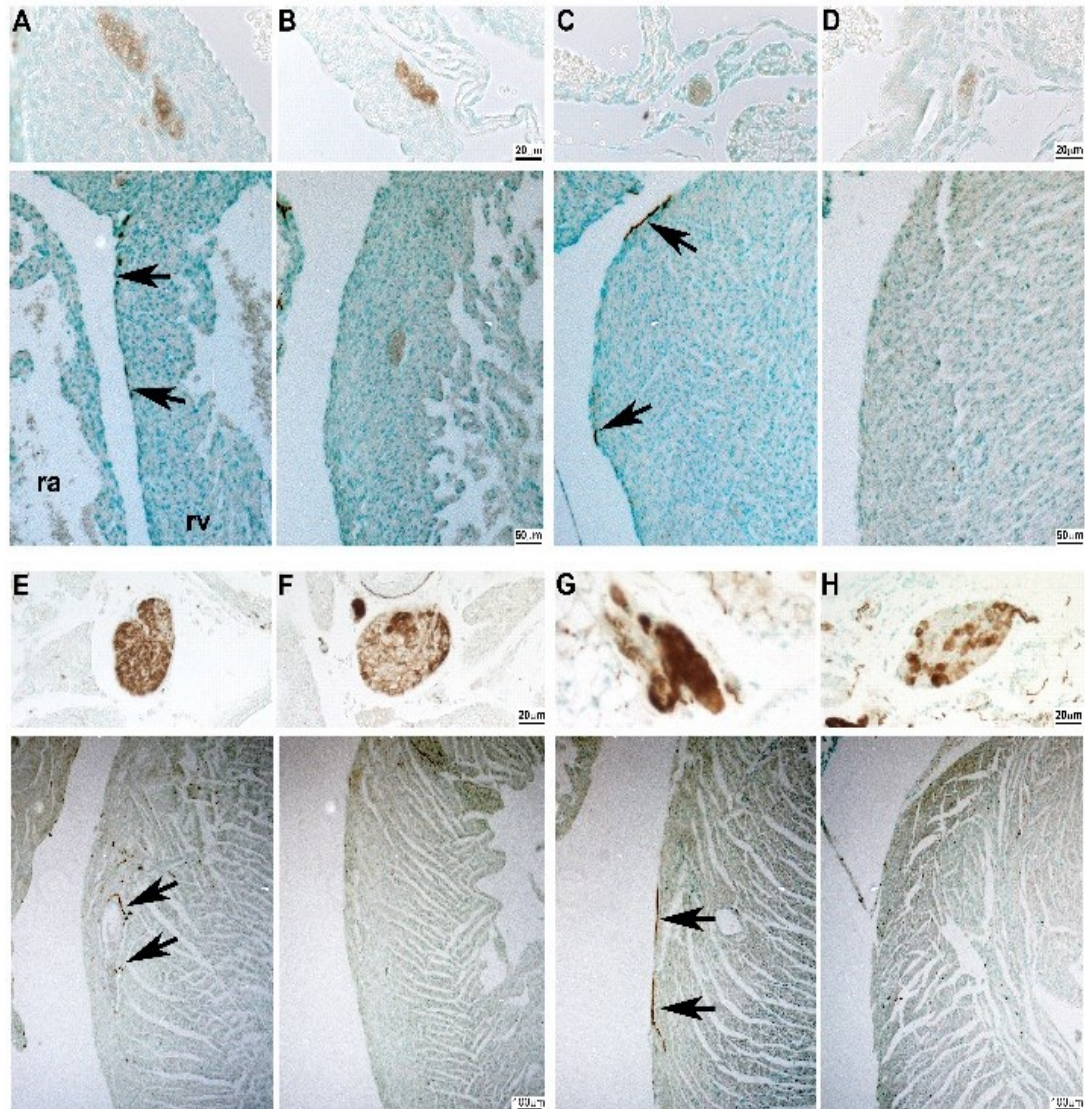
Figure 17. Temporal analysis of TH expression within cardiac ganglia and during cardiac innervation. Longitudinal sympathetic innervation of *Shp2* cKOs. **(A,B)** TH IHC detection of cardiac ganglia (upper panels) and sympathetic innervation of the ventricles (indicated via arrows in lower panels) of E16.5 hearts. Note both control (A) and cKO (B) cardiac ganglia appear to have normal TH expression, but there is diminished sympathetic innervation in the ventricle of the *Shp2* cKO. **(C,D)** P0 cKO cardiac ganglia (C) exhibit diminished TH expression compared to control (D), and there is decreased sympathetic cardiac

innervation evident in the *Shp2* cKO ventricles. **(E,F)** TH expression is diminished within P6 cKO cardiac ganglia and there is reduced sympathetic innervation (F) compared to wild-type littermate control (E). **(G,H)** TH IHC of cardiac ganglia and ventricle of a control (G) and mutant (H) at age P18. Note, that although the *Shp2* cKO ganglia are similar in size to controls, that the mutant ganglia have decreased TH expression only during postnatal stages. However, the mutant ventricles exhibit diminished TH-marked innervation at all ages examined. Scales bar in all upper panels is 20μm, A-D lower panels is 50μm and E-H lower panels is 100μm. (Figure adapted from Lajiness et al., 2014).

Significantly, global cardiac sympathetic innervation of the *Shp2* cKO was compromised. At day 0, nodules of TH-positive innervation is observed in control (arrows; Figure 16H) but not in *Shp2* cKO hearts (Figure 16I) and by P7 the mutant has substantially decreased TH-positive innervation (Figure 16J, K), particularly around the blood vessels supplying the ventricles (where sympathetic innervation is most pronounced in the control). Diminished TH-positive innervation was also observed in E16.5, P6, and P18 *Shp2* cKO hearts (Figure 17). Interestingly, despite diminished global cardiac sympathetic innervation, the epicardial-to-endocardial gradient was present in both controls and *Shp2* cKOs (Figure 18).To further validate diminished TH expression in the heart of *Shp2* cKOs, Western analysis performed on microdissected heart/ganglia regions confirmed that TH levels were decreased by 70% in Shp2 cKO hearts versus hearts of control littermates (Figure 16L).
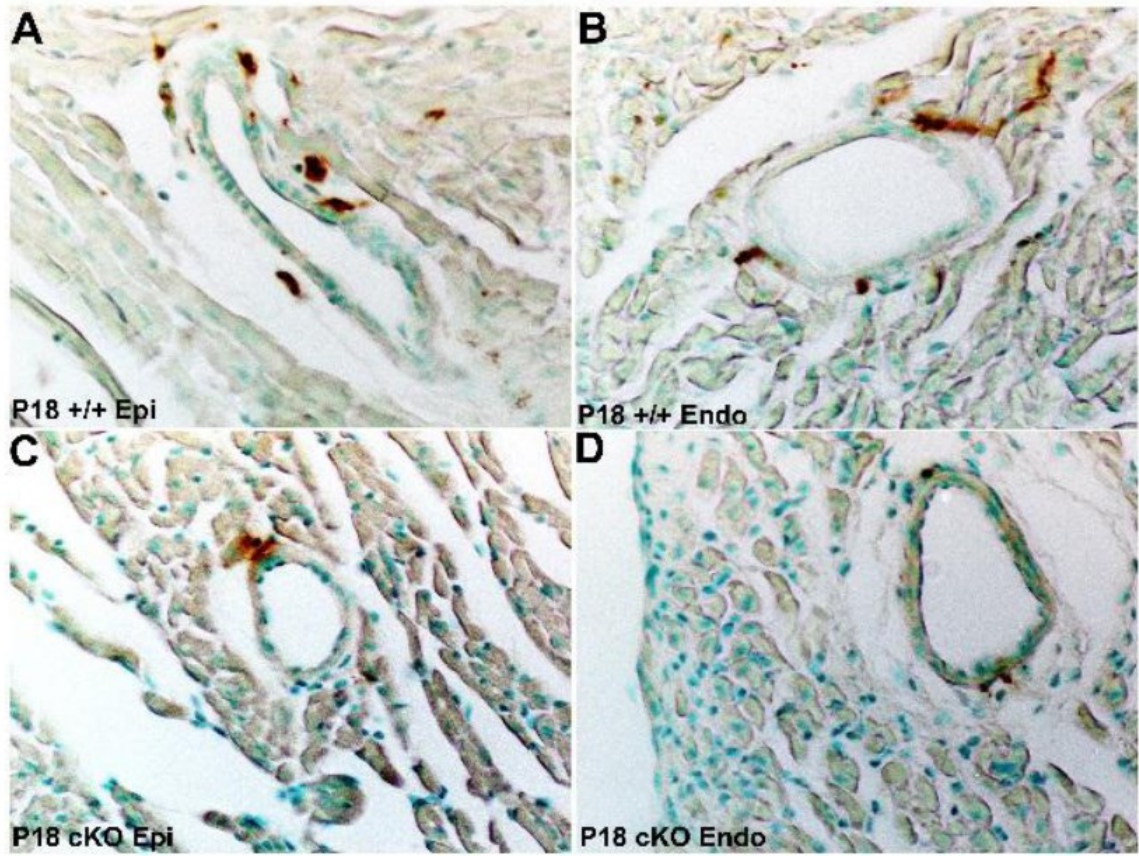
Figure 18. Although sympathetic innervation is globally decreased in cKOs, the epicardial-to-endocardial innervation gradient is preserved. (A,B) Tyrosine hydroxylase IHC of P18 littermate control showing sympathetic innervation surrounding a blood vessel in the subepicardial (A) as well as the subendocardial (B) region of the myocardium. **(C,D)** TH IHC of P18 cKO showing sympathetic innervation surrounding a blood vessel in the subepicardial (C) as well as the subendocardial (D) region of the myocardium. Note that there is less pronounced sympathetic innervation in the endocardial region of both control and *Shp2* cKO hearts when compared to their respective epicardial region (n=4-5 of each genotype). (Figure adapted from Lajiness et al., 2014).

Radioactive *in situ* hybridization was used to examine whether the ganglia of *Shp2* cKOs aberrantly express markers of early embryonic sympathetic neuronal differentiation. Both *Phox2a* and *Phox2b* mRNA were expressed in *Shp2* cKO but not control ganglia (Figure 19). Additional embryonically expressed sympathetic neuronal differentiation factors (*Gata3, Sox10,* and *Mash1*) were also investigated but found to be negative in both controls and mutants. *In situ* hybridization studies performed by Jian Wang, MS.
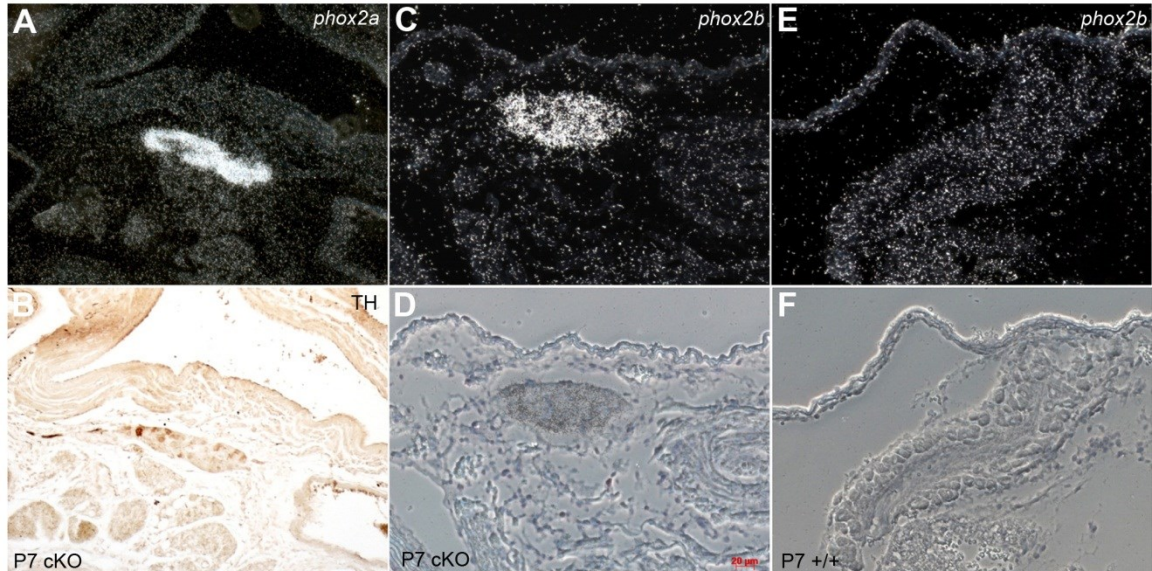
Figure 19. Postnatal *Shp2* cKOs aberrantly express the embryonic sympathetic neuronal differentiation markers *Phox2a* and *Phox2b*. (A,B) *In situ* hybridization of mutant cardiac ganglia showing aberrant expression of *Phox2a* (embryonic sympathetic neuronal differentiation marker; A) in the context of diminished TH expression (B). **(C,D)** *In situ* hybridization of mutant cardiac ganglia showing aberrant expression of *Phox2b* (embryonic sympathetic neuronal differentiation marker; C). Lower panel is a phase contrast image of the ganglia itself (D). **(E,F)** Representative *in situ* hybridization of control cardiac ganglia showing no expression of *Phox2b* (E). Lower panel is a phase contrast image of the ganglia (F). [Radioactive *in situ* data provided by Jian Wang]. (Figure adapted from Lajiness et al., 2014).

***Shp2* cKOs experience sinus bradycardia**

To investigate whether the observed Shp2-dependent innervation defect has any functional impact, longitudinal ECG analysis was carried out from P4 to P20, with readings taken every other day. These studies revealed that the *Shp2* cKOs exhibit sinus bradycardia (slow heart rate with normal P-wave present; two-way ANOVA, P=0.0012; Figure 20A,B) beginning at P12, corresponding to the developmental timing of sympathetic control of heart rate[53, 77]. At P6, before the sympathetic nervous system is thought to be functionally relevant for establishing basal heart rate, there is no difference in heart rate between *Shp2* cKOs and littermate controls (Figure 20A,B). However, by P12 the heart rate of the control pups significantly increased (the increase is associated with establishment of sympathetic control of heart rate) while the heart rate of *Shp2* cKOs did not show a corresponding increase (Figure 20A,B). There was no increase in the average heart rate of the control littermates from P12 to P17 (average heart rate of 501 and 506 bpm respectively). Similarly, there was no appreciable change in the average heart rate of *Shp2* cKOs between P12 and P17 although there was a slight trend toward decreasing heart rates over time (average heart rates of 460 and 414 respectively) (Figure 20A,B).
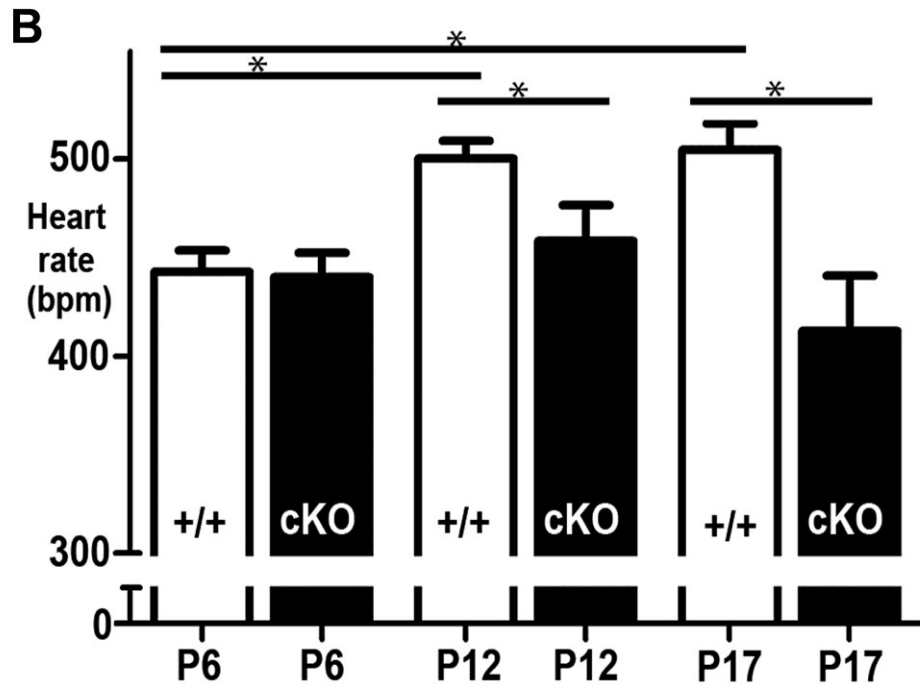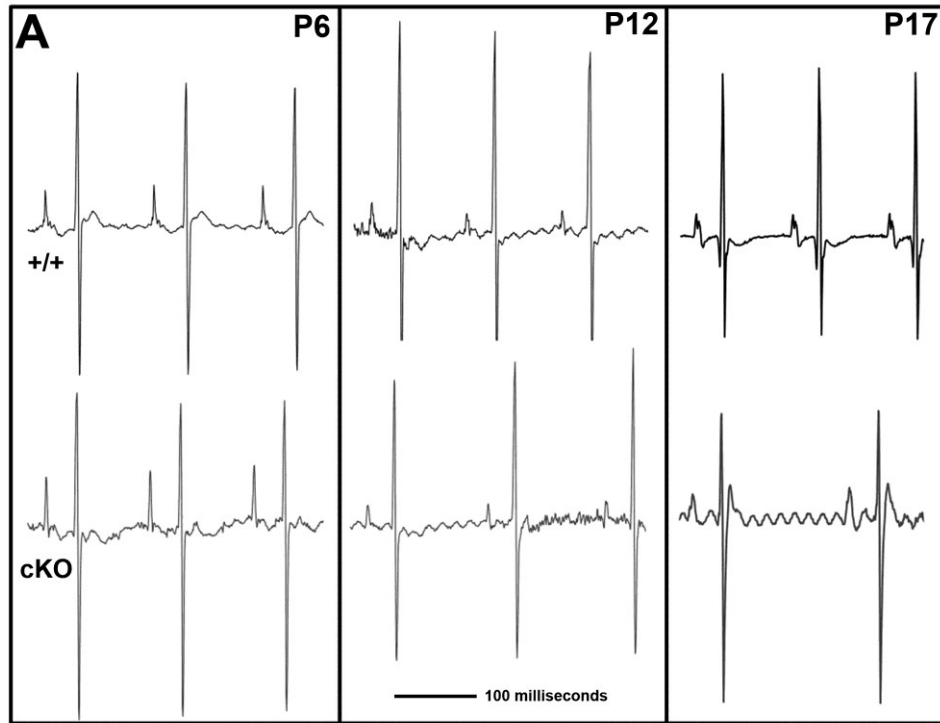
Figure 20. *Shp2* mutants exhibit progressive sinus bradycardia. (A)

Characteristic ECG traces from a wild-type littermate control and a *Shp2* cKO at

three different ages (P6, before sympathetic innervation is functionally relevant to

heart rate; P12, once sympathetic innervation is functionally established; and

P17, demonstrating the continual decline of heart rate as the phenotype

progresses) are shown. **(B)** Graphic representation of average heart rates

collected at the three ages in (A). The heart rate of control animals increased

over time from P6 to P12 and then plateaued while the *Shp2* cKO heart rate

never significantly changed (2-way ANOVA, Sidak's multiple comparisons

Control: P6vsP12 $p<0.05$, P6vsP17$p<0.05$, P12vs17=non-significant ($p>0.05$)

Shp2 cKO: none of the comparisons of any of the different time points were

significant; Control vs. *Shp2* cKO at a single time point: P6 non-significant, P12

$p<0.05$, P17 $p<0.05$ (n=7-19)). Error bars represent SEM. (Figure adapted from

Lajiness et al., 2014).

No other arrhythmias or anomalies in the ECG wave form (P-wave duration, PR, or QRS intervals) were observed throughout the study with the exception of a mild prolongation of the PR interval immediately preceding death (Table 1). However the first degree heart block (the clinical name for prolonged PR interval) never progressed to second degree heart block or initiated any arrhythmias. Furthermore, this finding may be complicated by other issues such as the weight loss that was observed in the final 24 hours of life. QT intervals were also examined, but the absence of a definitive T wave in many traces negated the utility of such an investigation.

Table 1. Longitudinal ECG functional data. Other than sinus bradycardia, no anomalies in the ECG wave form of *Shp2* cKOs were observed. Table 1 includes heart rate (HR, beats per minute), P-wave duration (in milliseconds), PR interval (in milliseconds), and QRS interval (in milliseconds) data collected from control and *Shp2* cKO littermates longitudinally (n=7-19). Bolded entries indicate significant differences (p-value<0.05) between control and *Shp2* cKO values at that time point. (Table from Lajiness et al., 2014).

	HR (BPM)	P (ms)	PR (ms)	QRS (ms)
P6 Control	443.84±10.9	11.57±0.48	40.18±2.05	12.88±0.42
P6 Mutant	441.26±12.26	12.41±0.83	43.67±1.14	12.92±0.71
P12 Control	501.34±8.93	11.01±0.43	32.2±0.42	10.21±0.26
P12 Mutant	**459.54±18.11**	10.82±0.58	33.48±0.61	10.65±0.22
P17 Control	505.56±13.36	10.43±0.31	30.16±0.39	9.88±0.19
P17 Mutant	**413.97±27.99**	10.34±0.32	**34.76±1.24**	10.72±0.24

To examine the underlying cause of the sinus bradycardia, several pharmacological interventions were employed. Due to the diminished sympathetic innervation observed in the cKO heart (see Figures 16 and 17) we hypothesized that the lack of adrenergic stimulation was directly responsible for the observed phenotype. To test this hypothesis, we directly activated the β-adrenergic receptors (the receptors that would normally be stimulated by sympathetic neuron release of norepinephrine) by administering an *i.p.* injection of the β1- and β2-adrenoreceptor agonist, isoproterenol. Isoproterenol increased the heart rate in both the control and *Shp2* cKOs by 30% with respect to their basal heart rates (Figure 21). Moreover, the relative increase is consistent with the results reported from isoproterenol challenge tests carried out in adult mice[147] and confirms that the *Shp2* cKO cardiomyocytes are capable of responding to adrenergic stimulation. In contrast, inhibiting parasympathetic activity with atropine had no significant effect on the heart rate of either *Shp2* cKO or littermate controls (Figure 22). This was not particularly surprising due to the fact that the parasympathetic influence on murine heart rate is often minimal and subject to change on differing genetic backgrounds[153, 154].
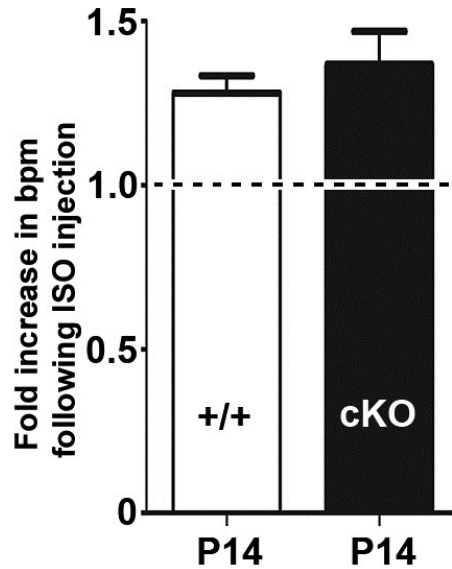
Figure 21. Isoproterenol increases heart rate in both control and *Shp2* cKOs. Graphic representation of heart rate increase (normalized to basal heart rate, indicated by dotted line) following *i.p.* injection of isoproterenol (2mg/kg body weight). Both mutant and control heart rates increased with isoproterenol administration (paired *t*-test; p=0.003); however, the genotype of the animal did not affect the degree to which the heart rate was elevated (2-way ANOVA interaction (genotype x treatment): p=0.905, (n=4-6)). Error bars represent SEM. (Figure adapted from Lajiness et al., 2014).
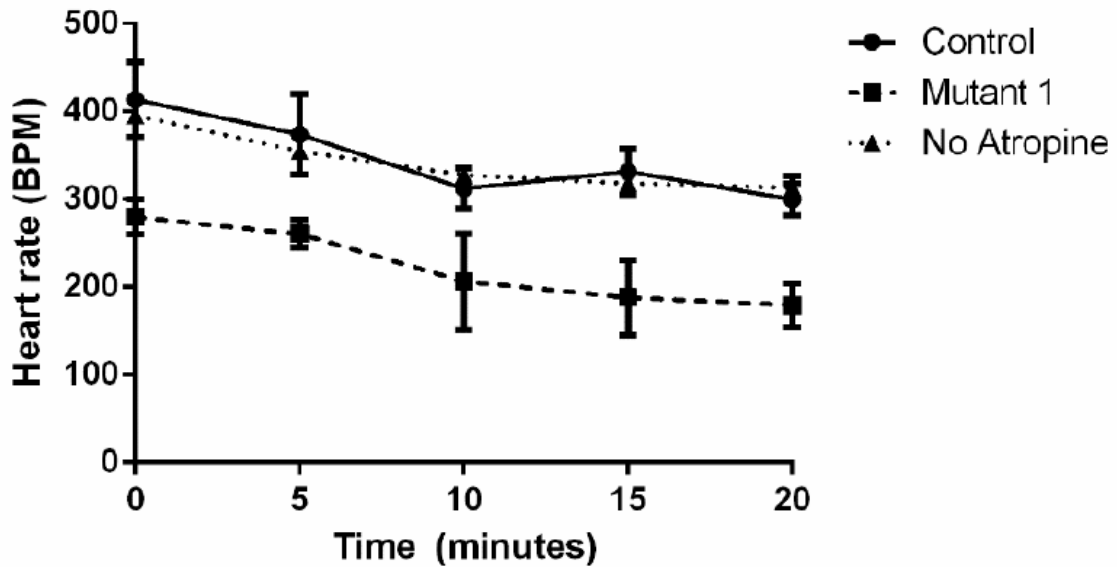
Figure 22. *Shp2* **cKO parasympathetic activity is unaffected**. Line graph depicting the longitudinal effect of atropine. The slight cardiodepressive trend over time is due to prolonged exposure to isoflurane as indicated by the "No Atropine" control. The effects of atropine are negligible in both the control and mutant indicating that elevated parasympathetic tone is not responsible for the slower heart rate in mutants (n=2-3 for each condition and genotype). (Figure adapted from Lajiness et al., 2014).

To exclude the possibility that the β-adrenergic receptors or their downstream

signaling effectors were misexpressed in *Shp2* cKOs, qPCR was used to

measure the levels of mRNAs encoding the *β1-adrenergic receptor* (the primary

adrenergic receptor expressed in the heart) as well as *adenylate cyclase-6* (the

enzyme that produces cAMP as a second messenger to propagate the

adrenergic signal). Levels of both targets were found to be equally expressed in

the hearts of P14 *Shp2* cKO as well as littermate controls (Figure 23). This result

corroborates findings reported in other models of NGF signaling alterations[155].

Furthermore, heart *Ngf* levels, (as quantified via qPCR) were found to be the

same between *Shp2* cKOs and controls for all ages investigated (Figure 24). This

was expected as regulation of NGF synthesis throughout development is

independent of sympathetic innervation or norepinephrine secretion at the target

organ[156]. Taken together, these data suggest that the diminished cardiac

innervation does not affect the induction of neurotrophic factors within the heart.
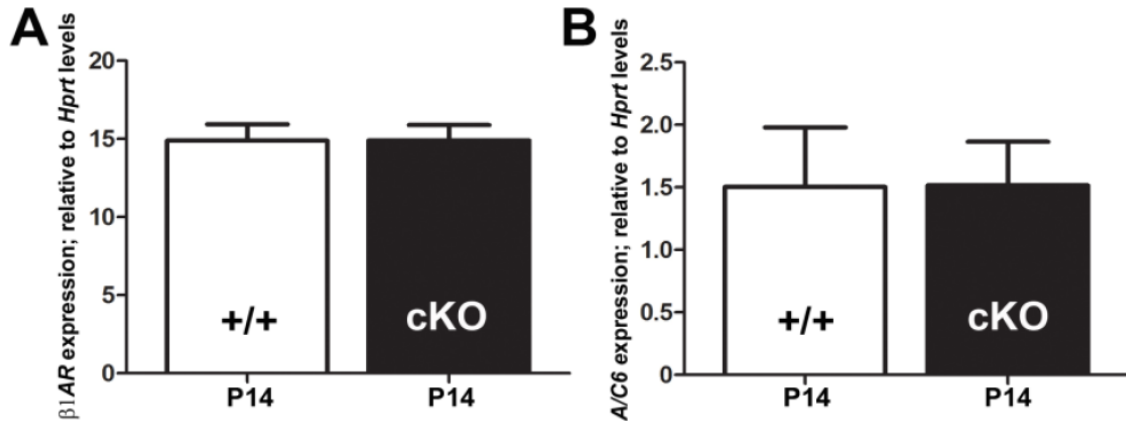
Figure 23. *Shp2* **cKO hearts exhibit normal expression of** *β1-adrenergic*

receptor **and** *adenylate cyclase-6* **mRNA. (A)** qPCR analysis of *β1-adrenergic*

receptor (*β1AR*) mRNA levels normalized to *Hprt* cDNA synthesis and loading

control, within P14 control and *Shp2* cKO isolated hearts demonstrating

equivalent expression levels (n=2). **(B)** qPCR analysis of *adenylate cyclase-6*

(*A/C6)* mRNA levels normalized to *Hprt* housekeeping control. Note that although

A/C6 expression levels are lower than *β1AR,* they are also similar in control and

Shp2 cKO isolated P14 hearts (n=2). Error bars represent SEM. [qPCR

experiments done in collaboration with Emily Blue, PhD]. (Figure adapted from

Lajiness et al., 2014).
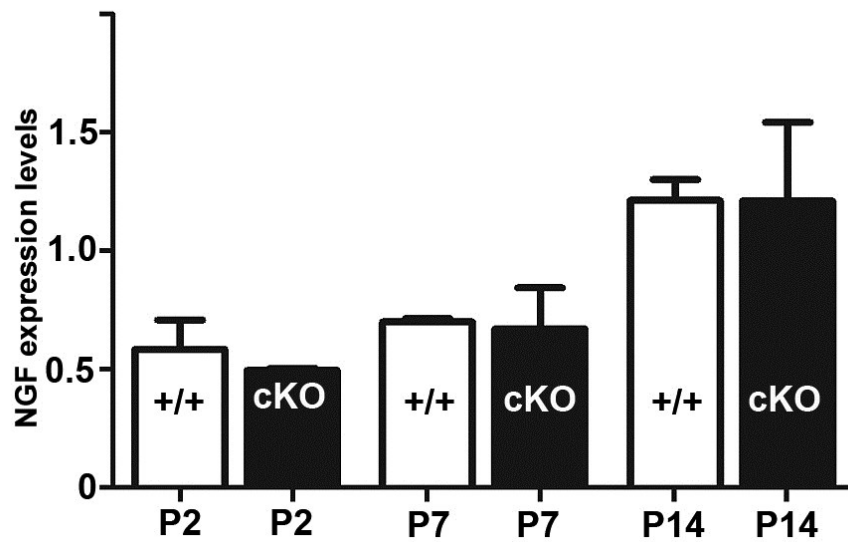
Figure 24. NGF expression is unaltered in *Shp2* cKOs. qPCR analysis

illustrating comparable levels of *Ngf* between control and *Shp2* cKO hearts

throughout the first 2 weeks of life. Error bars represent SEM. [qPCR

experiments done in collaboration with Emily Blue, PhD]. (Figure adapted from

Lajiness et al., 2014).

To rule out any potential abnormalities in the SA node as a possible contributing

factor to the sinus bradycardia observed, *Hcn4* expression was examined. HCN4

is a key channel located primarily in the SA node that helps maintain a regular

heart rhythm. Significantly, no disparities between *Hcn4* expression levels or

localization were detected between control and *Shp2* cKO SA nodes (Figure 25).
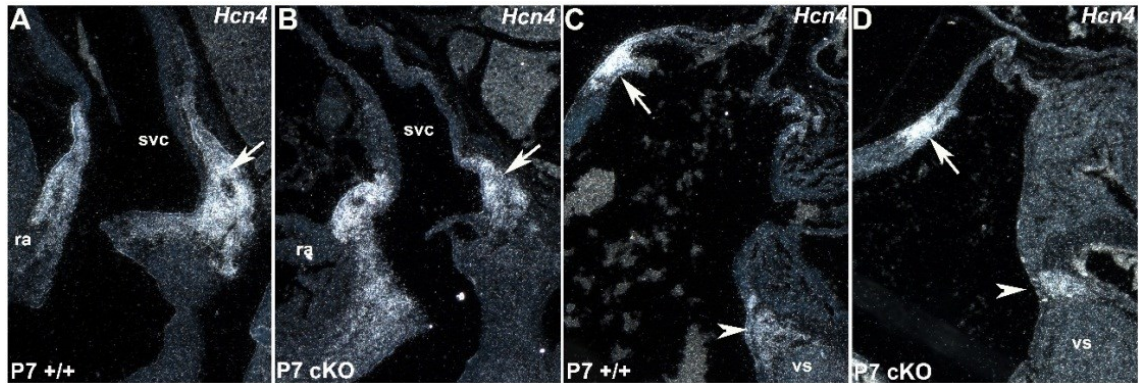
Figure 25. *Shp2* cKOs exhibit normal SA node structure and expression of

***Hcn4*.** *In situ* hybridization analysis of *Hcn4* expression in wild-type (A,C) and

Shp2 cKO (B,D) P7 hearts. *Hcn4* was similarly present in both control and *Shp2*

cKO SA nodes (arrows in A,B), the wall of the right atria (arrows in C,D) and on

top of the ventricular septums (arrowheads in C,D).Abbreviations: ra, right atria;

svc, superior vena cava; vs, ventricular septum. [Jian Wang performed the

radioactive *in situ* hybridization shown]. (Figure adapted from Lajiness et al.,

2014).

Also, as *Periostin-Cre* is expressed in cardiac fibroblasts which are responsible for insulating the intrinsic conduction system of the heart, *lacZ*-positive fibroblasts were quantified and found to be comparable between mutants and controls at all ages investigated (Figure 26A,B). Additionally, the levels of αSmooth muscle actin (a marker expressed by cardiac fibroblasts, particularly early in development) was equitable (Figure 26C), indicating that cKO cardiac fibroblasts are present, appropriately localized, and express normal markers.
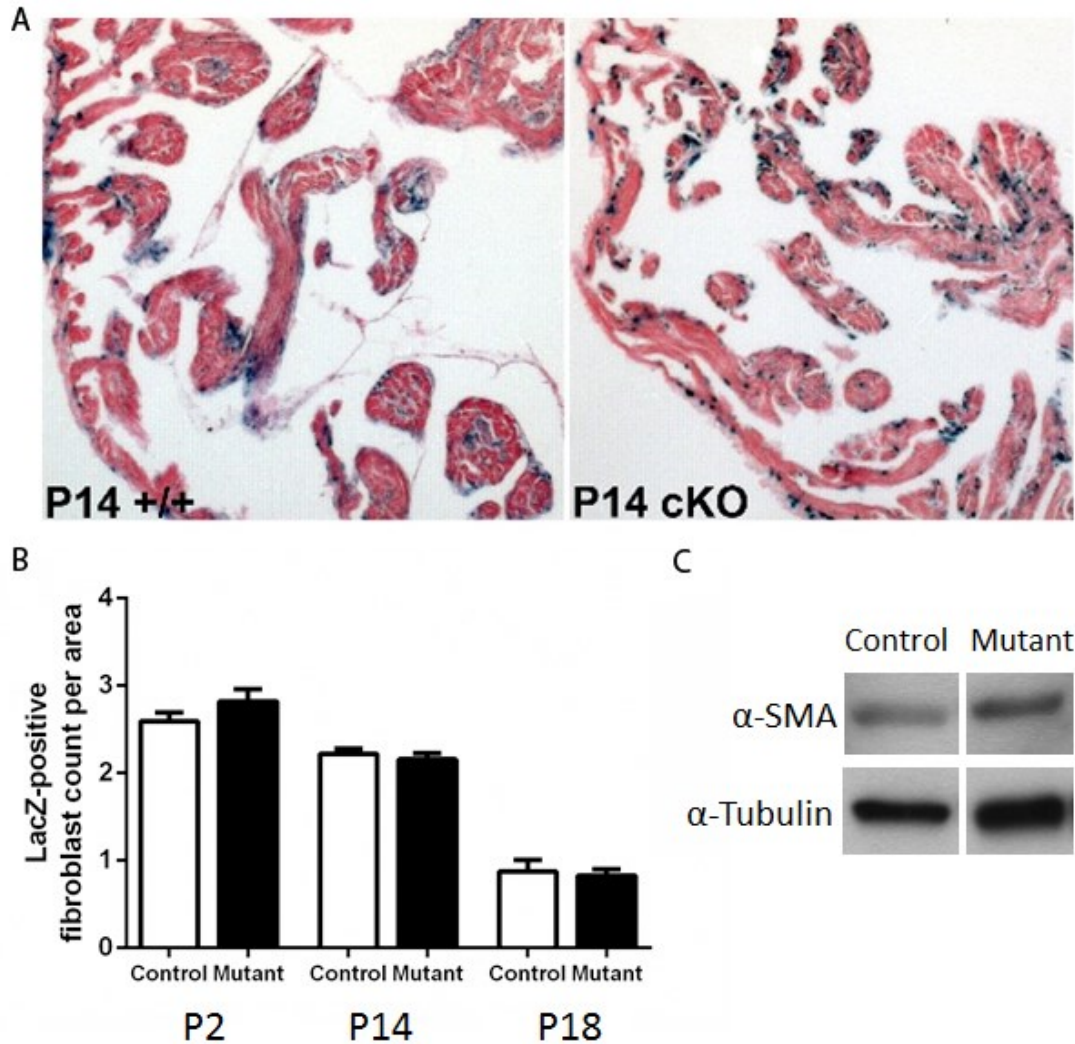
Figure 26. LacZ-positive cardiac fibroblasts are similar in number, localization, and expression patterns between *Shp2* cKOs and controls.

(A,B) Lineage mapping of *Periostin-Cre* expression via β-galactosidase staining and eosin counterstaining in histological sections revealed normal distribution and number of cardiac fibroblasts in both P14 controls and *Shp2* cKOs. **(B)** Quantification revealed that the relative proportion of LacZ-positive cardiac fibroblasts observed in atria at three different ages of control/*Shp2* cKO pairs is comparable in wild-types and *Shp2* cKOs (n=2-3). **(C)** Composite Western blot

confirming equivalent expression of α-smooth muscle actin in control and mutant

isolated P14 ventricles (n=4 pooled samples). Error bars represent SEM.

Although histology did not reveal any structural abnormalities, the microstructure of the control and *Shp2* cKO ventricular myocardium were further investigated via electron microscopy. Similar to the results obtained in the histological analysis, lineage mapping, and qPCR data presented earlier, the contractile apparatus and mitochondrial architecture did not differ between *Shp2* cKOs and littermate controls (Figure 27). These data indicate that *Periostin-Cre* mediated lineage-restricted loss of Shp2 does not adversely affect the *Shp2* cKO heart itself.
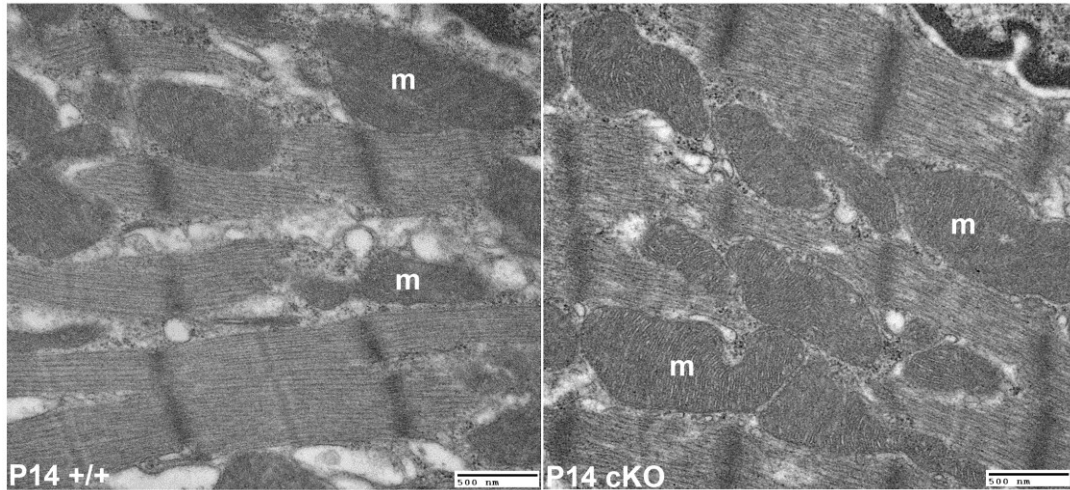
Figure 27. *Shp2* cKO hearts are structurally normal. Electron microscopy examination of control and mutant myocardium revealed normal contractile apparatus and mitochondrial (m) architecture in the P14 *Shp2* cKO and control hearts. Scale bar is 500nm. [IU EM core processed the heart tissue and collected the images shown]. (Figure adapted from Lajiness et al., 2014).

Decreased pERK is a primary signaling abnormality observed in Shp2 cKOs

Shp2 is an important factor in several signaling cascades, particularly in the modulation of the MAPK signaling cascades[110]. Published data have shown that cKO of Shp2 within pre-migratory NC results in diminished pERK signaling and that transient ERK1/2 activation is necessary for expression of smooth muscle and neural markers in NC *in vitro*[123]. Similarly, Shp2-deficent hematopoietic stem and progenitor cells show defective ERK and AKT activation[157]. In contrast, Shp2 impaired cardiomyoctes exhibit increased levels of phosphorylated AKT (pAKT)[158-160]. As they are the two major postnatal effector molecules studied in models of Shp2 dysregulation, we examined pERK and pAKT levels. Western analysis of microdissected heart/cardiac ganglia protein isolates (containing only the top of the hearts that are enriched for Cre-postive cells) revealed that pERK protein levels were decreased in *Shp2* cKOs by 50% at both E14.5 as well as P7 (Figure 28A,B). However, in the *Shp2* cKOs pAKT levels were unaltered both *in utero* and postnatally (Figure 28A,C). These results indicate that the ERK1/2 branch of the MAPK pathway as opposed to the AKT pathway is selectively affected in the *Shp2;Periostin-Cre* mutants and suggest that Shp2 activity in the post-migratory NC is essential for pERK-mediated differentiation and establishment of cardiac sympathetic neurons but not their survival which is dependent on AKT signaling.
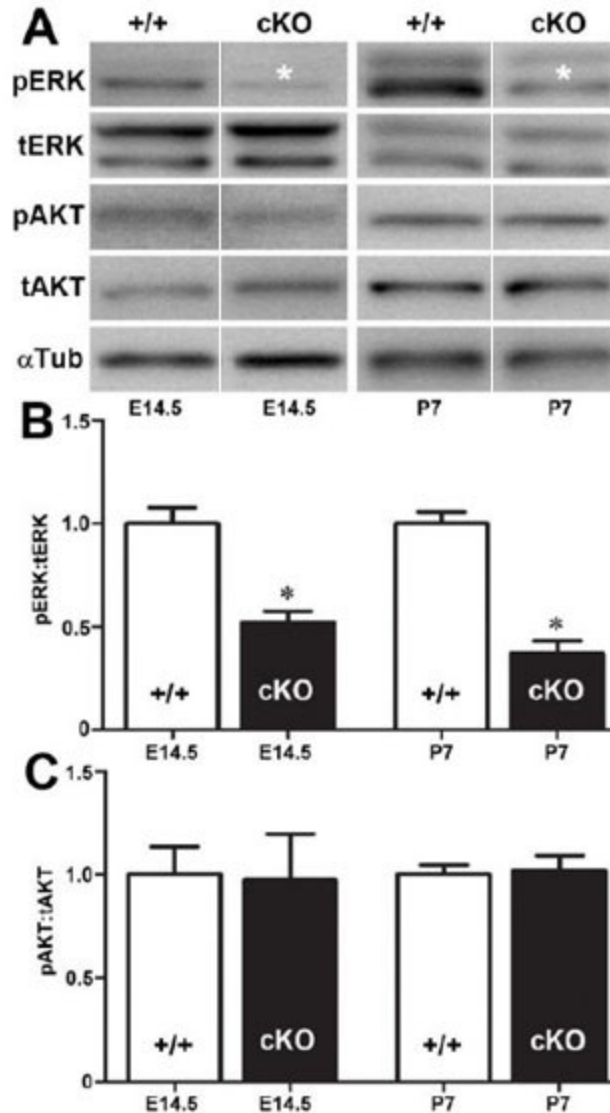
Figure 28. *Shp2* **cKOs exhibit a decrease in cardiac pERK signaling both embryonically and postnatally while pAKT signaling remains unaltered**. **(A)** Representative composite Western blot illustrating decreased pERK levels in mutant microdissected heart/cardiac ganglia (*) compared to wild-type at both E14.5 and P7, but equivalent total ERK levels (n=5). However, *Shp2* cKO pAKT levels were unaltered at these ages (n=3). **(B)** Densitometric quantification of pERK to tERK ratios at E14.5 and P7 (*t*-test, *p-value<0.05 (E14.5 p-value=0.0052; P7 p-value= 0.0008)). **(C)** Densitometric quantification of pAKT to

tAKT ratios (*t*-test, p-value=0.498 (E14.5); p-value=0.758 (P7)). Error bars

represent SEM. The significant reduction pERK levels suggests a

disproportionate amount of the active pERK signaling in our neonatal

microdissected heart/cardiac ganglia samples was within the NC/*Periostin-Cre*-

positive lineage. Moreover, unlike both total ERK1,2 and Shp2 which are

ubiquitously expressed, pERK levels are known to fluctuate within a dynamic

spatiotemporal tissue-restricted pattern in both mouse[161] and human tissues[162].

(Figure adapted from Lajiness et al., 2014).

Genetic restoration of pERK signaling rescues the cardiac innervation phenotype of *Shp2* cKOs

We next determined whether diminished pERK levels were directly responsible for the sympathetic innervation phenotype observed in *Shp2* cKOs. To reactivate ERK1/2 signaling, a conditional floxed-stop model of *caMEK1* (the effector directly upstream of ERK) was crossed onto the *Shp2;Periostin-Cre* background (Figure 29A). In this way, any cell expressing Cre will simultaneously delete *Shp2* and express caMEK1[138] in a lineage-restricted manner. The *Shp2;Periostin-Cre;caMEK* mice had significantly higher pERK levels than their non-caMEK1 expressing mutant littermates, and importantly, in the *Shp2;Periostin-Cre;caMEK* mice, pERK levels were comparable to wild-type age-matched littermate controls (Figure 29B). *Shp2;Periostin-Cre;caMEK* TH levels were similarly restored to wild-type levels (Figure 29C).
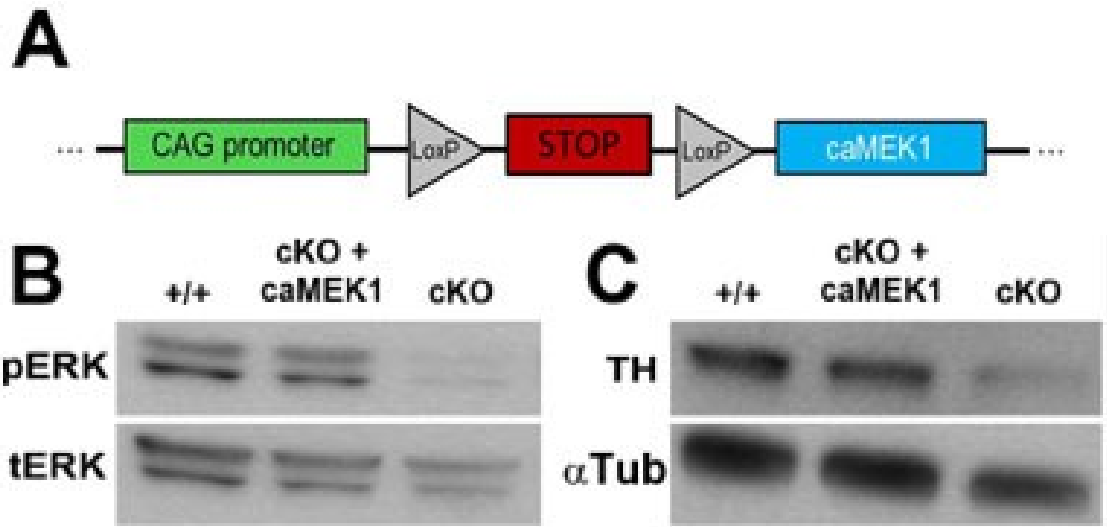
Figure 29. Schematic of genetic rescue and molecular characterization of resulting mice. (A) Schematic of *caMEK1* genetic construct. **(B)** Western analysis of P14 heart isolates demonstrated that pERK levels in a rescued mutant (cKO + caMEK1) are similar to those in wild-type littermates, while pERK in a *Shp2* cKO is still drastically decreased. **(C)** Western analysis of heart isolates demonstrated TH levels are also normalized in a rescued mutant and are similar to a wild-type littermate, but TH levels relative to α-tubulin loading control are still drastically decreased in *Shp2* cKO hearts. (Figure adapted from Lajiness et al., 2014).

Moreover, immunohistochemistry revealed restoration of TH expression throughout the *Shp2;Periostin-Cre;caMEK* cardiac ganglia (Figure 30A-C) as well as an increase in TH-positive innervation properly localized around the blood vessels in the myocardium of the *caMEK1* expressing cKO ventricle (Figure 30D-F). The restored sympathetic innervation on the dorsal surface of the P14 *Shp2;Periostin-Cre;caMEK* heart was verified via whole-mount TH-immunostaining. The latter analysis revealed substantially increased arborization in the "rescued" mutant as compared to the non-rescued *Shp2;Periostin-Cre* mutant (Figure 30G-I). Consequently, the heart rates of *Shp2;Periostin-Cre;caMEK* rescued mutants were normalized to control levels at all ages investigated (P14 shown; Figure 31). Thus, the rescue of sympathetic innervation functionally elevated the heart rates of the rescued mutants to those of littermate controls.
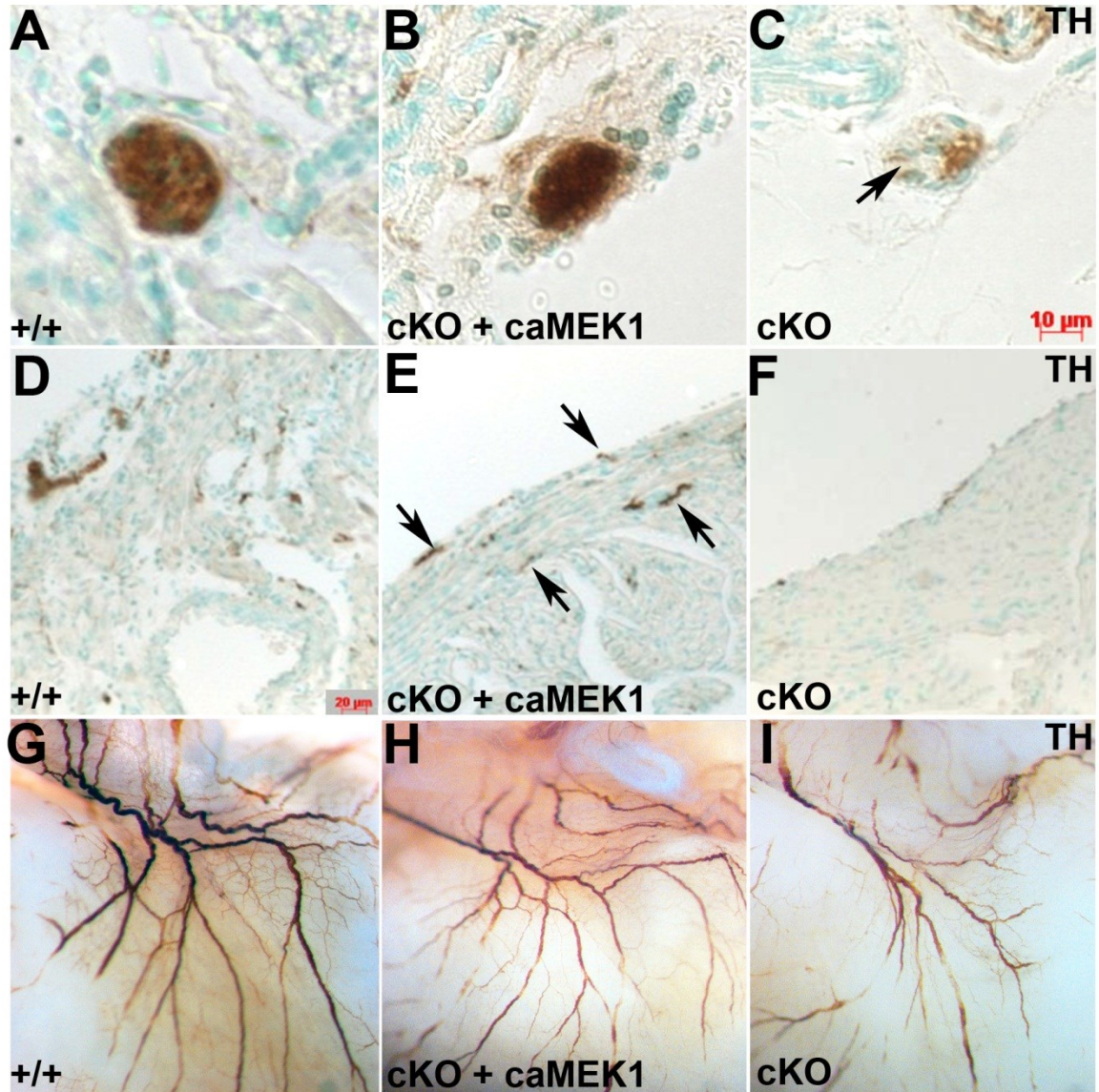
Figure 30. *Shp2;Periostin-Cre;caMEK1* **rescued mutants exhibit normalized cardiac sympathetic innervation. (A-C)** TH IHC of P14 control (A), rescue (B), and mutant (arrow, C) cardiac ganglia demonstrating a restoration of TH expression in the rescued mutant ganglia. **(D-F)** TH IHC of P14 control (D), rescue (E), and mutant (F) left ventricle demonstrating increased TH-positive innervation in the rescued mutant ventricle (arrows in E). **(G-I)** Whole mount TH IHC showing the dorsal surface pattern of sympathetic innervation in a P14

control (G), rescued mutant (H), and mutant (I) heart. (Figure adapted from

Lajiness et al., 2014).
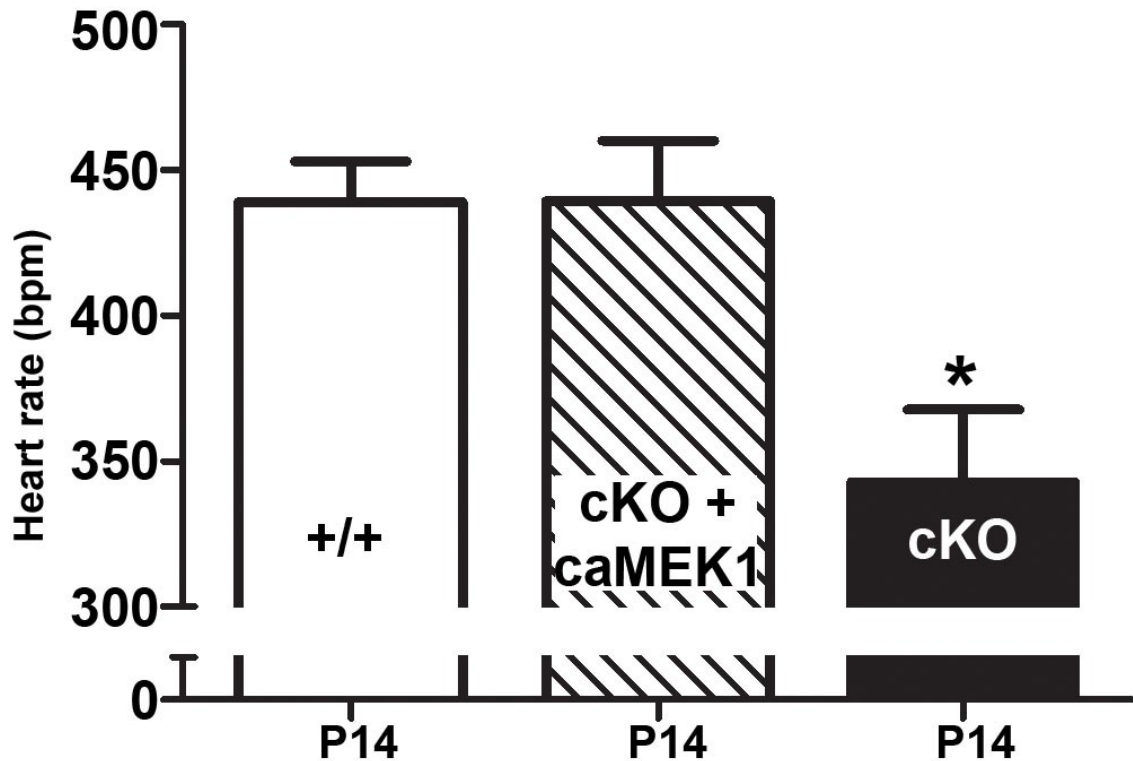
Figure 31. *Shp2;Periostin-Cre;caMEK* **rescued mutants exhibit normalized heart rates.** ECG analysis of average heart rates of control, rescue, and mutant littermates at P14 (1-way ANOVA p=0.0113; Tukey's multiple comparisons test: +/+ vs. rescue=non-significant, +/+ vs. cKO=significant (p<0.05), rescue vs. cKO=significant (p<0.05) n=5-20). Note that lineage-specific expression of caMEK1 restores the mutant heart rates. Error bars represent SEM. (Figure adapted from Lajiness et al., 2014).

One interesting aspect of the genetic intercross was that mixing the *Shp2*cKO model (on a predominantly C57BL/6 background) with the *caMEK1* model (on a pure FVB/N background) shifted the basal heart rates of both control and mutant littermates (Figure 32). This is not surprising as mice of different genetic backgrounds have widely divergent basal heart rates[163]. Since the shift in basal heart rate affected all genotypes to the same extent and the relationship between control and *Shp2* cKO heart rates was not altered, it was not investigated further. Rather, these data were considered evidence that the mechanism for cardiac sympathetic innervation described in this study holds true on more than one genetic background.
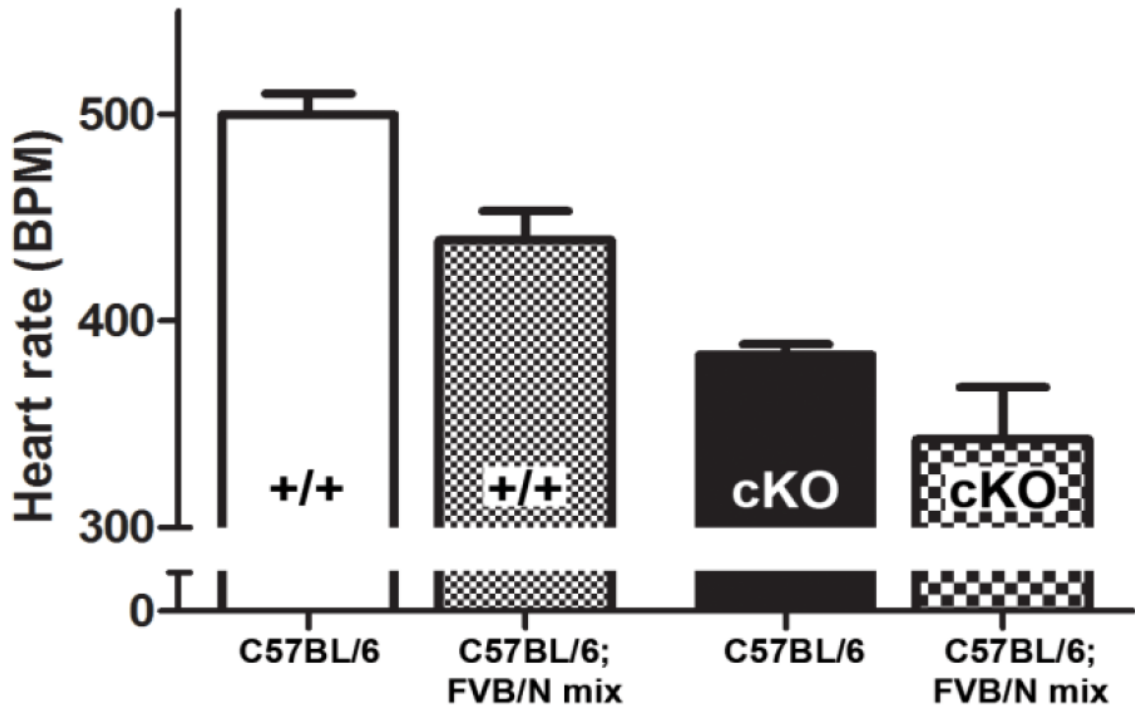
Figure 32. Genetic background effects on heart rate. Placing the C57BL/6 mice on a mixed C57BL/6;FVB/N background, equivalently altered basal heart rates in both *Shp2* cKO and control mice. Average heart rates of P14 mice of either C57BL/6 or mixed (C57BL/6;FVB/N) genetic background demonstrating that both control and *Shp2* cKO basal heart rates were similarly decreased on the mixed background (n=6-20). Error bars represent SEM.

Our studies revealed neurite outgrowth deficiency and overall diminished cardiac sympathetic innervation Shp2 cKOs. Taken together with the pERK-dependent rescue, these findings recapitulated previous *in vitro* work linking NGF, Shp2, pERK and sympathetic neuron differentiation. Thus, we propose a schematic detailing the likely signaling mechanism as explanation for these data (Figure 33). Briefly, NGF binds to its receptor TrkA which is associated with a complex including Shp2. Propagation of signaling results in localization of Ras to the membrane where GDP is exchanged for GTP. Ras bound to GTP activates RAF via phosphorylation which continues the activating phosphorylation cascade through MEK and ERK. Once phosphorylated, ERK translocates to the nucleus where it promotes sympathetic neuron differentiation and neurite outgrowth.
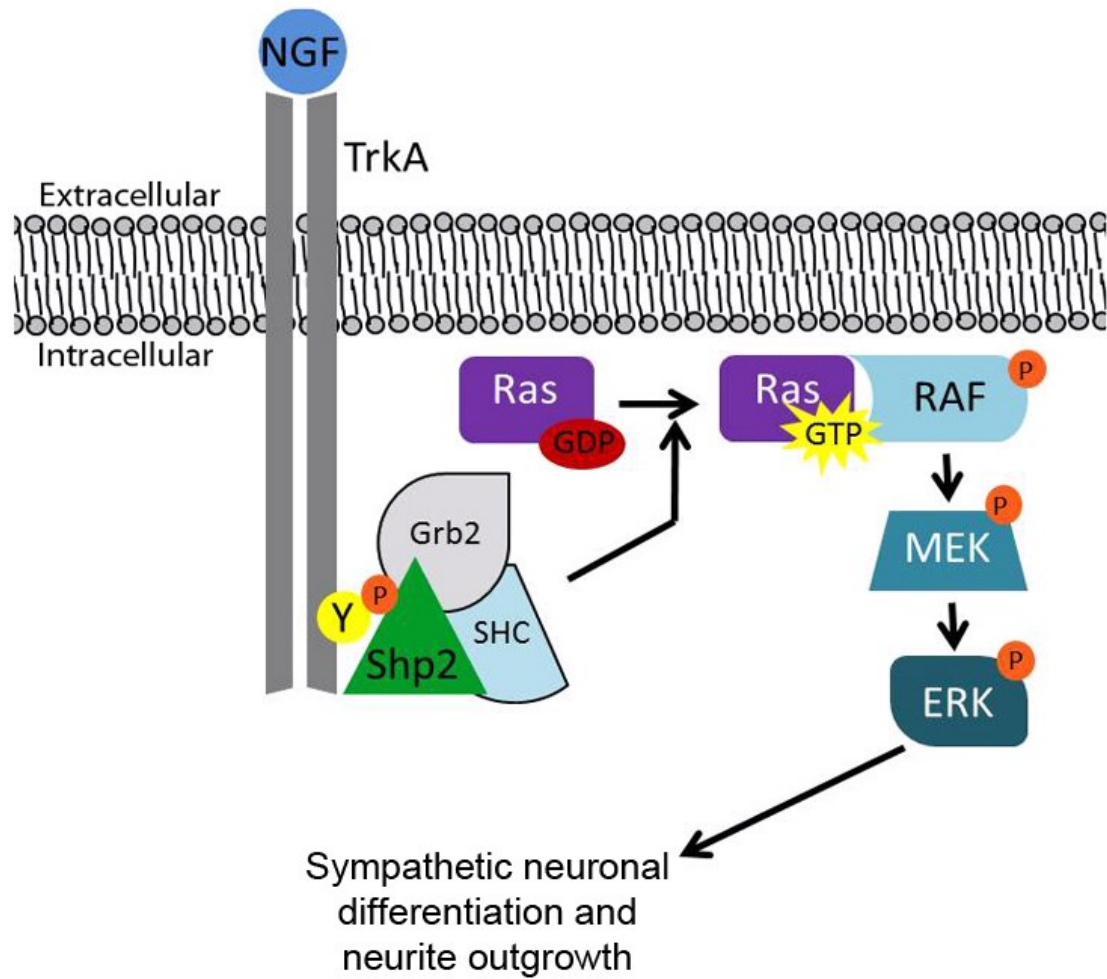
Figure 33. Proposed model for underlying signaling cascade responsible for the sympathetic innervation defects within *Shp2* cKOs. Schematic based off of work detailed in Rosario et al., 2007[92]. (Figure adapted from Lajiness et al., 2014).

Despite enacting a complete rescue of the cardiac phenotype, the "rescued"

Shp2;Periostin-Cre;caMEK mice still exhibited failure to thrive postnatallly with

growth curves similar to that of non-rescued *Shp2* cKOs (Figure 34). While half of

the rescued mutants observed (n=16) lived past weaning, all were dead by P40

(Figure 35). The doubling of the life-span of non-rescued mutants is significant;

however, the persistence of lethality despite the rescue of heart rate indicates

that not all aspects of the phenotype (particularly those with significant

contributions to lethality) are addressed by normalizing pERK levels.
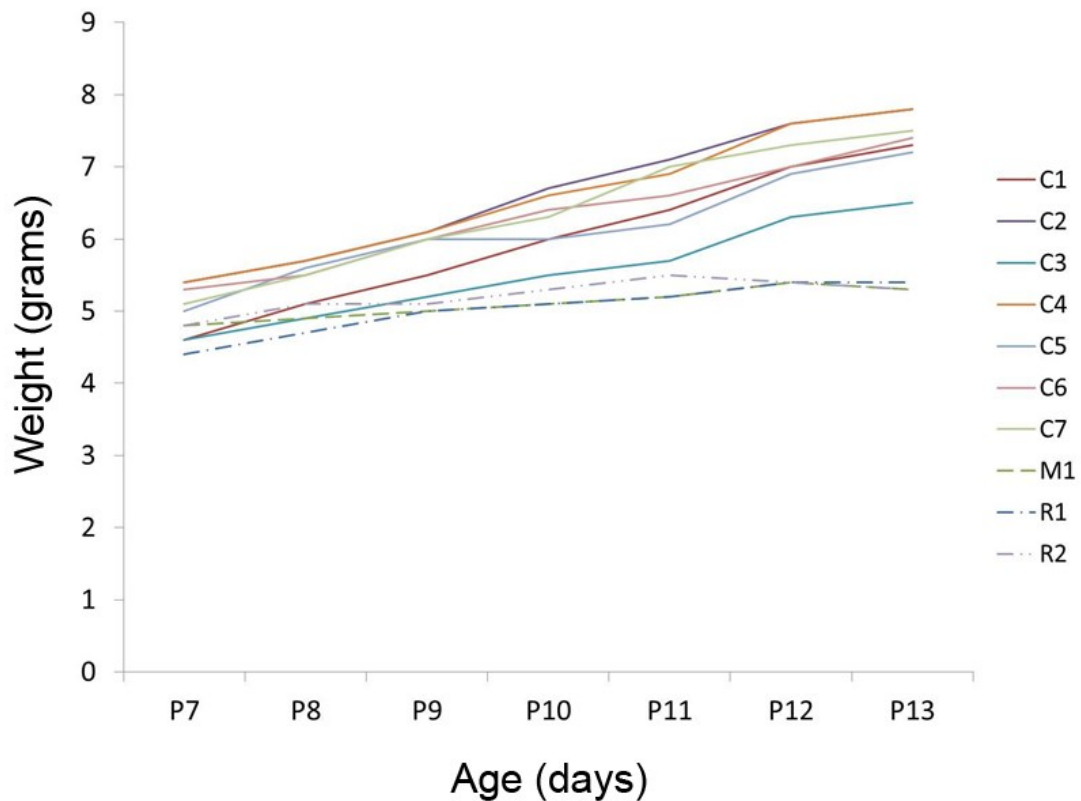
Figure 34. Growth curve of representative litter. Line graph of weight plotted from P7 to P13 of a litter of pups containing 7 controls (C1-C7), one non-rescued mutant (M1; *Shp2* cKO), and two rescued mutants (R1 and R2; *Shp2* cKO;*caMEK1*). Notice that the growth curve of the rescued mutants matches the growth curve of the non-rescued mutant. This trend was consistently observed (n=6 litters).
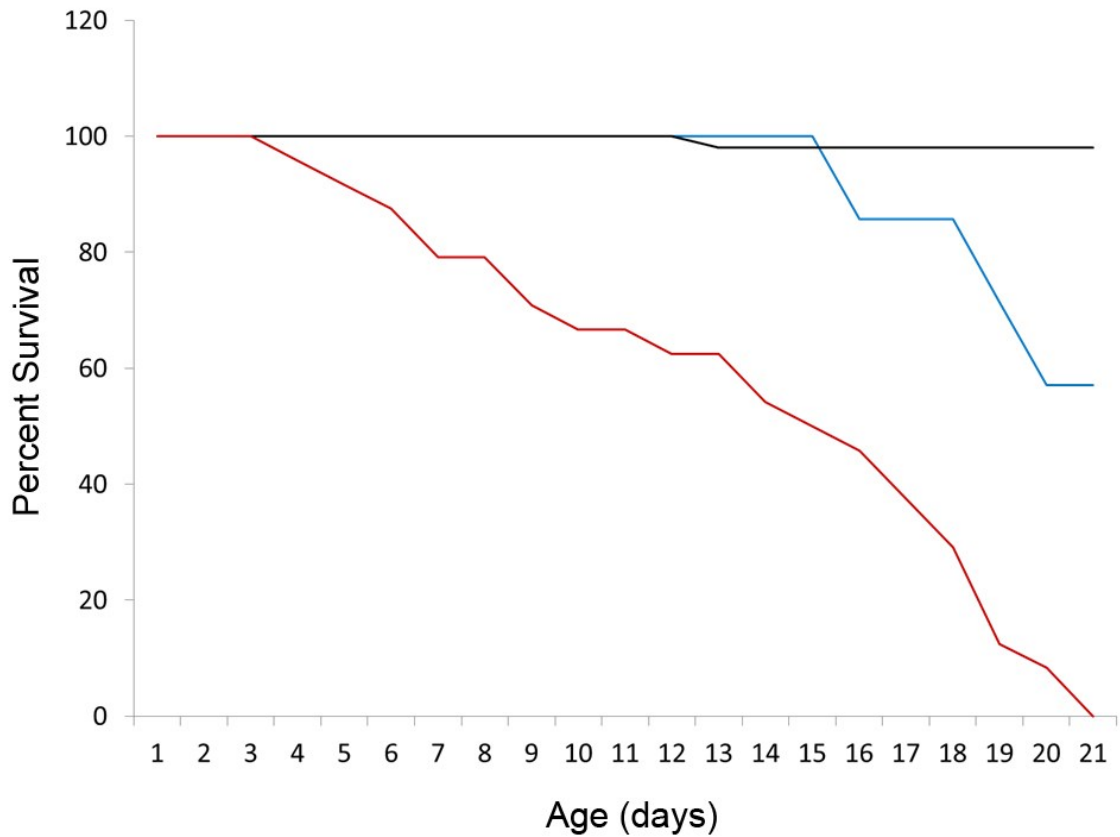
Figure 35. Survival curve of mutants vs. rescued mutants vs. controls. Line graph of percent surviving pups over time for control (black), rescued mutant (blue), and non-rescued mutant (red) pups. Notice that the MEK rescue delays lethality but does not prevent it (n=16).

DISCUSSION

The use of *Periostin-Cre*, which expresses Cre recombinase in post-migratory NC lineages from E10 onward, enabled us to selectively knock out expression of the Shp2 protein phosphatase during a previously unexplored window of NC development. Significantly, *Shp2;Periostin-Cre* mice were viable at birth in contrast to *Shp2;Wnt-1-Cre* mice which die at E13.5[126]. As *Periostin-Cre* is expressed in many of the same NC lineages as *Wnt-1-Cre*, we believe the timing of Cre recombinase expression and therefore loss of Shp2 to be critical for the phenotypic differences observed between the two mouse models. For example, loss of Shp2 at E8 results in loss of SCPs and immature SCs on peripheral nerves, structural craniofacial and cardiac abnormalities, diminished enteric innervation and incompatibility with postnatal life[126]. However, loss of Shp2 expression just 2 days later (after NC cell migration) results in a viable pup with SCPs and immature SCs present on peripheral nerves but deficient myelination, normal craniofacial and cardiac structure, and diminished but present enteric innervation. These findings indicate that Shp2 may play an important role in the pre-migratory or migratory phase of NC development as many effects are decreased or absent when Shp2 is deleted in post-migratory NC. Significantly, we have shown that *Periostin-Cre* is a genetic tool that can be applied to investigate an important yet previously unexamined developmental time point.

The lack of embryonic mortality allowed us to investigate postnatal phenotypes. We observed that enteric innervation begins to look sparse by P7 and continues to dwindle as the phenotype associated with loss of Shp2 progresses. The significance of this observation has not yet been established; however, these gastrointestinal innervation defects could correlate to functional deficits such as motility abnormalities.

Similarly, the diminished peripheral innervation was an interesting observation. In other models of NGF signaling cascade interruption, there is significantly reduced sensory innervation to target organs such as the skin and subcutaneous tissue as NGF is an important trophic and chemoattractant factor in these lineages[27, 81, 101]. The functional significance of diminished peripheral innervation has not been investigated in detail in our mouse model; however, the lack of innervation of the tongue may indicate that *Shp2* cKO pups have difficulty suckling and thus decreased nutrition may be a significant component of the failure to thrive observed.

Despite the range of clinically applicable phenotypes observed, this study primarily focused on exploring the role of Shp2 and downstream pERK signaling in the context of sympathetic innervation of the developing heart. Specifically, sympathetic neuron differentiation as well as sympathetic innervation establishment and maintenance were investigated. While much is known about the molecular mechanisms regulating sympathetic neuron growth and

differentiation *in vitro*, many of these pathways had yet to be investigated *in vivo*.

We generated a lineage specific KO of *Shp2* that exhibits postnatal failure of

sympathetic cardiac innervation. Furthermore, the fact that restoration of pERK

levels through expression of a constitutively active upstream MEK1 rescued the

cardiac innervation phenotype indicates that pERK signaling is necessary for

peripheral sympathetic innervation *in vivo*. Shp2 has been shown *in vitro* to be a

required intermediary linking NGF signaling to pERK elevation which is essential

for sympathetic neuron differentiation[85, 86, 92, 121, 122, 164-167]. Our study now

provides evidence that this holds true *in vivo* and has functional significance as

diminished cardiac sympathetic innervation results in bradycardia.

When the NGF-Shp2-ERK pathway is interrupted in model systems such as

PC12 cells (cell line derived from rat adrenal pheochromocytoma that is often

used as a model of sympathetic neuron survival and differentiation) and

explanted superior cervical ganglia via pharmacological or genetic means,

sympathetic neurons fail to differentiate (as indicated by the paucity of neurites

projected from the cell body)[85, 86, 92, 121, 122, 164-166]. Some *in vivo* models have

indicated an important role for NGF/MAPK signaling in sensory innervation

patterning[101]. However, other groups have attempted to investigate the effect of

Shp2 mutations on sympathetic innervation *in vivo* but were unable to

recapitulate the *in vitro* results[164]. Thus, our *Shp2* cKO is the first *in vivo* model to

demonstrate that Shp2 and subsequent pERK elevation are required for

sympathetic innervation of the developing heart.

It was interesting to note that although *Periostin-Cre* is expressed from E10.5 onward, phenotypic differences between *Shp2* cKOs and controls were not observed until after birth. This could be due to the fact that NGF and its downstream signaling is not required for sympathetic innervation until E16.5[90]. However, in the absence of an inducible Cre to temporally vary when Shp2 is deleted we cannot exclude the possibility that NC progenitors are altered or misspecified early in development and the effects are not manifested until after birth. This is a limitation of the current study and is an avenue of future research when the appropriate genetic tools become available.

While global cardiac sympathetic innervation was diminished in cKOs, it was interesting to note that the TH-positive intrinsic cardiac ganglia exhibited decreased neurite outgrowth and TH expression. This emphasizes that these structures are subject to the influences of Shp2 and pERK signaling. Furthermore, in the context of sinus bradycardia, our findings reinforce the functional role of TH-positive cardiac ganglia in the "heart brain" as well as the idea that they are involved in heart rate regulation particularly in the first 2-3 weeks of life[36, 37, 39, 42]. The dearth of axonal projections emanating from these ganglia suggest that there is a failure of sympathetic neurons to differentiate or to maintain their differentiated state in *Shp2* cKOs. The loss of sympathetic-specific TH expression despite continued expression of the generic neuronal marker NSβT further supports this conclusion. Together, these data suggest that the

NGF signaling pathway which is responsible for sympathetic neuron differentiation and maintenance during the early postnatal period may be the underlying mechanism for the altered sympathetic innervation observed in *Shp2* cKO hearts.

Aberrant expression of embryonic sympathetic neuron differentiation transcription factors such as *Phox2a* and *2b* which regulate TH and dopamine β-hydroxylase expression[67] further supports this hypothesis. However, as only a few time points were investigated, it is not known if *Phox2a* and *2b* expression is appropriately downregulated in *Shp2* cKOs at birth and then aberrantly re-expressed later in the postnatal period or if expression is simply never appropriately downregulated. The former would imply that sympathetic neurons differentiate initially and then dedifferentiate postnatally whereas the latter scenario would indicate that the cardiac sympathetic neurons never appropriately differentiate. Distinguishing these events could be investigated by performing *in situ* hybridization to examine late embryonic and early postnatal expression of *Phox2a* and *2b* which would shed light on Shp2 and pERK's roles in establishing versus maintaining a differentiated state in sympathetic neurons.

Additionally, the absence of apoptotic cells in mutant sympathetic ganglia emphasizes the fact that MAPK signaling is essential for differentiation but not for the survival of sympathetic neurons. While there have been reports that MAPK signaling can play a role in neuronal survival particularly in the context of

cytotoxic injury by agents such as cytosine arabinoside (AraC)[91, 168, 169], NGF is

thought to maintain a basal level of sympathetic neuron survival via PI3K/AKT

signaling which is not disturbed in our model. Thus, although these Shp2-

regulated protein kinases (including ERK) have pleotropic effects on the cell, they

likely elicit some of their effects by regulating downstream mediators of

sympathetic nervous system homeostatic gene expression.

Functionally, we have demonstrated that Shp2-dependent sympathetic deficiency

leads to sinus bradycardia. No other abnormalities or arrhythmias were observed

in the ECG traces to indicate any intrinsic cardiac pathology. Since the P-wave is

consistently present in both control and *Shp2* cKO traces and lasts for the same

duration, these data indicate that the SA node is appropriately initiating the action

potential which is efficiently disseminated throughout the atrial myocardium

resulting in the expected pattern of depolarization. Furthermore, the lack of

prolongation of PR intervals throughout the majority of ages investigated

indicates that the AV node is functioning appropriately. The minor PR

prolongation observed at P17 is most likely a product of significantly decreased

heart rates and, importantly, never progresses from 1st degree heart block to any

form of arrhythmia. The normal QRS complex indicates that the action potential

is efficiently transferred throughout the Purkinje fiber network with no conduction

delays or bundle branch blocks observed. Because this is a 3-lead ECG as

opposed to the more sophisticated 12-lead ECGs utilized in human studies, we

cannot examine parameters such as axis shifts. However, with the information

we have collected, there is no reason to suspect that any conduction abnormality or axis shift would be observed as a result of the loss of Shp2 expression.

As there is diminished sympathetic innervation in the *Shp2* cKO heart, and thus less catecholamines (*i.e.* norepinephrine) released to maintain an elevated heart rate, we reason that this deficiency is the direct cause of the bradycardia observed. Therefore, we hypothesized that delivering an exogenous β-adrenergic agonist (isoproterenol) would stimulate both the control and *Shp2* cKO heart to beat faster. Since isoproterenol did increase both the control and *Shp2* cKO heart rates equivalently, we were able to conclude that the mutant heart is functionally capable of responding to catecholamines and maintaining a rapid heart rate (decreasing the likelihood of conduction or structural defects as a cause of the bradycardia). This finding also indicates that Shp2 expression in post-migratory NC cells is not required for the heart to respond to catecholamines. Histological examination of the SA node indicated that the node was present and appropriately expressing the pacemaker cell marker HCN4. This finding of normal appearing histology is consistent with the presence of a regularly occurring P-wave on the ECG traces. If the SA node were structurally compromised to the point that the "pacemaker" function of the heart had been taken up by a secondary pacemaker such as the AV node, the heart rate would, indeed, be slower; however, the P-wave would be absent which is not the case in our model. Together, these data further exclude intrinsic SA node dysfunction as the primary cause of bradycardia in the *Shp2* cKOs.

As fibroblasts serve as the insulating component for the intrinsic conduction system of the heart and are affected by the genetic modification driven by *Periostin-Cre*, alterations in fibroblast number or localization were investigated. No aberrancies in either parameter were found in *Shp2* cKO cardiac fibroblasts and the fibroblasts appropriately expressed αsmooth muscle actin. While cardiac fibroblasts, particularly in neonates, express αsmooth muscle actin ,one important consideration when using αsmooth muscle actin as an indicator of cardiac fibroblasts is that injury to the heart causes cardiac fibroblasts differentiate into myofibroblasts which drastically increase expression of αsmooth muscle actin (reviewed in Lajiness et al., 2013[151]). As neither structural injury to the heart nor fibrosis is present in our model, we do not think that this fact alters the interpretation of our data. Importantly, the number of LacZ-positive (*i.e.* genetically modified) cardiac fibroblasts decreased with age. Since the number of fibroblasts affected is decreasing as the bradycardia is worsening, it is not likely that cardiac fibroblasts are involved in the pathomechanism of the bradycardia.

Similarly, the distribution of cardiac sympathetic innervation was investigated. Specifically, the proportion of TH-positive fibers in the epicardial region of the myocardium (the "outside" surface of the heart) compared to the endocardial region of the myocardium (the "inside" surface of the heart) was of particular interest. In a "normal" heart there is more sympathetic innervation in the epicardium compared to the endocardium. Absence of this epicardial-to-

endocardial gradient has been associated with bradycardia in other mouse models[97]. Despite the global decrease in cardiac sympathetic innervation of *Shp2* cKO hearts, the fact that the epicardial-to-endocardial gradient was intact in all ages examined indicates that this is not a contributing factor to the sinus bradycardia observed in *Shp2* cKOs. Furthermore, as administration of atropine to inhibit the parasympathetic innervation did not elevate heart rate, increased parasympathetic tone is not responsible for the slowed heart rate. Therefore, having eliminated the other most likely explanations, we concluded that the diminished sympathetic tone is the direct cause of the sinus bradycardia observed in *Shp2* cKOs. This hypothesis was further verified by rescuing the sympathetic innervation phenotype by conditionally expressing caMEK1 which abolished the sinus bradycardia.

MEK1 is an ideal target for a genetic rescue of our model as the only known substrate of MEKs are ERK1/2, and reciprocally, the only known activators of ERK1/2 are MEK1/2[121]. Both MEK1 and MEK2 are known to activate ERKs; however, MEK1 has been more extensively studied and is considered the more physiologically relevant isoform particularly downstream of RAS. *In vitro* studies have revealed that MEK1 but not MEK2 associates with RAS in a signaling complex when NIH 3T3 cells are serum starved and then stimulated with fetal calf serum[170]. Specifically, in PC12 cells an inactivating mutation in MEK1 blocks sympathetic differentiation while activating mutations facilitate neurite outgrowth even in the presence of dominant-negative Shp2 or in the absence of NGF[86, 122].

Introduction of caMEK1 driven by the same conditional system as our *Shp2* cKO, allowed us to simultaneously delete Shp2 and express caMEK in post-migratory NC. Significantly, this model resulted in a physiological increase in pERK levels (restored to control levels) as unchecked elevation of pERK can result in cardiac valvular and septal abnormalities[171].

The spatiotemporal precision of this genetic model has allowed us to begin to parse out the ERK-dependent from the ERK-independent effects of *Shp2* cKO. The rescued mutants (*Shp2;Periostin-Cre;caMEK*) still exhibit failure to thrive and eventually die (100% lethality by P40) although a significant portion (~50%) survive past weaning whereas all non-rescued mutants (*Shp2* cKOs) die prior to P21. The lack complete rescue of lethality indicates that there may be both ERK-dependent and ERK–independent mechanisms contributing to the eventual death of the organism. For example, the altered peripheral and enteric innervation, although not the focus of this study, could be contributing factors to lethality in both the cKO and rescued model. Specifically, in addition to following a similar pattern of growth, rescued mutants do noticeably exhibit the same gait abnormalities and grasping phenotype observed in *Shp2* cKOs. This phenotype is observed as early as P7 in both genotypes.

It is possible that these aspects are not rescued because they are not dependent on pERK levels and that a different molecular mechanism is the cause. An alternative explanation is that there is not complete rescue due to the fact that

dynamic pERK regulation cannot be achieved through constitutive expression of caMEK1. This genetic model effectively increases basal pERK levels to that seen in controls; however, it also separates the regulation of pERK levels from NGF and other growth factor signaling. This itself can have physiologic ramifications and must be carefully considered as a confounding factor.

Significantly, our findings indicate that establishment of sympathetic innervation of the heart is an ERK-dependent event as all aspects of the cardiac innervation phenotype observed in the *Shp2* cKO were rescued by lineage-restricted caMEK1. This model provides a useful tool in which to identify lineage-specific proximate targets of Shp2 during autonomic innervation and establishment of a mature functioning cardiovascular system.

Through lending mechanistic insight to early sympathetic innervation and heart rate regulation, our *Shp2* cKO model also allows for investigation of how the loss of Shp2 function in diseases such as LS can lead to the ECG abnormalities characteristic of the syndrome[108, 112]. While these abnormalities are not extremely well characterized and often complicated by structural cardiac defects[112, 114, 172, 173], our cKO mouse provides an opportunity to study Shp2's spatiotemporal role in establishing aberrant ECG patterning in isolation from compounding structural cardiac defects. It is important to remember, however, that our *Shp2* cKO is not a model for LS as LS exhibits a mutation in the Shp2 protein expressed from one of the two alleles encoding the protein as opposed to absence of Shp2 protein

expression all together. Additionally, it is thought that LS mutant Shp2 acts in a complicated mechanism possibly involving dominant negative effects as the catalytically inactive version of Shp2 is in the open conformation (traditionally the active conformation) which may allow it to outcompete the normal Shp2 for binding sites at RTKs[102, 108]. Furthermore, the LS mutation occurs in all cells from conception onward. Despite these differences, the knowledge gained about NC biology and how it contributes to the establishment and maintenance of sympathetic innervation in the heart though these studies can be applied to many diseases including LS. In addition, these studies contribute to our general knowledge of sympathetic innervation and the various interruptions to its development that can occur embryonically as well as postnatally.

FUTURE STUDIES

Future studies will focus on investigating aspects of the *Shp2* cKO (with and without the MEK1 rescue) phenotypes potentially involved in lethality such as the altered enteric innervation and peripheral innervation abnormalities initially observed at P7.

Further investigation of enteric innervation will involve whole-mount NSβT IHC of gut sections at various time points throughout development (P7, P13, P15, and P18 have already been investigated so this work would primarily focus on earlier stages to establish when the phenotype is first observed). This will allow for a longitudinal approach to examine the progression of the phenotype over time. Furthermore, incorporation of functional studies to ascertain if the diminished enteric innervation results in abnormal or protracted peristaltic activity may be informative. Also, the etiology of enteric ganglia absence would be interesting to examine. Evaluating whether this is due to decreased proliferation or apoptosis can be accomplished with IHC. An in-depth histological analysis of the many layers of intestinal tissue may be useful even if only to eliminate structural abnormalities as a pathomechanism for the failure to thrive phenotype observed postnatally.

In addition, pups were observed to have gait abnormalities and grasping phenotypes often associated with myelination defects[107, 174-177]. These were

observed at P7, prior to weight loss or heart rate abnormalities. As the 3.9kb Periostin promoter has been shown to be expressed in Schwann cells by E14[137] and Shp2 is known to play an important role in myelination[101, 126, 134, 135], the potential presence of a myelination phenotype in the *Shp2* cKOs was investigated. To examine a possible myelination defect, we explored whether or not Schwann cell precursors (SCPs) migrate and immature SCs persist on peripheral nerves embryonically. Hematoxylin and eosin (H&E) stained sections of embryonic dorsal root ganglia indicated that, indeed, SCPs migrated and immature SCs were present on peripheral nerves at E14.5 and 16.5 (Figure 36). Further investigation revealed that although SCs are present on peripheral nerves, preliminary data suggest that the myelin generated by mutant SCs is much thinner in trigeminal (Figure 37) as well as sciatic (Figure 38) nerves. Additionally, axonal loss was observed in the sciatic nerve of *Shp2* cKO pups (Figure 38). Interestingly, expression of caMEK1 appears to rescue the myelination phenotype in the trigeminal nerve (Figure 37), but does not alter the myelination nor the axonal loss in the sciatic nerve (Figure 38). These findings, although preliminary, may explain the gait abnormalities and most likely contribute to the failure to thrive phenotype that eventually leads to lethality. However, it is important to remember that hypomyelination, although sometimes associated with failure to thrive and early postnatal lethality, can also be compatible with life as seen in the Trembler mice (a model of Charcot-Marie-Tooth disease)[178, 179].
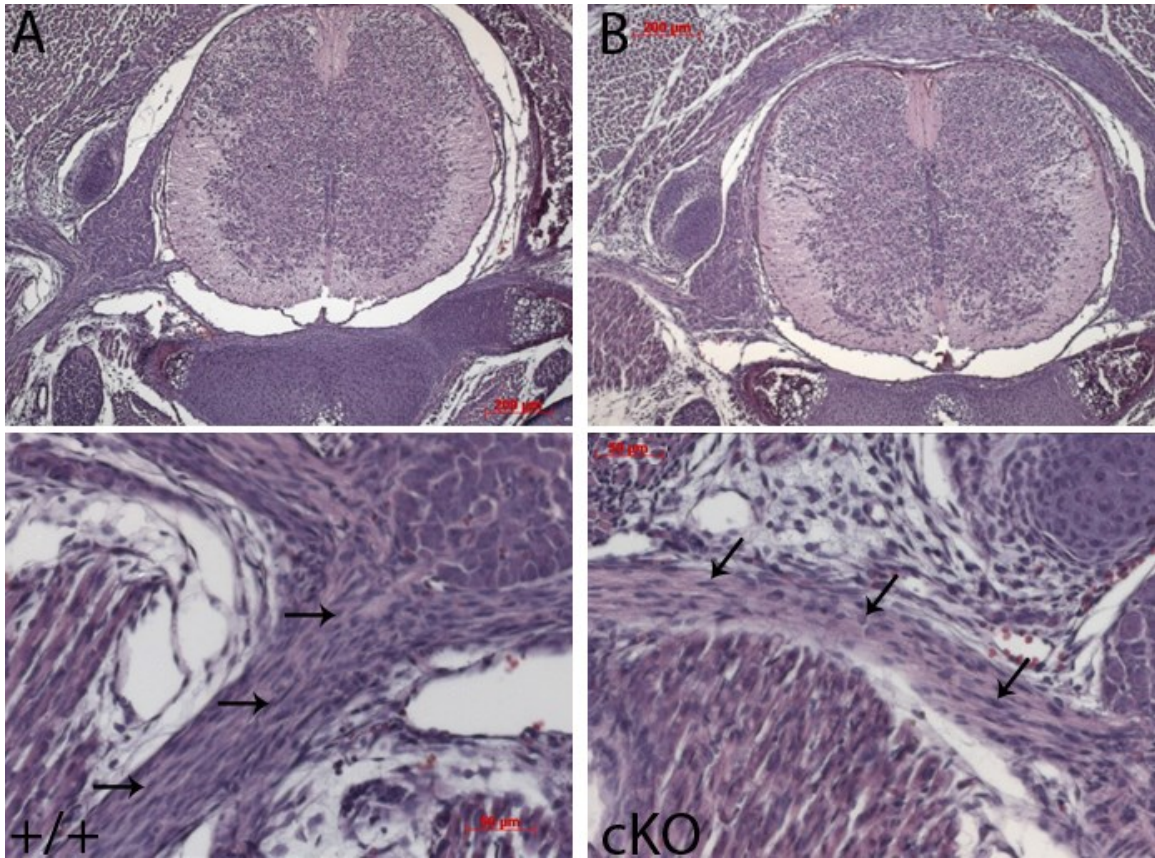
Figure 36. Immature SCs are present on *Shp2* cKO peripheral nerves embryonically. (A) E16.5 control dorsal root ganglia (low mag, top panel; high mag, lower panel) showing migration of SCPs onto peripheral nerves as evidenced by hemotoxylin positive nuclei present (see arrows). **(B)** E16.5 mutant dorsal root ganglia illustrating that *Shp2* cKOs also have SCPs present on peripheral nerves embryonically (see arrows; n=2).
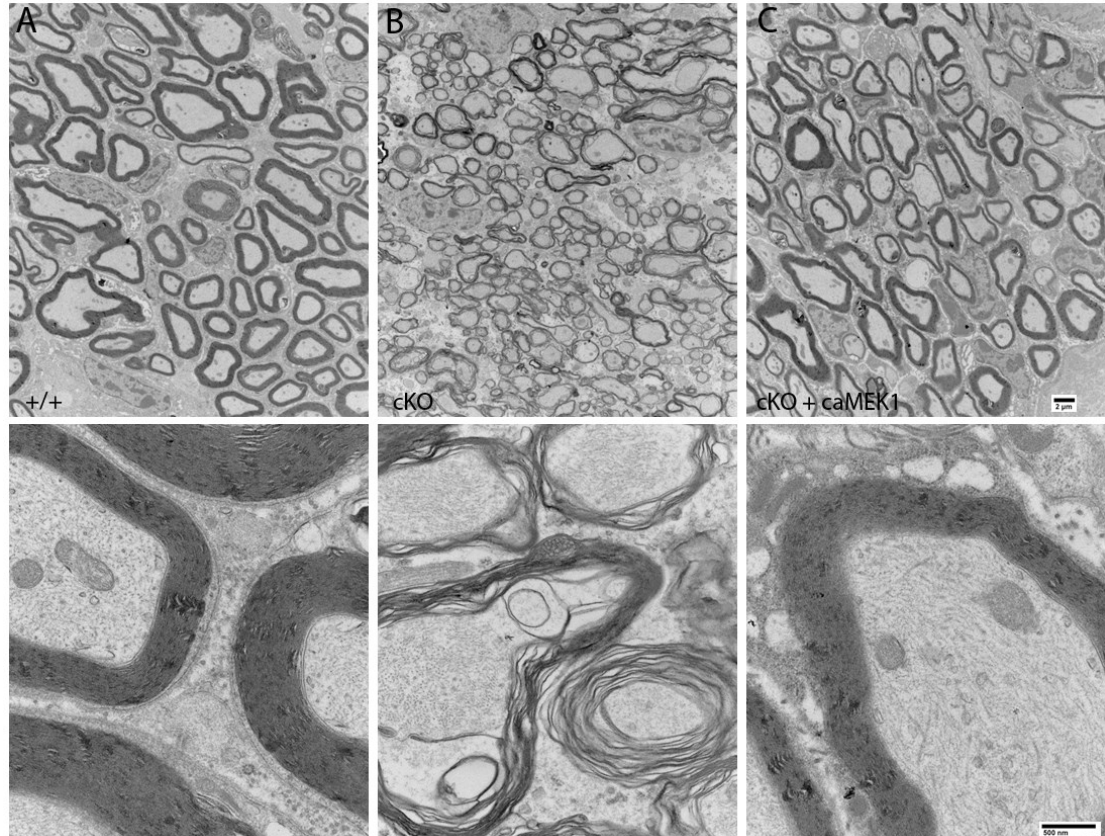
Figure 37. A myelination defect is observed in trigeminal nerves of *Shp2* cKOs and appears to be rescued by caMEK1 expression. (A) P17 control EM of trigeminal nerve at low power (2,900X; top panel) and high power (30,000X; lower panel). **(B)** P17 *Shp2* cKO EM of trigeminal nerve at low power (2,900X; top panel) and high power (30,000X; lower panel). **(C)** P17 rescued mutant EM of trigeminal nerve at low power (2,900X; top panel) and high power (30,000X; lower panel). Notice the thin layers of myelin in the cKO compared to the thick, cohesive myelin in the control and rescued mutant (n=2-3). [IU EM core processed nerve tissue and assisted in collecting images].
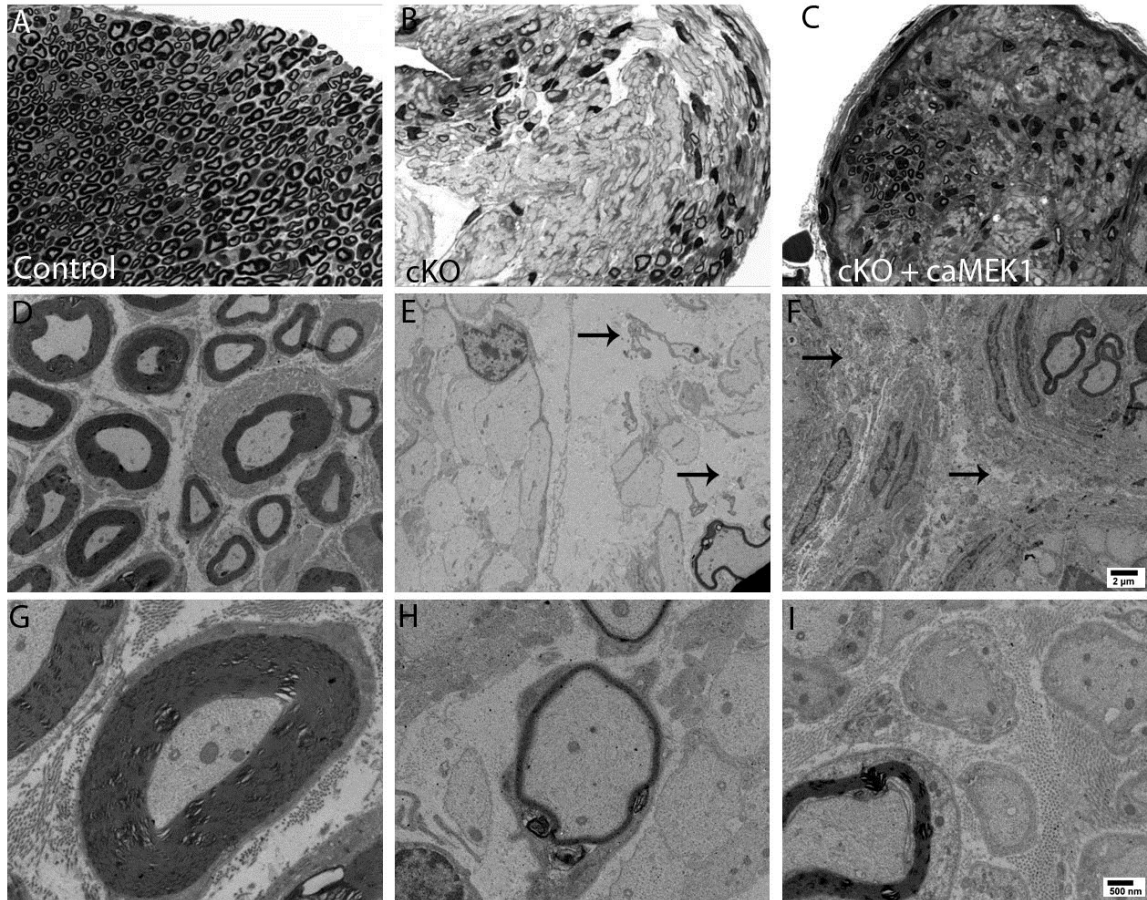
Figure 38. Diminished myelination and axonal loss observed in sciatic nerves of *Shp2* cKOs and rescued mutants. (A-C) Thick section of P17 control (A), *Shp2* cKO (B), and rescued mutant (C) sciatic nerve (cross-section). Note the dark uniform myelination surrounding individual axons in the control that is largely absent from the mutant and rescued mutant nerve. **(D-F)** TEM image of P17 control (D), *Shp2* cKO (E), and rescued mutant (F) sciatic nerve (2,900 X). Note the predominance of unmyelinated/minimally myelinated axons in the *Shp2* cKO and rescued mutant samples. Also, there is significant axonal loss in the *Shp2* cKO (E, arrows) and rescued mutant (F, arrows) which is not present in the control nerve. **(G-I)** TEM image of P17 control (G), *Shp2* cKO (H), and rescued mutant (I) sciatic nerve (11,000 X). Note the predominance of

123

unmyelinated/minimally myelinated axons in the *Shp2* cKO and rescued mutant

samples (n=2-3). [IU EM core processed nerve tissue, assisted in collecting

imagaes, and provided thick sections].

Several preliminary studies have already been performed to begin to parse out the myelination defects present in the *Shp2* cKO and *Shp2;Periostin-Cre;caMEK1* mouse models. Kelly Monk, PhD at Washington University has been a valuable collaborator and has advised on planning future experiments as well as interpretation of TEM data. To date, I have collected samples of trigeminal and sciatic nerves at P17 and examined them via TEM. Preliminary analysis indicates that there is a myelination defect observed in *Shp2* cKOs which appears to be rescued by expression of caMEK1 in the trigeminal nerve; however, diminished myelination as well as axonal loss is observed in the sciatic nerves of both non-rescued and rescued mutants which most likely accounts for the persistence of the gait abnormalities in the rescued mutants.

At present, these data only represent investigation of two or three animals of each genotype and are still preliminary. Several caveats need to be addressed to complete the myelination story. For example, it is still unclear as to whether the observed myelination phenotype is a primary or secondary effect particularly as the samples were harvested at P17 when the *Shp2* cKOs are already experiencing significantly diminished health. Furthermore, despite the fact that the *Periostin* promoter that drives Cre recombinase expression in our model has been shown to be expressed in SCs as early as E14[137], the recombination efficiency in SCs of the trigeminal nerve and sciatic nerve has not been investigated in the early postnatal stage. Notwithstanding the preliminary nature of these studies, these findings of decreased myelination and axonal loss in the

peripheral nervous system serve to place our cardiac focused story in the overall context of the entire organism. The advantage of *in vivo* studies as compared to *in vitro* studies is the context. There are only so many aspects of biochemical signaling pathways and physiology that can be accurately replicated *in vitro*. The body of recent literature on cardiac innervation suggests that there are complex interactions between sympathetic, parasympathetic, and sensory neurons within the "heart brain" which serve to regulate the heart's function[36-42]. While the sympathetic innervation of the heart is not myelinated, a subset of the sensory innervation is. Therefore, thoroughly characterizing the myelination phenotype of *Shp2* cKOs can further inform what we already know about the cardiac innervation in this model.

Future work could focus on collecting samples at earlier time points (Dr. Monk has suggested P0 (before myelination is really established) and P7 (an intermediate time point)). Examination of these developmental time points will shed light on the process that leads to the myelination defect. Again, proliferation and apoptosis studies via IHC may be informative as to the etiology of this loss. Furthermore, Dr. Monk has suggested staining for important myelin proteins such as P0 to investigate the structural integrity of the myelin that is present as the separation of the myelin layers observed in Figure 37 may be indicative of a structural defect in the myelin layers. However, it is also possible that this separation observed is an effect of processing and must be investigated further.

Functional studies may also be incorporated to evaluate the motility phenotypes observed in both rescued and non-rescued mutants. Additionally, nerve conduction studies to quantitatively determine the rate of action potential transmission through an isolated peripheral nerve such as the sciatic would yield critical information as to how the structural phenotype observed by TEM is directly affecting the animal in terms of action potential propagation. This is also one of the few tests that would be capable of detecting an intermediate phenotype or partial rescue in the rescued mutants due to its quantitative nature.

Collectively these histological and functional investigations along with molecular analyses designed to probe signaling pathways involved in the observed phenotypes will serve to further delineate the ERK-dependent versus ERK-independent effects observed in our *Shp2* cKO. The gastrointestinal and myelination manifestations of Shp2 loss are of particular interest due to their clinical implications. Furthermore, the fact that abnormalities in both the enteric and peripheral nervous system are much more severe in early models of NC Shp2 loss (specifically *Wnt-1-Cre* driven deletion[126]) underscores the utility of *Periostin-Cre* as a genetic tool to examine complex developmental processes in the NC.

REFERENCES

1.   Knecht AK, Bronner-Fraser M. Induction of the neural crest: a multigene process. *Nat Rev Genet.* 2002;3(6):453-461.

2.   Nieto A. The early steps of neural crest development. *Mechanisms of Development.* 2001;105:27-35.

3.   Chai Y, Jiang X, Ito Y, Bringas PJ, Han J, Rowitch D, Soriano P, McMahon A, Sucov H. Fate of the mammalian cranial neural crest during tooth and mandibular morphogenesis. *Development.* 2000;127(8):1671-1679.

4.   Kirby M, Bockman D. Neural crest and normal development: a new perspective. *Anat Rec.* 1984;209(1):1-6.

5.   Snider P, Olaopa M, Firulli AB, Conway SJ. Cardiovascular development and the colonizing cardiac neural crest lineage. *ScientificWorldJournal.* 2007;7:1090-1113.

6.   Newgreen D, Dufour S, Howard M, Landman K. Simple rules for a "simple" nervous system? Molecular and biomathematical approaches to enteric nervous system formation and malformation. *Dev Biol.* 2013;382(1):305-319.

7.   Musser M, Michelle Southard-Smith E. Balancing on the crest - Evidence for disruption of the enteric ganglia via inappropriate lineage segregation and consequences for gastrointestinal function. *Dev Biol.* 2013;382(1):359-364.

8.   Huber K. The sympathoadrenal cell lineage: specification, diversification, and new perspectives. *Dev Biol.* 2006;298(2):335-343. Epub 2006 Jul 2014.

9.   Betters E, Liu Y, Kjaeldgaardb A, Sundströmc E, García-Castro MI. Analysis of early human neural crest development. *Developmental Biology.* 2010;344:578-592.

10.   Wu X, Howard M. Two Signal Transduction Pathways Involved in the Catecholaminergic Differentiation of Avian Neural Crest-Derived Cells *In Vitro*. *Molecular and Cellular Neuroscience.* 2001;18:394-406.

11.   Bockman D, Kirby M. Dependence of thymus development on derivatives of the neural crest. *Science.* 1984;223(4635):498-500.

12. Hutson M, Kirby M. Neural crest and cardiovascular development: a 20-year perspective. *Birth Defects Res C Embryo Today.* 2003;69(1):2-13.

13. Neeb Z, Lajiness J, Bolanis E, Conway S. Cardiac outflow tract anomalies. *Wiley Interdiscip Rev Dev Biol.* 2013;2(4):449-530.

14. Iwashita T, Kruger G, Pardal R, Kiel M, Morrison S. Hirschsprung disease is linked to defects in neural crest stem cell function. *Science.* 2003;301(5635):972-976.

15. Burns A, Douarin N. The sacral neural crest contributes neurons and glia to the post-umbilical gut: spatiotemporal analysis of the development of the enteric nervous system. *Development.* 1998;125(21):4335-4347.

16. Fujimoto T, Hata J, Yokoyama S, Mitomi T. A study of the extracellular matrix protein as the migration pathway of neural crest cells in the gut: analysis in human embryos with special reference to the pathogenesis of Hirschsprung's disease. *J Pediatr Surg.* 1989;24(6):550-556.

17. Creazzo TL, Godt RE, Leatherbury L, Conway SJ, Kirby ML. Role of cardiac neural crest cells in cardiovascular development. *Annu Rev Physiol.* 1998;60:267-286.

18. Gurjarpadhye A, Hewett KW, Justus C, Wen X, Stadt H, Kirby ML, Sedmera D, Gourdie RG. Cardiac neural crest ablation inhibits compaction and electrical function of conduction system bundles. *Am J Physiol Heart Circ Physiol.* 2007;292(3):H1291-1300.

19. Bronner M, LeDouarin N. Development and evolution of the neural crest: An overview. *Developmental Biology.* 2012;366:2-9.

20. Sauer B, Henderson N. Site-specific DNA recombination in mammalian cells by the Cre recombinase of bacteriophage P1. *Proc Natl Acad Sci U S A.* 1988;85(14):5166-5170.

21. Soriano P. Generalized lacZ expression with the ROSA26 Cre reporter strain. *Nat Genet.* 1999;21(1):70-71.

22. Macatee T, Hammond B, Arenkiel B, Francis L, Frank D, Moon A. Ablation of specific expression domains reveals discrete functions of ectoderm- and endoderm-derived FGF8 during cardiovascular and pharyngeal development. *Development.* 2003;130(25):6361-6374.

23. Olaopa M, Zhou H, Snider P, Wang J, Schwartz R, Moon A, Conway S. Pax3 is essential for normal cardiac neural crest morphogenesis but is not required during migration nor outflow tract septation. *Dev Biol.* 2011;356(2):308-322

24. Danielian P, Muccino D, Rowitch D, Michael S, McMahon A. Modification of gene activity in mouse embryos in utero by a tamoxifen-inducible form of Cre recombinase. *Curr Biol.* 1998;8(24):1323-1326.

25. Lewis A, Vasudevan H, O'Neill A, Soriano P, Bush J. The widely used Wnt1-Cre transgene causes developmental phenotypes by ectopic activation of Wnt signaling. *Dev Biol.* 2013;379(2):229-234.

26. Brewer S, Feng W, Huang J, Sullivan S, Williams T. Wnt1-Cre-mediated deletion of AP-2alpha causes multiple neural crest-related defects. *Dev Biol.* 2004;267(1):135-153.

27. Snider W. Functions of the Neurotrophins during Nervous System Development: What the Knockouts Are Teaching Us. *Cell.* 1994;77:627-638.

28. Yamauchi Y, Abe K, Mantani A, Hitoshi Y, Suzuki M, Osuzu F, Kuratani S, Yamamura K. A novel transgenic technique that allows specific marking of the neural crest cell lineage in mice. *Dev Biol.* 1999;212(1):191-203.

29. Dubois N, Hofmann D, Kaloulis K, Bishop J, Trumpp A. Nestin-Cre transgenic mouse line Nes-Cre1 mediates highly efficient Cre/loxP mediated recombination in the nervous system, kidney, and somite-derived tissues. *Genesis.* 2006;44(8):355-360.

30. Ke Y, Zhang EE, Hagihara K, Wu D, Pang Y, Klein R, Curran T, Ranscht B, Feng GS. Deletion of Shp2 in the brain leads to defective proliferation and differentiation in neural stem cells and early postnatal lethality. *Mol Cell Biol.* 2007;27(19):6706-6717.

31. Zurborg S, Piszczek A, Martínez C, Hublitz P, Al Banchaabouchi M, Moreira P, Perlas E, Heppenstall P. Generation and characterization of an Advillin-Cre driver mouse line. *Mol Pain.* 2011;7(66).

32. Triposkiadis F, Karayannis G, Giamouzis G, Skoularigis J, Louridas G, Butler J. The sympathetic nervous system in heart failure physiology, pathophysiology, and clinical implications. *J Am Coll Cardiol.* 2009;54(19):1747-1762.

33. Rhoades, Rodney A., and George A. Tanner. Medical Physiology. 1st ed. Boston: Little Brown and Company, 1995.

34. Le, Tao, Vikas Bhushan, and Neil Vasan. First Aid for the USMLE Step 1 2010. 20th ed. New York: McGraw-Hill, 2010.

35. Shi X, Stevens G, Foresman B, Stern S, Raven P. Autonomic nervous system control of the heart: endurance exercise training. *Med Sci Sports Exerc.* 1995;27(10):1406-1413.

36.   Kukanova B, Mravec B. Complex intracardiac nervous system. *Bratisl Lek Listy.* 2006;107(3):45-51.

37.   Horackova M, Slavikova J, Byczko Z. Postnatal development of the rat intrinsic cardiac nervous system: a confocal laser scanning microscopy study in whole-mount atria. *Tissue Cell.* 2000;32(5):377-388.

38.   Habecker B, Bilimoria P, Linick C, Gritman K, Lorentz C, Woodward W, Birren S. Regulation of cardiac innervation and function via the p75 neurotrophin receptor. *Auton Neurosci.* 2008;140(1-2):40-48.

39.   Huang M, Friend D, Sunday M, Singh K, Haley K, Austen K, Kelly R, Smith T. An intrinsic adrenergic system in mammalian heart. *J Clin Invest.* 1996;98(6):1298-1303.

40.   Rysevaite K, Saburkina I, Pauziene N, Noujaim S, Jalife J, Pauza D. Morphologic pattern of the intrinsic ganglionated nerve plexus in mouse heart. *Heart Rhythm.* 2011;8(3):448-454.

41.   Rysevaite K, Saburkina I, Pauziene N, Vaitkevicius R, Noujaim S, Jalife J, Pauza D. Immunohistochemical characterization of the intrinsic cardiac neural plexus in whole-mount mouse heart preparations. *Heart Rhythm.* 2011;8(5):731-738.

42.   Hoard J, Hoover D, Mabe A, Blakely R, Feng N, Paolocci N. Cholinergic neurons of mouse intrinsic cardiac ganglia contain noradrenergic enzymes, norepinephrine transporters, and the neurotrophin receptors tropomyosin-related kinase A and p75. *Neuroscience.* 2008;156:129-142.

43.   Burnstock G. Review lecture. Neurotransmitters and trophic factors in the autonomic nervous system. *J Physiol.* 1981;313:1-35.

44.   Ahlquist R. A study of the adrenotropic receptors. *Am J Physiol.* 1948;152(3):586-600.

45.   Schmidt K, Weinshenker D. Adrenaline Rush: The Role of Adrenergic Receptors in Stimulant-Induced Behaviors. *Mol Pharmacol.* 2014.

46.   Jensen B, O'connell T, Simpson P. Alpha-1-Adrenergic Receptors in Heart Failure: The Adaptive Arm of the Cardiac Response to Chronic Catecholamine Stimulation. *J Cardiovasc Pharmacol.* 2013.

47.   Hein L, Altman J, Kobilka B. Two functionally distinct alpha2-adrenergic receptors regulate sympathetic neurotransmission. *Nature.* 1999;402(6758):181-184.

48.   Berthelsen S, Pettinger W. A functional basis for classification of alpha-adrenergic receptors. *Life Sci.* 1977;21(5):595-606.

49.   Levick, J. R.. <u>An Introduction to Cardiovascular Physiology</u>. 5th ed. Great Britian: Hodder Arnold, 2010.

50.   Podrid P, Fuchs T, Candinas R. Role of the sympathetic nervous system in the genesis of ventricular arrhythmia. *Circulation.* 1990;82:103-113.

51.   Brown M, Brown D, Murphy M. Hypokalemia from beta2-receptor stimulation by circulating epinephrine. *N Engl J Med.* 1983;309(23):1414-1419.

52.   Atwood G, Kirshner N. Postnatal Development of Catecholamine Uptake and Storage of the Newborn Rat Heart. *Developmental Biology.* 1976;49:532-538.

53.   Robinson RB. Autonomic receptor--effector coupling during post-natal development. *Cardiovasc Res.* 1996;31:68-76.

54.   Francis N. Cellular and Molecular Determinants of Sympathetic Neuron Development. *Annu. Rev. Neurosci.* 1999;22:541-566.

55.   Vincentz JW, Rubart M, Firulli AB. Ontogeny of cardiac sympathetic innervation and its implications for cardiac. *Pediatr Cardiol.* 2012;33(6):923-928.

56.   Mercer E, Hoyle G, Kapur R, Brinster R, Palmiter R. The dopamine beta-hydroxylase gene promoter directs expression of E. coli lacZ to sympathetic and other neurons in adult transgenic mice. *Neuron.* 1991;7(5):703-716.

57.   Ieda M, Fukuda K. Cardiac innervation and sudden cardiac death. *Curr Cardiol Rev.* 2009;5(4):289-295.

58.   Cao J, Chen L, KenKnight B, Ohara T, Lee M, Tsai J, Lai W, Karagueuzian H, Wolf P, Fishbein M, Chen P. Nerve sprouting and sudden cardiac death. *Circ Res.* 2000;86(7):816-821.

59.   Packer M. The neurohormonal hypothesis: a theory to explain the mechanism of disease progression in heart failure. *J Am Coll Cardiol.* 1992;20(1):248-254.

60.   Verrier R, Antzelevitch C. Autonomic aspects of arrhythmogenesis: the enduring and the new. *Curr Opin Cardiol.* 2004;19(1):2-11.

61.   Loring J, Erickson C. Neural crest cell migratory pathways in the trunk of the chick embryo. *Dev Biol.* 1987;121(1):220-236.

62.   Anderson D. Molecular control of cell fate in the neural crest: the sympathoadrenal lineage. *Annu Rev Neurosci.* 1993;16:129-158.

63. Guillemot F, Lo L, Johnson J, Auerbach A, Anderson D, Joyner A. Mammalian achaete-scute homolog 1 is required for the early development of olfactory and autonomic neurons. *Cell.* 1993;75(3):463-476.

64. Howard M, Stanke M, Schneider C, Wu X, Rohrer H. The transcription factor dHAND is a downstream effector of BMPs in sympathetic neuron specification. *Development.* 2000;127(18):4073-4081.

65. Pattyn A, Morin X, Cremer H, Goridis C, Brunet J. The homeobox gene Phox2b is essential for the development of autonomic neural crest derivatives. *Nature.* 1999;399(6734):366-370.

66. Lim K, Lakshmanan G, Crawford S, Gu Y, Grosveld F, Engel J. Gata3 loss leads to embryonic lethality due to noradrenaline deficiency of the sympathetic nervous system. *Nat Genet.* 2000;25(2):209-212.

67. Stanke M, Junghans D, Geissen M, Goridis C, Ernsberger U, Rohrer H. The Phox2 homeodomain proteins are sufficient to promote the development of sympathetic neurons. *Development.* 1999;126(18):4087-4094.

68. Morin X, Cremer H, Hirsch M, Kapur R, Goridis C, Brunet J. Defects in sensory and autonomic ganglia and absence of locus coeruleus in mice deficient for the homeobox gene Phox2a. *Neuron.* 1997;18(3):411-423.

69. Coppola E, d'Autreaux F, Rijli F, Brunet J. Ongoing roles of Phox2 homeodomain transcription factors during neuronal differentiation. *Development.* 2010;137(24):4211-4220.

70. Cochard P, Goldstein M, Black I. Ontogenetic appearance and disappearance of tyrosine hydroxylase and catecholamines in the rat embryo. *Proc Natl Acad Sci U S A.* 1978;75(6):2986-2990.

71. Ernsberger U, Patzke H, Tissier-Seta J, Reh T, Goridis C, Rohrer H. The expression of tyrosine hydroxylase and the transcription factors cPhox-2 and Cash-1: evidence for distinct inductive steps in the differentiation of chick sympathetic precursor cells. *Mech Dev.* 1995;52(1):125-136.

72. Ernsberger U. Role of neurotrophin signalling in the differentiation of neurons from dorsal root ganglia and sympathetic ganglia. *Cell Tissue Res.* 2009;336(3):349-384.

73. Cochard P, Paulin D. Initial expression of neurofilaments and vimentin in the central and peripheral nervous system of the mouse embryo in vivo. *J Neurosci.* 1984;4(8):2080-2094.

74. Groves A, George K, Tissier-Seta J, Engel J, Brunet J, Anderson D. Differential regulation of transcription factor gene expression and phenotypic markers in developing sympathetic neurons. *Development.* 1995;121(3):887-901.

75. Schneider C, Wicht H, Enderich J, Wegner M, Rohrer H. Bone morphogenetic proteins are required in vivo for the generation of sympathetic neurons. *Neuron.* 1999;24(4):861-870.

76. Shoba T, Tay S. Nitrergic and peptidergic innervation in the developing rat heart. *Anat Embryol (Berl).* 2000;201(6):491-500.

77. Rimmer K, Harper AA. Developmental changes in electrophysiological properties and synaptic transmission in rat intracardiac ganglion neurons. *J Neurophysiol.* 2006;95(6):3543-3552.

78. De Champlain J, Malmfors T, Olson L, Sachs C. Ontogenesis of peripheral adrenergic neurons in the rat: pre- and postnatal observations. *Acta Physiol Scand.* 1970;80(2):276-288.

79. Snider WD. Nerve Growth Factor Enhances Dendritic Arborization of Sympathetic Ganglion Cells in Developing Mammals *The Journal of Neuroscience.* 1988;8(7):2628-2634.

80. Standen N. The postnatal development of adrenoceptor responses to agonists and electrical stimulation in rat isolated atria. *Br J Pharmacol.* 1978;64(1):83-89.

81. Saygili E, Kluttig R, Rana OR, Saygili E, Gemein C, Zink MD, Rackauskas G, Weis J, Schwinger RHG, Marx N, Schauerte P. Age-related regional differences in cardiac nerve growth factor expression. *Age (Dordr).* 2012;34(3):659-667.

82. Klesse LJ, Meyers KA, Marshall CJ, Parada LF. Nerve growth factor induces survival and differentiation through two distinct. *Oncogene.* 1999;18(12):2055-2068.

83. Virdee K, Tolkovsky A. Activation of p44 and p42 MAP kinases is not essential for the survival of rat sympathetic neurons. *Eur J Neurosci.* 1995;7(10):2159-2169.

84. Virdee K, Tolkovsky A. Inhibition of p42 and p44 mitogen-activated protein kinase activity by PD98059 does not suppress nerve growth factor-induced survival of sympathetic neurones. *J Neurochem.* 1996;67(5):1801-1805.

85. Kaplan DR, Miller FD. Neurotrophin signal transduction in the nervous system. *Curr Opin Neurobiol.* 2000;10(3):381-391.

86.   Marshall CJ. Specificity of receptor tyrosine kinase signaling: transient versus sustained extracellular signal-regulated kinase activation. *Cell.* 1995;80(2):179-185.

87.   Mazzoni IE, Said FA, Aloyz R, Miller FD, Kaplan D. Ras regulates sympathetic neuron survival by suppressing the p53-mediated cell. *J Neurosci.* 1999;19(22):9716-9727.

88.   Virdee K, Xue L, Hemmings B, Goemans C, Heumann R, Tolkovsky A. Nerve growth factor-induced PKB/Akt activity is sustained by phosphoinositide 3-kinase dependent and independent signals in sympathetic neurons. *Brain Res.* 1999;837(1-2):127-142.

89.   Xue L, Murray J, Tolkovsky A. The Ras/phosphatidylinositol 3-kinase and Ras/ERK pathways function as independent survival modules each of which inhibits a distinct apoptotic signaling pathway in sympathetic neurons. *J Biol Chem.* 2000;275(12):8817-8824.

90.   Ieda M, Fukuda K, Hisaka Y, Kimura K, Kawaguchi H, Fujita J, Shimoda K, Takeshita E, Okano H, Kurihara Y, Kurihara H, Ishida J, Fukamizu A, Federoff H, Ogawa S. Endothelin-1 regulates cardiac sympathetic innervation in the rodent heart by controlling nerve growth factor expression. *J Clin Invest.* 2004;113(6):876-884.

91.   Thompson J Fau - Dolcet X, Dolcet X Fau - Hilton M, Hilton M Fau - Tolcos M, Tolcos M Fau - Davies AM, Davies AM. HGF promotes survival and growth of maturing sympathetic neurons by PI-3 kinase. *Mol Cell Neurosci.* 2004;27(4):441-452.

92.   Rosario M, Franke R, Bednarski C, Birchmeier W. The neurite outgrowth multiadaptor RhoGAP, NOMA-GAP, regulates neurite extension. *J Cell Biol.* 2007;178(3):503-516.

93.   Smeyne R, Klein R, Schnapp A, Long L, Bryant S, Lewin A, Lira S, Barbacid M. Severe sensory and sympathetic neuropathies in mice carying a disrupted Trk/NGF receptor gene. *Nature.* 1994;368:246-249.

94.   Ruit KG, Snider WD. Administration or deprivation of nerve growth factor during development. *J Comp Neurol.* 1991;314(1):106-113.

95.   Crowley C, Spencer SD, Nishimura MC, Chen KS, Pitts-Meek S, Armanini MP, Ling LH, McMahon SB, Shelton DL, Levinson AD, et al. Mice lacking nerve growth factor display perinatal loss of sensory and. *Cell.* 1994;76(6):1001-1011.

96.   Gorin P, Johnson E. Experimental autoimmune model of nerve growth factor deprivation: effects on developing peripheral sympathetic and sensory neurons. *Proc Natl Acad Sci U S A.* 1979;76(10):5382-5386.

97.   Ieda M, Kanazawa H, Kimura K, Hattori F, Ieda Y, Taniguchi M, Lee J, Matsumura K, Tomita Y, Miyoshi S, Shimoda K, Makino S, Sano M, Kodama I, Ogawa S, Fukuda K. Sema3a maintains normal heart rhythm through sympathetic innervation patterning. *Nat Med.* 2007;13(5):604-612.

98.   Maden C, Gomes J, Schwarz Q, Davidson K, Tinker A, Ruhrberg C. NRP1 and NRP2 cooperate to regulate gangliogenesis, axon guidance and target innervation in the sympathetic nervous system. *Dev Biol.* 2012;369(2):277-285.

99.   Hof P, Pluskey S, Dhe-Paganon S, Eck MJ, Shoelson SE. Crystal structure of the tyrosine phosphatase SHP-2. *Cell.* 1998;92(4):441-450.

100.   Qu C. The SHP-2 tyrosine phosphatase: signaling mechanisms and biological functions. *Cell Res.* 2000;10(4):279-288.

101.   Newbern JM, Li X, Shoemaker SE, Zhou J, Zhong J, Wu Y, Bonder D, Hollenback S, Coppola G, Geschwind DH, Landreth GE, Snider WD. Specific functions for ERK/MAPK signaling during PNS development. *Neuron.* 2011;69(1):91-105.

102.   Edouard T, Montagner A, Dance M, Conte F, Yart A, Parfait B, Tauber M, Salles JP, Raynal P. How do Shp2 mutations that oppositely influence its biochemical activity result in syndromes with overlapping symptoms? *Cell Mol Life Sci.* 2007;64(13):1585-1590.

103.   Stewart RA, Sanda T, Widlund HR, Zhu S, Swanson KD, Hurley AD, Bentires-Alj M, Fisher DE, Kontaridis MI, Look AT, Neel BG. Phosphatase-dependent and -independent functions of Shp2 in neural crest cells underlie LEOPARD syndrome pathogenesis. *Dev Cell.* 2010;18(5):750-762.

104.   Grossmann KS, Rosario M, Birchmeier C, Birchmeier W. The tyrosine phosphatase Shp2 in development and cancer. *Adv Cancer Res.* 2010;106:53-89.

105.   Tartaglia M, Gelb BD, Zenker M. Noonan syndrome and clinically related disorders. *Best Pract Res Clin Endocrinol Metab.* 2011;25(1):161-179.

106.   Digilio MC, Conti E, Sarkozy A, Mingarelli R, Dottorini T, Marino B, Pizzuti A, Dallapiccola B. Grouping of multiple-lentigines/LEOPARD and Noonan syndromes on the PTPN11 gene. *Am J Hum Genet.* 2002;71(2):389-394.

107.   Wu X, Simpson J, Hong JH, Kim KH, Thavarajah NK, Backx PH, Neel BG, Araki T. MEK-ERK pathway modulation ameliorates disease phenotypes in a mouse model of Noonan syndrome associated with the Raf1(L613V) mutation. *J Clin Invest.* 2011;121(3):1009-1025.

108. Kontaridis MI, Swanson KD, David FS, Bardford D, Neel BG. PTPN11 (SHP2) mutations in LEOPARD syndrome have dominant negative, not activating, effects. *J. Biol. Chem.* 2006;281:6785-6792.

109. Tartaglia M, Martinelli S, Stella L, Bocchinfuso G, Flex E, Cordeddu V, Zampino G, Burgt I, Palleschi A, Petrucci TC, Sorcini M, Schoch C, Fao R, Emanuel PD, Gelb BD. Diversity and functional consequences of germline and somatic PTPN11 mutations in human disease. *Am. J. Hm. Genet.* 2006;78:279-290.

110. Neel B, Gu H, Pao L. The 'Shp'ing news: SH2 domain-containing tyrosine phosphatases in cell signaling. *Trends Biochem Sci.* 2003;28(6):284-293.

111. Zhang EE, Chapeau E, Hagihara K, Feng GS. Neuronal Shp2 tyrosine phosphatase controls energy balance and metabolism. *Proc Natl Acad Sci U S A.* 2004;101(45):16064-16069.

112. Torres J, Russo P, Tobias J. Anaesthetic implications of LEOPARD syndrome. *Paediatr Anaesth.* 2004;14(4):352-356.

113. Tartaglia M, Zampino G, Gelb B. Noonan syndrome: clinical aspects and molecular pathogenesis. *Mol Syndromol.* 2010;1(1):2-26.

114. Woywodt A, Welzel J, Haase H, Duerholz A, Wiegand U, Potratz J, Sheikhzadeh A. Cardiomyopathic lentiginosis/LEOPARD syndrome presenting as sudden cardiac arrest. *Chest.* 1998;113(5):1415-1417.

115. Limongelli G, Pacileo G, Calabro R. Is sudden cardiac death predictable in LEOPARD syndrome? *Cardiol Young.* 2006;16(6):599-601.

116. Sarkozy A, Digilio MC, Dallapiccola B. Leopard syndrome. *Orphanet J Rare Dis.* 2008;3:13.

117. Bentires-Alj M, Kontaridis MI, Neel BG. Stops along the RAS pathway in human genetic disease. *Nat Med.* 2006;12(3):283-285.

118. Tidyman W, Rauen K. The RASopathies: developmental syndromes of Ras/MAPK pathway dysregulation. *Curr Opin Genet Dev.* 2009;19(3):230-236.

119. Nakamura T, Gulick J, Pratt R, Robbins J. Noonan syndrome is associated with enhanced pERK activity, the repression of which can prevent craniofacial malformations. *Proc Natl Acad Sci U S A.* 2009;106(36):15436-15441.

120. Nakamura T, Colbert M, Krenz M, Molkentin JD, Hahn HS, Dorn GW, 2nd, Robbins J. Mediating ERK 1/2 signaling rescues congenital heart defects

in a mouse model of Noonan syndrome. *J Clin Invest.* 2007;117(8):2123-2132.

121. Cowley S, Paterson H, Kemp P, Marshall CJ. Activation of MAP kinase kinase is necessary and sufficient for PC12 differentiation and for transformation of NIH 3T3 cells. *Cell.* 1994;77(6):841-852.

122. Wright JH, Drueckes P, Bartoe J, Zhao Z, Shen SH, Krebs EG. A role for the SHP-2 tyrosine phosphatase in nerve growth-induced PC12 cell. *Mol Biol Cell.* 1997;8(8):1575-1585.

123. Nakamura T, Gulick J, Colbert MC, Robbins J. Protein tyrosine phosphatase activity in the neural crest is essential for normal heart and skull development. *Proc Natl Acad Sci U S A.* 2009;106(27):11270-11275.

124. Saxton T, Pawson T. Morphogenetic movements at gastrulation require the SH2 tyrosine phosphatase Shp2. *Proc Natl Acad Sci U S A.* 1999;96(7):3790-3795.

125. Chen B, Bronson RT, Klaman LD, Hampton TG, Wang JF, Green PJ, Magnuson T, Douglas PS, Morgan JP, Neel BG. Mice mutant for Egfr and Shp2 have defective cardiac semilunar valvulogenesis. *Nat Genet.* 2000;24(3):296-299.

126. Grossmann KS, Wende H, Paul FE, Cheret C, Garratt AN, Zurborg S, Feinberg K, Besser D, Schulz H, Peles E, Selbach M, Birchmeier W, Birchmeier C. The tyrosine phosphatase Shp2 (PTPN11) directs Neuregulin-1/ErbB signaling throughout Schwann cell development. *Proc Natl Acad Sci U S A.* 2009;106(39):16704-16709.

127. Saxton TM, Ciruna BG, Holmyard D, Kulkarni S, Harpal K, Rossant J, Pawson T. The SH2 tyrosine phosphatase shp2 is required for mammalian limb development. *Nat Genet.* 2000;24(4):420-423.

128. Uhlen P, Burch PM, Zito CI, Estrada M, Ehrlich BE, Bennett AM. Gain-of-function/Noonan syndrome SHP-2/Ptpn11 mutants enhance calcium oscillations and impair NFAT signaling. *Proc Natl Acad Sci U S A.* 2006;103(7):2160-2165.

129. Mirsky R, Jessen K, Brennan A, Parkinson D, Dong Z, Meier C, Parmantier E, Lawson D. Schwann cells as regulators of nerve development. *J Physiol Paris.* 2002;96(1-2):17-24.

130. Newbern J, Birchmeier C. Nrg1/ErbB signaling networks in Schwann cell development and myelination. *Semin Cell Dev Biol.* 2010;21(9):922-928.

131. Monje P, Soto J, Bacallao K, Wood P. Schwann cell dedifferentiation is independent of mitogenic signaling and uncoupled to proliferation: role of

cAMP and JNK in the maintenance of the differentiated state. *J Biol Chem.* 2010;285(40):31024-31036.

132. Taveggia C, Zanazzi G, Petrylak A, Yano H, Rosenbluth J, Einheber S, Xu X, Esper R, Loeb J, Shrager P, Chao M, Falls D, Role L, Salzer J. Neuregulin-1 type III determines the ensheathment fate of axons. *Neuron.* 2005;47(5):681-694.

133. Murphy P, Topilko P, Schneider-Maunoury S, Seitanidou T, Baron-Van Evercooren A, Charnay P. The regulation of Krox-20 expression reveals important steps in the control of peripheral glial cell development. *Development.* 1996;122(9):2847-2857.

134. Dong Z, Sinanan A, Parkinson D, Parmantier E, Mirsky R, Jessen K. Schwann cell development in embryonic mouse nerves. *J Neurosci Res.* 1999;56(4):334-348.

135. Voiculescu O, Charnay P, Schneider-Maunoury S. Expression Pattern of a Krox-20/Cre Knock-in Allele in the Developing Hindbrain, Bones, and Peripheral Nervous System. *Genesis.* 2000;26(2):123-126.

136. Joseph N, Mosher J, Buchstaller J, Snider P, McKeever P, Lim M, Conway S, Parada L, Zhu Y, Morrison S. The loss of Nf1 transiently promotes self-renewal but not tumorigenesis by neural crest stem cells. *Cancer Cell.* 2008;13(2):129-140.

137. Lindsley A, Snider P, Zhou H, Rogers R, Wang J, Olaopa M, Kruzynska-Frejtag A, Koushik SV, Lilly B, Burch JB, Firulli AB, Conway SJ. Identification and characterization of a novel Schwann and outflow tract endocardial cushion lineage-restricted periostin enhancer. *Dev Biol.* 2007;307(2):340-355.

138. Krenz M, Gulick J, Osinska H, Colbert M, Molkentin J, Robbins J. Role of ERK1/2 signaling in congenital valve malformations in Noonan syndrome. *Proc Natl Acad Sci U S A.* 2008;105(48):18930-18935.

139. Lajiness JD, Snider P, Wang J, Feng GS, Krenz M, Conway SJ. SHP-2 deletion in post-migratory neural crest cells results in impaired cardiac sympathetic innervation. *Proc Natl Acad Sci U S A.* 2014.

140. Chuma S, Nakatsuji N. Autonomous transition into meiosis of mouse fetal germ cells in vitro and its inhibition by gp130-mediated signaling. *Dev Biol.* 2001;229(2):468-479.

141. Snider P, Hinton RB, Moreno-Rodriguez RA, Wang J, Rogers R, Lindsley A, Li F, Ingram DA, Menick D, Field L, Firulli AB, Molkentin JD, Markwald R, Conway SJ. Periostin is required for maturation and extracellular matrix

stabilization of noncardiomyocyte lineages of the heart. *Circ Res.* 2008;102(7):752-760.

142. Morikawa Y, D'Autreaux F, Gershon M, Cserjesi P. Hand2 determines the noradrenergic phenotype in the mouse sympathetic nervous system. *Dev Biol.* 2007;307(1):114-126.

143. Conway S. In situ hybridization of cells and tissue sections. *Methods Mol Med.* 1996;6:193-206.

144. Koushik S, Wang J, Rogers R, Moskophidis D, Lambert N, Creazzo T, Conway S. Targeted inactivation of the sodium-calcium exchanger (Ncx1) results in the lack of a heartbeat and abnormal myofibrillar organization. *FASEB J.* 2001;15(7):1209-1211.

145. Zhou H, Wang J, Rogers R, Conway S. Lineage-specific responses to reduced embryonic Pax3 expression levels. *Dev Biol.* 2008;315(2):369-382.

146. Roth DM, Swaney JS, Dalton ND, Gilpin EA, Ross J, Jr. Impact of anesthesia on cardiac function during echocardiography in mice. *Am J Physiol Heart Circ Physiol.* 2002;282(6):H2134-2140.

147. Hohimer AR, Davis LE, Hatton DC. Repeated daily injections and osmotic pump infusion of isoproterenol cause similar increases in cardiac mass but have different effects on blood pressure. *Can J Physiol Pharmacol.* 2005;83(2):191-197.

148. Rose R, Kabir M, Backx P. Altered heart rate and sinoatrial node function in mice lacking the cAMP regulator phosphoinositide 3-kinase-gamma. *Circ Res.* 2007;101(12):1274-1282.

149. Takeda N, Manabe I, Uchino Y, Eguchi K, Matsumoto S, Nishimura S, Shindo T, Sano M, Otsu K, Snider P, Conway SJ, Nagai R. Cardiac fibroblasts are essential for the adaptive response of the murine heart to pressure overload. *J Clin Invest.* 2010;120(1):254-265.

150. Lajiness JD, Conway SJ. The Dynamic Role of Cardiac Fibroblasts in Development and Disease. *J Cardiovasc Transl Res.* 2012;5:739-748.

151. Lajiness J, Conway S. Origin, development, and differentiation of cardiac fibroblasts. *J Mol Cell Cardiol.* 2013.

152. Katz D, Nicolelis M, Simon S. Nutrient tasting and signaling mechanisms in the gut. IV. There is more to taste than meets the tongue. *Am J Physiol Gastrointest Liver Physiol.* 2000;278(1):6-9.

153. Shusterman V, Usiene I, Harrigal C, Lee J, Kubota T, Feldman A, London B. Strain-specific patterns of autonomic nervous system activity and heart failure susceptibility in mice. *Am J Physiol Heart Circ Physiol.* 2002;282(6):H2076-2083.

154. Saba S, London B, Ganz L. Autonomic blockade unmasks maturational differences in rate-dependent atrioventricular nodal conduction and facilitation in the mouse. *J Cardiovasc Electrophysiol.* 2003;14(2):191-195.

155. Steinberg S, Rosen T, Malfatto G, Rosen M. Beta adrenergic modulation of cardiac rhythm in a rat model of altered sympathetic neural development. *J Mol Cell Cardiol.* 1991;23:47-52.

156. Clegg D, Large T, Bodary S, Reichardt L. Regulation of nerve growth factor mRNA levels in developing rat heart ventricle is not altered by sympathectomy. *Dev Biol.* 1989;134(1):30-37.

157. Chan G, Cheung L, Yang W, Milyavsky M, Sanders A, Gu S, Hong W, Liu A, Wang X, Barbara M, Sharma T, Gavin J, Kutok J, Iscove N, Shannon K, Dick J, Neel B, Braun B. Essential role for Ptpn11 in survival of hematopoietic stem and progenitor cells. *Blood.* 2011;117(16):4253-4261.

158. Schramm C, Fine D, Edwards M, Reeb A, Krenz M. The PTPN11 loss-of-function mutation Q510E-Shp2 causes hypertrophic cardiomyopathy by dysregulating mTOR signaling. *Am J Physiol Heart Circ Physiol.* 2012;302(1):231-243.

159. Marin T, Keith K, Davies B, Conner D, Guha P, Kalaitzidis D, Wu X, Lauriol J, Wang B, Bauer M, Bronson R, Franchini K, Neel B, Kontaridis M. Rapamycin reverses hypertrophic cardiomyopathy in a mouse model of LEOPARD syndrome-associated PTPN11 mutation. *J Clin Invest.* 2011;121(3):1026-1043.

160. Ishida H, Kogaki S, Narita J, Ichimori H, Nawa N, Okada Y, Takahashi K, Ozono K. LEOPARD-type SHP2 mutant Gln510Glu attenuates cardiomyocyte differentiation and promotes cardiac hypertrophy via dysregulation of Akt/GSK-3beta/beta-catenin signaling. *Am J Physiol Heart Circ Physiol.* 2011;301(4):H1531-1539. .

161. Corson L, Yamanaka Y, Lai K, Rossant J. Spatial and temporal patterns of ERK signaling during mouse embryogenesis. *Development.* 2003;130(19):4527-4537.

162. Rouleau C, Matécki S, Kalfa N, Costes V, de Santa Barbara P. Activation of MAP kinase (ERK1/2) in human neonatal colonic enteric nervous system. *neurogastroenterol Motil.* 2009;21(2):207-214.

163. Hoit B, Kiatchoosakun S, Restivo J, Kirkpatrick D, Olszens K, Shao H, Pao Y, Nadeau J. Naturally occurring variation in cardiovascular traits among inbred mouse strains. *Genomics.* 2002;79(5):679-685.

164. Chen B, Hammonds-Odie L, Perron J, Masters BA, Bixby JL. SHP-2 mediates target-regulated axonal termination and NGF-dependent neurite. *Dev Biol.* 2002;252(2):170-187.

165. Gill JS, Schenone AE, Podratz JL, Windebank AJ. Autocrine regulation of neurite outgrowth from PC12 cells by nerve growth factor. *Brain Res Mol Brain Res.* 1998;57(1):123-131.

166. Grewal SS, York RD, Stork PJ. Extracellular-signal-regulated kinase signalling in neurons. *Curr Opin Neurobiol.* 1999;9(5):544-553.

167. Perron J, Bixby J. Distinct neurite outgrowth signaling pathways converge on ERK activation. *Mol Cell Neurosci.* 1999;13(5):362-378.

168. D'Alessio A, Cerchia L, Amelio I, Incoronato M, Condorelli G, de Franciscis V. Shp2 in PC12 cells: NGF versus EGF signalling. *Cell Signal.* 2007;19(6):1193-1200.

169. Anderson CN, Tolkovsky AM. A role for MAPK/ERK in sympathetic neuron survival: protection against a p53-dependent, JNK-independent induction of apoptosis by cytosine arabinoside. *J Neurosci.* 1999;19(2):664-673.

170. Jelinek T, Catling A, Reuter C, Moodie S, Wolfman A, Weber M. RAS and RAF-1 form a signalling complex with MEK-1 but not MEK-2. *Mol Cell Biol.* 1994;14(12):8212-8218.

171. Araki T, Chan G, Newbigging S, Morikawa L, Bronson RT, Neel BG. Noonan syndrome cardiac defects are caused by PTPN11 acting in endocardium to enhance endocardial-mesenchymal transformation. *Proc Natl Acad Sci U S A.* 2009;106(12):4736-4741.

172. Smith R, Pulicicchio L, Holmes A. Generalized lentigo: electrocardiographic abnormalities, conduction disorders and arrhythmias in three cases. *Am J Cardiol.* 1970;25(4):501-506.

173. Limongelli G, Sarkozy A, Pacileo G, Calabro P, Digilio M, Maddaloni V, Gagliardi G, Di Salvo G, Iacomino M, Marino B, Dallapiccola B, Calabro R. Genotype-phenotype analysis and natural history of left ventricular hypertrophy in LEOPARD syndrome. *Am J Med Genet A.* 2008;146A(5):620-628.

174. Silva J, Sharma S, Hughes B, Yu Y, Cowell J. Homozygous inactivation of the LGI1 gene results in hypomyelination in the peripheral and central nervous systems. *J Neurosci Res.* 2010;88(15):3328-3336.

175. Henry E, Eicher E, Sidman R. The mouse mutation claw paw: forelimb deformity and delayed myelination throughout the peripheral nervous system. *J Hered.* 1991;82(4):287-294.

176. Nelis E, Timmerman V, De Jonghe P, Van Broeckhoven C, Rautenstrauss B. Molecular genetics and biology of inherited peripheral neuropathies: a fast-moving field. *Neurogenetics.* 1999;2(3):137-148.

177. Scherer S, Wrabetz L. Molecular mechanisms of inherited demyelinating neuropathies. *Glia.* 2008;56(14):1578-1589.

178. Nicks J, Lee S, Kostamo K, Harris A, Sookdeo A, Notterpek L. Long-term analyses of innervation and neuromuscular integrity in the Trembler-J mouse model of Charcot-Marie-Tooth disease. *J Neuropathol Exp Neurol.* 2013;72(10):942-954.

179. Suter U, Welcher A, Ozcelik T, Snipes G, Kosaras B, Francke U, Billings-Gagliardi S, Sidman R, Shooter E. Trembler mouse carries a point mutation in a myelin gene. *Nature.* 1992;356(6366):241-244.

CURRICULUM VITAE

Jacquelyn D. Lajiness

Education

2005-2009	Hope College, Holland, MI	B.S.: Biology B.A.: Chemistry
2009-2014	Indiana University	Ph.D.: Biochemistry Minor: Life Sciences
2009-2016	Indiana University	M.D. (in progress)

Honors, Awards, Fellowships

2005	Salutatorian, Rockford High School, Rockford, MI
2005-2009	Trustee Scholarship, Hope College
April 2006	First Year Biology Book Award, Hope College
April 2006	First Year Chemistry Book Award, Hope College
2007-2009	Beckman Scholarship, Arnold and Mabel Beckman Foundation
April 2007	Kleinheksel Award for excellence in sophomore level Mathematics, Hope College
April 2007	Organic Book Award, Hope College
2007-2009	Jaecker Chemistry Scholarship, Hope College
2009	B.S. and B.A.--Summa Cum Laude, Hope College
2005-2009	Dean's List, Hope College
March 2012	Biochemistry and Molecular Biology Research Day poster award, IUSM

2013	American Heart Association Midwest Predoctoral Fellowship
November 2013	APSA Midwest Regional Meeting poster award
2013-present	National Heart, Lung, Blood Institute F30 HL116106

Research and Training Experience

Hope College
Undergraduate research, Department of Chemistry, 2005-2009
Brent Krueger, Ph.D.

Project title: The Study of the Structural Dynamics and Binding of Biopolymers via the Use of Fluorescence-Detected Resonance Energy Transfer (FRET).

Indiana University School of Medicine
MSTP student, Department of Biochemistry and Cellular Biology, 2011-2014
Simon Conway, Ph.D

Dissertation title: Shp2 Deletion in Post-migratory Neural Crest Cells Results in Impaired Cardiac Sympathetic Innervation

Dissertation Committee: Drs. Maureen A. Harrington, David A. Ingram, R. Mark Payne, and Michael Rubart

Conferences Attended

Lydia R. Hartsell[†], Nora E. Kuiper[†], <u>Jacquelyn D. Lewis</u>[†], Conrad M. Tobert, Dr. Brent P. Krueger, and Dr. Michael J. Pikaart. Utilizing Fluorescence Spectroscopy and Computation to Better Understand Protein/DNA Interactions. 52nd Annual Biophysical Society National Meeting. Long Beach, California. February 2-6, 2008.
[†]Authors contributed equally to this work

<u>Jacquelyn D. Lewis</u>, David A. Paul, Dr. Michael J. Pikaart, Dr. Brent P. Krueger. The Study of the Structural Dynamics and Binding of Biopolymers via the Use of Fluorescence-Detected Resonance Energy Transfer (FRET). Beckman Symposium. Irvine, California. July 23-25, 2008.

Jacquelyn D. Lewis, David A. Paul, Dr. David P. Millar, Dr. Michael J. Pikaart, Dr. Brent P. Krueger. The Study of the Structural Dynamics and Binding of Biopolymers via the Use of Fluorescence-Detected Resonance Energy Transfer (FRET). Council on Undergraduate Research: "Posters on the Hill." Washington, D.C. May 5, 2009.

Jacquelyn D. Lajiness, Paige Snider, and Simon J. Conway.Shp2, Neural Crest, and Neonatal Death.2012 Biochemistry and Molecular Biology Research Day. Indianapolis, IN. March 30, 2012.

Jacquelyn D. Lajiness, Paige Snider, and Simon J. Conway.Shp2, Neural Crest, and Neonatal Death.2012 Weinstein Cardiovascular Development Conference. Chicago, IL. May 2-4, 2012.

Jacquelyn D. Lajiness, Paige Snider, and Simon J. Conway.Shp2, neural crest, and neonatal death. First Annual South-Central Regional MD/PhD Conference. Louisville, KY. September 8, 2012.

Jacquelyn D. Lajiness, Paige Snider, and Simon J. Conway. Protein tyrosine phosphatase Shp2 and neonatal cardiac innervation. APSA 9th Annual Meeting. Chicago, IL. April 26-28, 2013.

Jacquelyn D. Lajiness, Paige Snider, and Simon J. Conway. Protein tyrosine phosphatase Shp2 and neonatal cardiac innervation.28th Annual National MD/PhD Student Conference. Keystone, CO. July 26-28, 2013.

Jacquelyn D. Lajiness, Paige Snider, and Simon J. Conway. Protein tyrosine phosphatase Shp2 and neonatal cardiac innervation.51st Midwest Society for Developmental Biology meeting. St. Louis, MO. September 26-28, 2013.

Jacquelyn D. Lajiness, Paige Snider, and Simon J. Conway. Protein tyrosine phosphatase Shp2 and neonatal cardiac innervation. APSA Midwest Regional Meeting. Columbus, OH. November 9, 2013.

Jacquelyn D. Lajiness, Paige Snider, and Simon J. Conway.Protein tyrosine phosphatase Shp2 and neonatal cardiac innervation. APSA 10th Annual Meeting. Chicago, IL. April 25-27, 2014.

Invited Lectures

January, 2012   "Shp2 and Neonatal Sudden Death", Neonatal Medicine Working Group Conference, Indiana University School of Medicine

January, 2012	"Shp2 and Neonatal Sudden Death", MSTP student seminar, Indiana University School of Medicine
January, 2013	"Protein tyrosine phosphatase Shp2 and neonatal cardiac innervation", MSTP student seminar, Indiana University School of Medicine
April, 2013	"Protein tyrosine phosphatase Shp2 and neonatal cardiac innervation", Neonatal Medicine Working Group Conference, Indiana University School of Medicine
September, 2013	"Protein tyrosine phosphatase Shp2 and neonatal cardiac innervation", 51st Midwest Society for Developmental Biology meeting, St. Louis, MO.
March, 2014	"Protein tyrosine phosphatase Shp2 and neonatal cardiac innervation", Department of Biochemistry, Indiana University School of Medicine

Peer Reviewed Publications

Lajiness JD, Conway SJ. The Dynamic Role of Cardiac Fibroblasts in Development and Disease. *J Cardiovasc Transl Res.* 2012;5:739-48.

Neeb Z, Lajiness J, Bolanis E, Conway S. Cardiac outflow tract anomalies. *Wiley Interdiscip Rev Dev Biol.* 2013;2(4):449-530.

Lajiness J, Conway S. Origin, development, and differentiation of cardiac fibroblasts. *J Mol Cell Cardiol.* 2013. (In press)

Lajiness JD, Snider P, Wang J, Feng GS, Krenz M, Conway SJ. SHP-2 deletion in post-migratory neural crest cells results in impaired cardiac sympathetic innervation. *Proc Natl Acad Sci*. 2014. (In press)

Gehlhausen JR, Park SJ, Shew M, Staser K, Rhodes SD, Menon K, Lajiness JD, Mwanthi M, Wang X, Yuan J, Samuels B,Territo P, Nalepa G, Yang FC, Conway S, Giovannini M, Stemmer-Rachamimov A, Yates C, Clapp DW. A conditional NF2 mouse model of schwannoma genesis that recapitulates human disease. *J Clin Invest.* (Submitted)